

Project B3.1: Cities as Water Supply Catchments - Green Cities and Microclimate

Report:

Design and implementation of VTUF-3D, a new
micro-climate model in support of modelling of Water
Sensitive Urban Design features

Kerry Nice (Other contributors, Andrew Coutts, Nigel Tapper, Jason Beringer

March 3, 2016

Contents

1	Executive Summary	1
2	Introduction	1
2.1	Project overview	1
2.2	Water sensitive urban design (WSUD) as mitigation and adaptation	1
2.3	Goals of modelling the benefits of WSUD	2
2.4	Research objectives	3
3	Literature Review	5
3.1	Inclusion of vegetation in urban models	5
3.2	Methods to model T_{mrt} impacts of vegetation	5
3.3	Inclusion of vegetation in UCM modelling	5
3.4	Vegetation modelling at a local or micro scale using SEB	6
3.5	Direct modelling using CFD techniques	6
3.6	Possible tools to model urban vegetation at a micro-scale	7
3.6.1	TUF-3D	7
3.6.2	MAESPA	7
3.7	Tool creation for modelling urban vegetation	9
3.8	Research gaps in modelling urban micro-climates	10
4	Modifications to TUF-3D urban micro-climate model to support assessments of WSUD influences on HTC at a micro-scale in urban canyons	11
4.1	TUF-3D Modifications Design Details	11
4.1.1	Overview of changes	11
4.1.2	TUF-3D unmodified shading logic	11
4.1.3	Integrating vegetation shading and modified ray tracing logic in VTUF-3D	14
4.1.4	MAESPA vegetation transmission and energy balance functionality overview	17
4.1.5	VTUF-3D and MAESPA configuration changes	17
4.2	Configuration generation	19
4.2.1	Overview	19
4.2.2	Create streets and buildings	20
4.2.3	Create post-processing scripts	20
4.2.4	Domain creation	20

4.2.5	MAESPA configurations creation	21
4.2.6	MAESPA tree parameterizations	21
4.2.6.1	MAESPA olive tree (<i>Olea europaea</i>) parameterization	22
4.2.6.2	MAESPA brushbox tree (<i>Lophostemon Confertus</i>) parameterization	22
4.2.6.3	MAESPA grass parameterization	23
4.3	Running VTUF-3D	24
4.3.1	Overview of changes in TUF-3D	24
4.3.2	MAESPA energy flux conversions	25
4.3.3	Loading MAESPA data	25
4.3.4	Radiation transmission in Maespa	26
4.3.5	VTUF-3D use of Maespa shading values	26
4.3.6	VTUF-3D use of Maespa differential shading values	27
4.3.7	Adding physiological vegetation processes	27
4.3.8	Energy balance partitioning during simulation timesteps	28
4.4	VTUF-3D Post-processing	29
4.4.1	Tmrt and UTCI	30
4.4.2	Design conclusions	30
5	Validation and assessment of improved performance of the VTUF-3D model to model urban areas	31
5.1	VTUF-3D Validation Details	31
5.1.1	Overview of validation process	31
5.1.2	Model testing and validation using Preston dataset	31
5.1.3	Model testing and validation using City of Melbourne, George and Gipps St. dataset	39
5.1.4	Model testing and validation using George St. dataset	40
5.1.5	Model testing and validation using City of Melbourne, Gipps St. dataset .	42
5.1.6	Model testing and validation using Lincoln Sq dataset	47
5.2	Future tasks	47
5.2.1	Model testing and validation using Hughesdale dataset	47
5.2.2	Model testing and validation using Smith St dataset	47
6	A systematic assessment of WSUD scenarios and urban morphologies using newly improved VTUF-3D model in support of HTC at a micro-climate level in urban areas	51
6.1	VTUF-3D Scenarios Details	51

6.1.1	Overview of scenarios	51
6.1.2	Preston Scenarios	51
6.1.3	City of Melbourne Gipps St. scenarios	51
6.1.4	Sensitivity scenarios	54
7	Future plans	57
8	Conclusion	57
	References	58

List of Figures

1	WSUD techniques and urban micro-climate	2
2	WSUD techniques and urban micro-climate	3
3	Basic cubic cell and surface patch structure of TUF-3D	8
4	An example TUF-3D domain with a bounding wall and the sub-domain S_d (chosen to coincide with the central urban unit) in lighter shades	8
5	MAESPA process flowchart	9
6	MAESPA water balance flowchart	9
7	VTUF-3D model process flow	12
8	Building height arrays	13
9	Initial view angles ray tracing	13
10	TUF-3D unmodified shading	14
11	Vegetation height arrays	15
12	Integration of MAESPA tree model into VTUF-3D radiation fluxes routines	15
13	TUF-3D modified shading, timestep ray tracing	16
14	VTUF-3D modified shading, reverse ray tracing	18
15	TUF-3D/MAESPA vegetation/radiation interactions	18
16	VTUF-3D energy balance modelling with vegetation MAESPA tiles	19
17	TUF-3D energy balance modelling with MAESPA tiles	28
18	Preston suburb and modelled area	31
19	Digitization of Preston suburban street	32
20	Building heights (0, 5, 10m)	33
21	Building heights (0, 5, 10m)	33
22	Rnet RMSE VTUF-3D vs. observations comparison for Preston runs	34

23	Rnet d VTUF-3D vs. observations comparison for Preston runs	35
24	PrestonBase6 run 30 day hourly average VTUF-3D flux comparisons to Preston flux observations	36
25	PrestonBase6 energy closure (VTUF-3D and observations), $Q* - Qg - Qh - Qe = 0$	36
26	PrestonBase6 predicted vs. observations	37
27	PrestonBase6 daytime predicted vs. observations	37
28	PrestonBase6 nighttime predicted vs. observations	38
29	PrestonBaseNoVeg1 run 30 day hourly average VTUF-3D flux comparisons to Preston flux observations	38
30	PrestonBaseNoVeg1 predicted vs. observations	39
31	George St/Gipps St - Modelled domains with 4 and 3 observation stations located on street	39
32	Building heights (top) / Vegetation cover (bottom) - George St (left), Gipps St. (right)	40
33	Energy closure of George St	41
34	Results of George St. Tmrt and UTCI for 24 February 2014 1500.	42
35	George St. point comparison of Tsfc of 4 observation stations to modelled points	43
36	George St. point comparison of Tmrt of 4 observation stations to modelled points	43
37	George St. point comparison of UTCI of 4 observation stations to modelled points	44
38	George St. 30 day averages, 4 observation stations compared to modelled points	44
39	Energy closure of VTUF-3D and observations for Gipps St.	45
40	Gipps St. point comparison of Tmrt of 3 observation stations to modelled points	45
41	Gipps St. point comparison of Tsfc of 3 observation stations to modelled points .	46
42	Gipps St. point comparison of UTCI of 3 observation stations to modelled points	46
43	Lincoln Square domain	47
44	Lincoln Square building heights	48
45	Lincoln Square vegetation heights	48
46	Comparisons of modelled Tsfc to observed transits of Lincoln Sq. on 14 January 2014 3pm	49
47	Comparisons of modelled UTCI to observed transits of Lincoln Sq. on 14 January 2014 3pm	49
48	Hughesdale suburb and observation station locations	49
49	Smith St. contains detailed physiological observations of isolated trees	50
50	Preston, 4 scenarios of zero trees, half trees, existing Preston tree canopy cover, and double trees	52

51	Preston Scenarios-UTCI at 0m for 4 scenarios of zero trees, half trees, existing Preston tree canopy cover, and double trees	52
52	Modelled UTCI of 4 Preston scenarios over 13-14 February 2004 / UTCI differences between baseline existing Preston trees and other scenarios	53
53	Modelled Tcan of 4 scenarios over 13-14 February 2004 / Tcan differences between baseline existing trees and other scenarios	53
54	Gipps St. 5 scenarios of zero trees, half trees, existing Gipps St. tree canopy cover, double trees, and quadruple trees.	54
55	Gipps St. UTCI (averaged at 0m height) of scenarios of zero trees, half trees, existing Gipps St. tree canopy cover, double trees, and quadruple trees.	55
56	Gipps St. UTCI (averaged at 0m height) for 5 scenarios over 23-24 February 2014 / UTCI differences between baseline scenario and other Gipps St. scenarios	55
57	Modelled Tcan of 5 Gipps St. scenarios (and forcing Tair) over 23-24 February 2014 / Tcan differences between baseline existing Gipps St. trees scenario and other scenarios	56

List of Tables

1	Ray tracing results	16
2	MAESPA tree parameterizations common attributes	22
3	MAESPA olive tree (<i>Olea europaea</i>) parameterization, tree dimensions for 5x5m grid (rescale for taller/shorter), values adapted from Coutts (2014)	22
4	MAESPA olive tree (<i>Olea europaea</i>) parameterization	23
5	MAESPA brushbox tree (<i>Lophostemon Confertus</i>) parameterization, tree dimensions for 5x5m grid (rescale for taller/shorter), values adapted from Coutts (2015b)	23
6	MAESPA brushbox tree (<i>Lophostemon Confertus</i>) parameterization	24
7	MAESPA grass layer as a box tree on the ground covering the plot area, values adapted from Coutts (2015a)	24
8	MAESPA grass layer as a box tree on the ground covering the plot area	25
9	MAESPA variables loaded	26
10	VTUF-3D validation matrix	31
11	Preston simulations compared	34
12	George St Tmrt predicted vs. observations	41
13	George St Tsfc predicted vs. observations	41
14	George St UTCI predicted vs. observations	42
15	Gipps St. Tmrt predicted vs. observations	42
16	Gipps St. Tsfc predicted vs. observations	43

17 Gipps St. UTCI predicted vs. observations	44
--	----

List of Symbols

T_{mrt} mean radiant temperature

zH mean building height,m

1 Executive Summary

There will be an executive summary here.

2 Introduction

2.1 Project overview

Urban areas are facing a growing number of problems which include increasing ageing populations, increased population density, rapid conversion of green areas in to urban areas, trends towards increased average temperatures and increasing temperature extremes, and the increasing understanding of impacts to human health of extreme temperatures. These leave urban areas in an increasingly dangerous position. From an examination of a range of different studies examining cooling effects of urban greenery, it is clear that increased vegetation and water does have an impact, from city-wide scale down to a micro-climate street level scale. Shading and water evaporation are cited as the main drivers of these cooling effects. Also cited are factors of vegetation density, orientation, and amounts of irrigation used.

In coming years, strategies are needed to adapt to and deal with these challenges. Incorporating water sensitive urban design (WSUD) principles into urban areas can be an effective way to deal with many of these problems. However, guidance on how to most effectively use WSUD is lacking, as well as solid quantitative assessments of how well WSUD can perform in urban areas. In addition, no suitable tool exists to make these assessments. Therefore, this project will create a tool suited to this purpose, validate it, and then use it to quantify the effectiveness of WSUD, its most effective use, and determine a WSUD best practice. With this tool and the guidance gained from it, WSUD can be used in the most effective ways to help solve many of these pressing problems.

2.2 Water sensitive urban design (WSUD) as mitigation and adaptation

In examining the possible mitigation and adaptation strategies available to provide HTC in urban areas in light of all the challenges facing these areas, the use of Water Sensitive Urban Design (WSUD) can be considered an extension of both the cases of urban morphology changes and urban greening. Through increased incorporation of water sensitive principles into an urban landscape (Wong & Brown 2009), trees and other vegetation are added to fulfil a number of ecosystem services such as nutrient/pollution filtration, shading, and cooling through evapotranspiration. Stormwater is captured and stored and reused instead of being expelled from the system as waste water, allowing maintenance of the vegetation and increased use of water without having to draw more heavily on external sources.

Many of the changes reverse conditions Oke (1982) cites as contributors to urban heat island (UHI). These include air pollution reduction, conversion of impervious surfaces to pervious to promote water infiltration to the soil, reduction of sensible heat fluxes by shifting the surface energy balance towards greater latent energy fluxes, and by using natural cooling reduce the amount of artificial cooling needed (and their associated anthropogenic heat emissions).

While there is a body of research, highlighted by Bowler et al. (2010), showing that parks act as cooler parts of urban areas, there has been less work done examining bringing park elements into urban areas and how that can bring those cooling benefits to the urban area at large. New urban development or re-development designed to encourage evapotranspiration and energy dispersal through latent energy fluxes can reduce the need for artificial air conditioning (saving

the amount of anthropogenic heat released as well as a savings in CO₂ emissions) (Coutts et al. 2010).

WSUD features can facilitate this through features such as rainwater tanks, rain-gardens, wetlands, swales, infiltration systems, tree-pits, and porous pavements which increase soil moisture and increase the vegetation and availability of water in urban areas. The use of these features (using the methods shown in Figure 1) can promote changes at a local/neighbourhood scale such as larger scale shading and cooling plumes from irrigated open space and water bodies. Impacts on HTC will also be felt at the micro-scale (Figure 2) through increased shading, reduced sensible heat fluxes and ground heat storage.

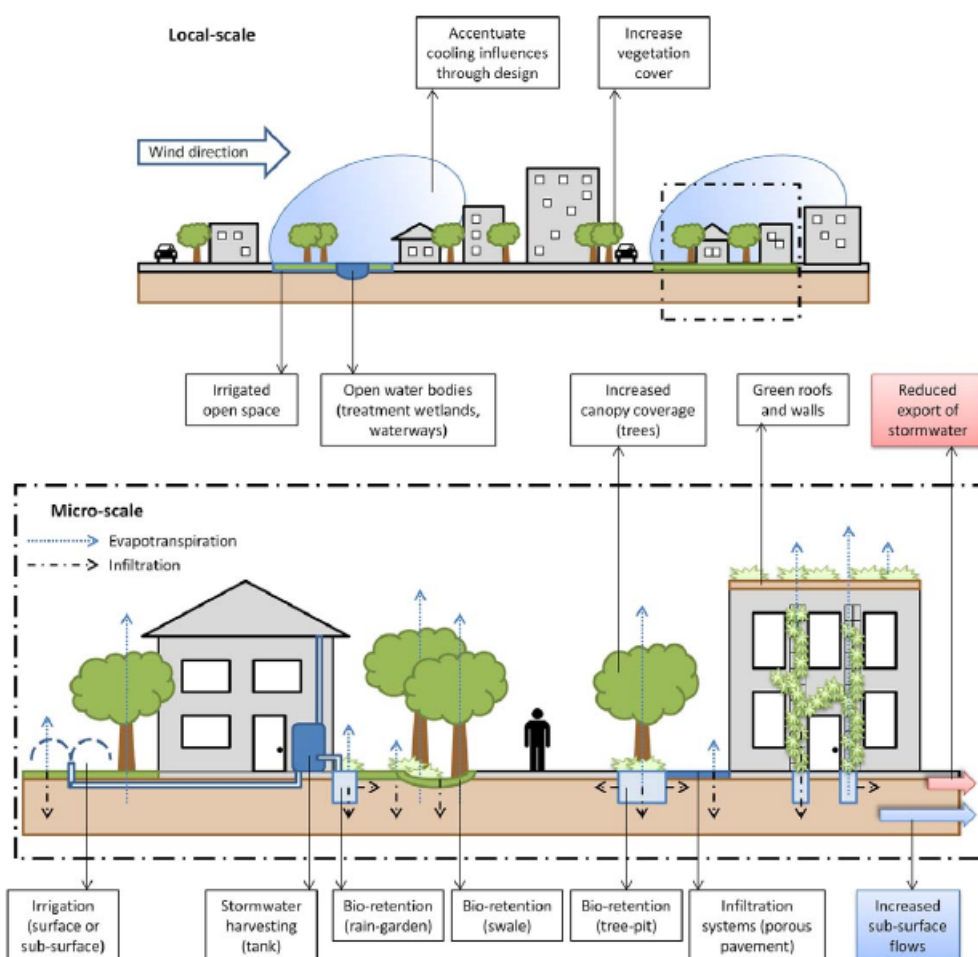


Figure 1: WSUD techniques and urban micro-climate (Coutts et al. 2012, p. 6)

2.3 Goals of modelling the benefits of WSUD

Some rough estimates can be drawn about how much cooling can be expected from adding urban greenery. Modelling can be attempted, but as will be shown in the literature review, no modelling tool exists yet to examine a wide variety of WSUD scenarios at a human scale (micro-climate scaled) to determine HTC benefits in urban areas. Observational studies are important to give an understanding of the processes within urban areas and to provide baseline validation data sets for models. However, collecting observational data is time consuming and difficult. More importantly, observations can only be used to study existing urban morphologies. Modelling tools are required to study different scenarios and new variations of features of an

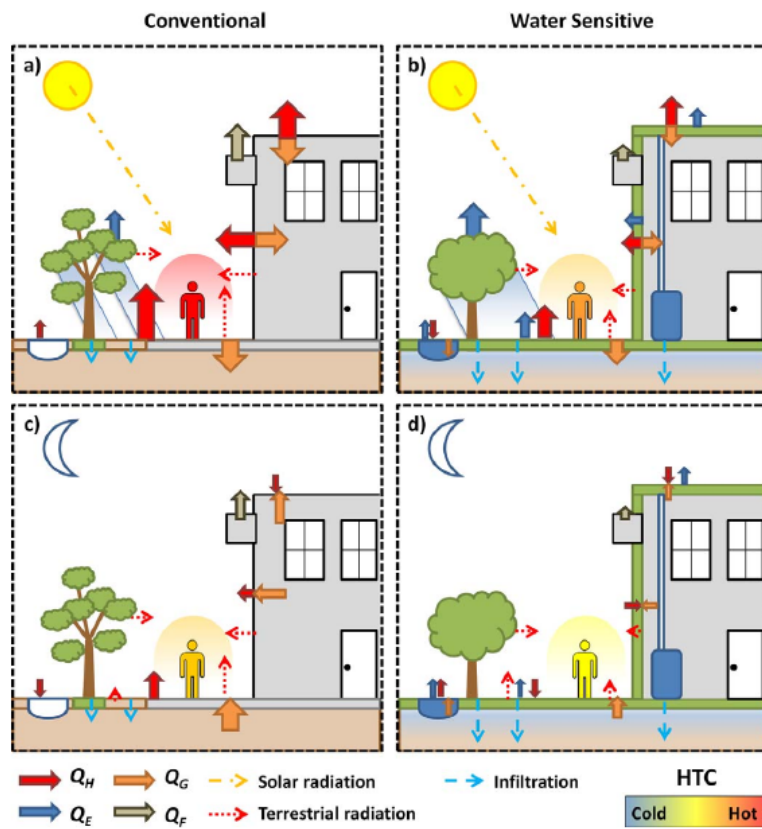


Figure 2: WSUD techniques and urban micro-climate (Coutts et al. 2012, p. 10)

urban area (buildings and materials and orientations, vegetation, surface types, and water features) to find optimal arrangements and determine best practice for their usage for HTC benefits in urban areas. Therefore, quantifying the positive climatic impacts of WSUD on HTC in urban areas at a micro-climate level requires a new tool set to be created and validated. After the tool is ready, it can be used in a systematic assessment of scenarios to determine the micro-climatic advantages of different WSUD features in a variety of urban configurations.

2.4 Research objectives

In order to achieve this aim, a number of objectives will need to be completed. The key research objectives proposed for this project are:

1. Preparation of a modelling tool to model specialised requirements of WSUD features for HTC at a micro-scale level.

Needs to:

- Predict climate parameters in 3-D urban environments.
- Accurate predictions of mean radiant temperatures in complex urban geometry.
- Capture the processes driving energy and water budgets of urban climates and interactions of the three layers of soil, plants, and atmosphere and their interactions with buildings and urban surfaces.

- Predict at a sufficient resolution (micro-scaled) to resolve human interactions with their surroundings and supply necessary parameters to calculate human thermal comfort index values.
 - Contain functionality to directly model or parameterise a variety of WSUD features.
- 2. Validations and assessments follow to determine level of model improvement** over existing models and the suitability to accurately capture important dynamics of WSUD and assess HTC improvements.
- Test VTUF-3D's ability to model the Coutts et al. (2007) Preston (Melbourne, Australia) data set, using predicted energy flux comparisons as a measurement of accuracy.
 - Model the three scenarios of White et al. (2012) (George St., Gipps St., and Bourke St.) over a number of representative days using temporal and spatial observed UTCI and Tmrt values as a measurement of accuracy.
 - Use the Motazedian (2015) Lincoln Square transits and observations of Tsfc and UTCI as a validation of VTUF-3D's spatial predictions accuracy.
 - Use the White et al. (2012) observation campaign to study a single isolated tree, a Queensland Brush Box (*Lophostemon confertus*) to validate VTUF-3D's ability to model this widely used street tree.
 - Use the Gebert et al. (2012) tree study campaign data to validate VTUF-3D's ability to model WSUD based tree pits.

3. Determine the impact of WSUD treatments on HTC comfort at a micro-scale in urban areas.

Assess:

- Modifications of temperatures (air and radiant) as well as HTC indexes (PMV, UTCI, etc), spatially and temporally at a micro-climate scale through the implementation of vegetation and WSUD features.
- The effectiveness of WSUD features in moderating effects of heat waves and temperature extremes.
- Optimal arrangements of WSUD features to maximise the cooling benefits at least cost using present and possible future urban morphologies.
- Synthesise guidelines for WSUD usage to most effectively promote human thermal comfort at a micro-scale in urban areas.

Run scenarios:

- Run basic tree cover variation scenarios based on the validation scenarios, examining the impact of varying amounts of tree canopy on HTC in these domains.
- Conduct sensitivity study using amount of vegetation, location of vegetation, characteristics of vegetation (tree height, leaf area index, number of trees, height, and tree placement), and soil moisture levels to isolate the most important parameters.

3 Literature Review

3.1 Inclusion of vegetation in urban models

The inclusion of vegetation within models has been attempted in a number of different ways, but not all of them are adequate to fulfil the requirements needed in HTC studies. The lack of T_{mrt} in particular has been a barrier to proper assessments of HTC as well as sufficiently detailed spatial predictions to allow HTC calculations from individual trees and elements of vegetation.

Urban vegetation has been accounted for in a number of different ways, using a number of different techniques and at different scales. Vegetation has been added to larger scale models a parametrisations. Vegetation has also been added to urban canopy models (UCM), many which model urban areas in a idealized way. Representations of vegetation have been added to surface energy balance (SEB) models. Finally, computational fluid dynamics (CFD) based models and other direct modelling techniques have been used to model the vegetation directly.

As will be shown in the following sections, some methods can calculate T_{mrt} and capture some but not all the effects of vegetation. The only currently available method to directly model vegetation at a micro-scale is using CFD based methods. This has implications for this study and this problem must be overcome to have a widely available and less computationally intense method to assess HTC impacts of vegetation.

3.2 Methods to model T_{mrt} impacts of vegetation

There have been attempts to quantify the impacts of vegetation through its influence on T_{mrt} , which is an important factor in human thermal comfort. In Tan et al. (2015), the approach taken was to observe and measure rates of plant evapotranspiration of a rooftop garden, as well as its albedo then regression modelling was used to predict T_{mrt} . While a relation was found between the two parameters and T_{mrt} , other important influences of vegetation might have not been considered in this modelling.

SOLWEIG (SOLWEIG 2011) and the RayMan model (Matzarakis et al. 2007; 2010) can be used to calculate the impacts of vegetation on the T_{mrt} . In both, vegetation is accounted for through sky view factors and the shading effect of vegetation, but do not consider the other possible cooling effects of increased latent energy fluxes and the repartitioning of the energy balances. Both these models appear to be useful tools to assess the influence of vegetation T_{mrt} (and its influence on HTC) but there remain limitations on their overall uses in assessing vegetation influences.

3.3 Inclusion of vegetation in UCM modelling

While meso-scaled atmospheric models do not have sufficient resolution to resolve individual urban features (such as streets, buildings, and vegetation), their coupling with urban canopy models (UCMs) has allowed their influence to be included in the results. As the scale of these models is city-wide or neighbourhood-scaled at best, they can capture temporal patterns, but are insufficient in spacial resolution to capture the effects of individual elements of vegetation or even small groupings of vegetation. However, these models can still be useful tools to look at such questions as cooling impacts of modifying a city's canopy cover and those impacts of heat related mortality (Chen et al. 2014).

For single layer UCMs, these parametrisations include the Town Energy Balance (TEB) model (Masson 2000), a single slab UCM (Kusaka et al. 2001), simple urban energy balance model for meso-scale simulations (SUMM) (Kanda et al. 2005), an energy balance UCM (Harman & Belcher 2006), and the community land model (CLM3) (Oleson et al. 2008). Of these, only Masson (2000) has included latent heat fluxes and urban hydrology.

TEB-Veg (Lemonsu et al. 2012) has added vegetation to the urban canyons using the Soil Biosphere and Atmosphere (ISBA) module (Noilhan & Planton 1989), running it twice in grid squares which contain tiles of vegetation and of urban vegetation. Using the results from these calculation steps, the fluxes are aggregated in proper proportions to roofs, walls, roads, and gardens.

Lee & Park (2008) and Lee (2011) describes the Vegetated Urban Canopy Model (VUCM). This model contains a nearly complete scheme for modelling vegetation. It uses the big leaf model as the basis for its urban canopy modelling.

However, there are still some gaps. Modelling of WSUD features requires additional hydrological scenarios, including irrigation, water filtration and retention features, such as is included in SUEWS's hydrology.

Multi-layer UCMs include parametrisation from Martilli et al. (2002); Kondo et al. (2005); Vu et al. (2002); Otte & Lacser (2004); Dupont et al. (2004). Of these, only Dupont et al. (2004) consider some number of vegetation tile types in the urban environment to modify momentum and turbulence budgets but not the building and tree interactions.

Modifications of Martilli et al. (2002) have added radiation interactions and tree foliate effects (Krayenhoff et al. 2014) and spatial averaged mean air flows within buildings and urban canopies (Krayenhoff et al. 2015).

Modifications to UCM parametrisation to include vegetation have added significant abilities to assess the impacts of urban vegetation. However, as these they are all local scaled at best, they still lack sufficient resolution to detail HTC impacts of vegetation.

3.4 Vegetation modelling at a local or micro scale using SEB

Models, modelling at a number of scales including local and micro-scaled, have been able to include vegetation and used to look at effects of urban vegetation. This family of models use Surface Energy Balance (SEB) techniques as the basis to resolve the radiation movement within the modelling domain.

Surface Urban Energy and Water Balance Scheme (SUEWS) (Järvi et al. 2011) uses a simple approach to model the surface energy balance (SEB) of an urban area. Vegetation is not directly modelled but accounted for in the repartitioning of the available energy based on the percentage breakdown of land cover as input variables for a model run.

SUEWS would be suitable for most urban modelling and looking at vegetation effects at a city-wide or neighborhood scale. However, as with meso-scaled models coupled with UCMs, the results will lack the micro-climate detail needed to make HTC assessments of individual elements of vegetation.

3.5 Direct modelling using CFD techniques

Direct simulations using CFD techniques have also been progressing rapidly. Models of this category largely evolved modelling micro-scale wind flow to look at pollution dispersion in

urban areas, such as MIMO (Kunz et al. 2000) and MITRAS (Mikroskaliges Chemie, Transport und Strömungsmodell) (Schlüzen et al. 2011). Neither model is available outside of a research context and both models are very difficult to configure and operate which limits their wide spread suitability modelling WSUD features.

ENVI-met (Bruse 1999) is another CFD based model which has been increasingly used for study of vegetation impacts at a micro-scale (Wang et al. 2015; Lehmann et al. 2014; Konarska et al. 2014; Declet-Barreto et al. 2012; Shahidan et al. 2012). However, a number of published studies where there was an attempt to validate ENVI-met results have encountered difficulties. Alitoudert, F and Mayer (2006) found that the values predicted by the model were probably overstated due to higher than expected radiation fluxes predicted by the model. Krüger et al. (2011) focused on wind speeds as a validation for ENVI-met's accuracy and found initial wind speeds of greater than 2 m/s to be unreliable and a limitation.

A final approach to micro-climate modelling taken particularly by a number of researchers in Japan is hand-coding simulations using CFD frameworks such as OpenFOAM (OpenFOAM 2011) or STAR-CD (CD-adapco 2011).

Only a handful of studies have attempted modelling human thermal comfort impacts of vegetation (Gromke et al. 2015) or other important WSUD features such as water bodies (Tominaga et al. 2015) using CFD techniques (excluding ENVI-met studies).

3.6 Possible tools to model urban vegetation at a micro-scale

TUF-3D

The TUF-3D model fits into the surface energy balance class of models but is first introduced here instead because of the possibilities it presents in creating a tool which can model urban vegetation at a micro-scale. The Temperatures of Urban Facets in 3D (TUF-3D) model (Krayenhoff & Voogt 2007) simulates energy balances through a 3D raster model (Figure 3, 4).

However, other types of vegetation, especially trees, are not currently modelled in TUF-3D. The model does not currently account for water in urban canyons in any stage of the water cycle.

These features will be added to the model as a phase (section 2.4) of this thesis creating a completed tool which can be used to examine WSUD scenarios in detail at a micro-scale. TUF-3D was built from radiative flux movements from the ground up and that's where its strength lies, as surface temperatures and mean radiant temperatures are critical for determining HTC. The simplifications in the convection scheme are anticipated to strike the suitable balance between complexity and computational intensity and accuracy and resolution.

MAESPA

In order to model the vegetation in the TUF-3D domains, a model capable of modelling trees and vegetation is needed. For this task, MAESPA has been chosen.

MAESPA is a soil-plant-atmosphere model and provides forest canopy radiation absorption and photosynthesis functionality, in addition to water balances. It is a process based model (PBM), modelling the interactions among environmental drivers, plant and canopy structure, leaf physiology and soil water availability and their combined effects on water use and carbon uptake.

For MAESPA, the functionality of the canopy components was largely described by Wang & Jarvis (1990) with its origins in the MAESTRO model. The canopy of individual trees is built

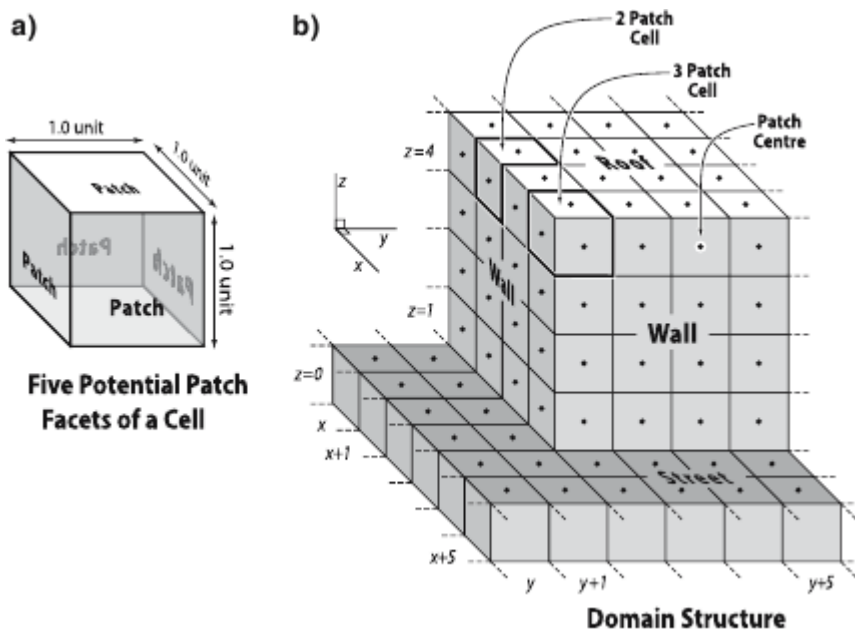


Figure 3: Basic cubic cell and surface patch structure of TUF-3D (Krayenhoff & Voogt 2007, p. 437)

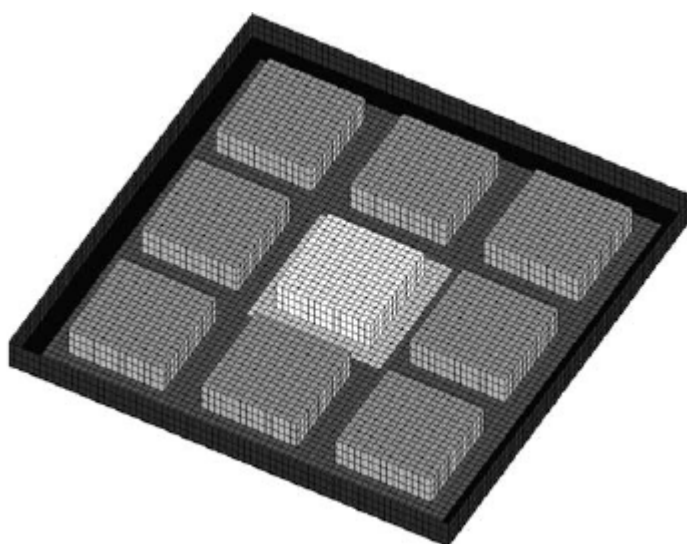


Figure 4: An example TUF-3D domain with a bounding wall and the sub-domain S_d (chosen to coincide with the central urban unit) in lighter shades (Krayenhoff & Voogt 2007, p. 437)

based on several possible shapes (cones, cylinders, ellipsoids, etc.) and using parameters of length, height, and width. These canopies are broken down into a number of grid points. Radiation transfer (of direct and diffuse radiation) and interactions (shading effects and sun movement) from three different wavelengths (photosynthetically active radiation (PAR), near infra-red (NIR), and long-wave) are modelled in the crown grid points.

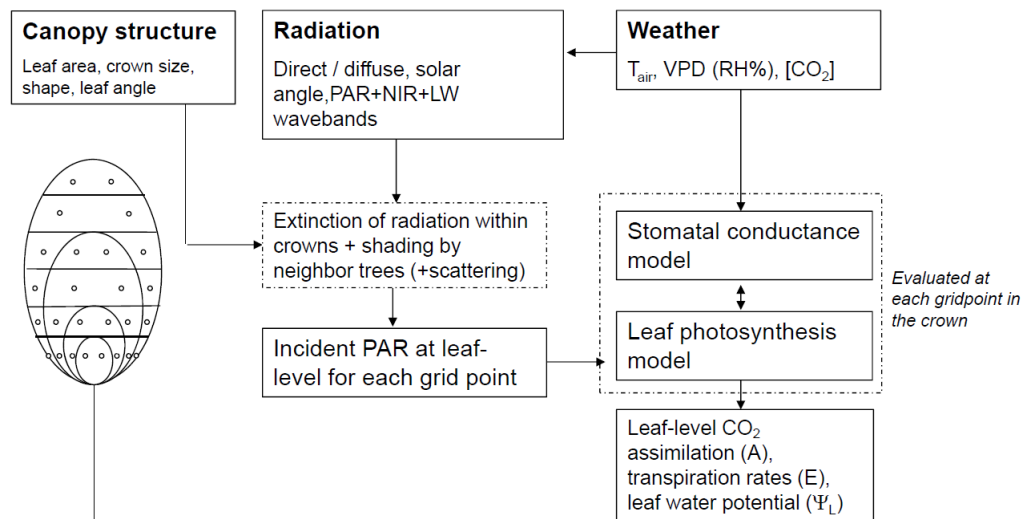


Figure 5: MAESPA process flowchart (Duursma & Medlyn 2012)

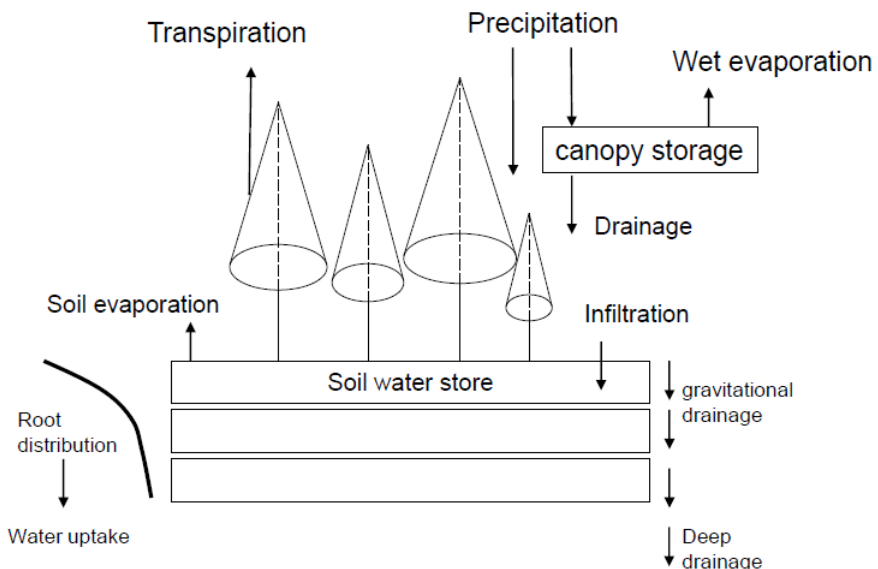


Figure 6: MAESPA water balance flowchart (Duursma & Medlyn 2012)

3.7 Tool creation for modelling urban vegetation

It is anticipated that the marriage of the TUF-3D model with the MAESPA model will create a tool suitable for modelling urban vegetation at a micro-scale. The creation and validation of this tool will be the major task of this thesis. Afterwards, the tool will be used to quantify the cooling effects of urban greening. The theoretical basis of, as well as the current state of observational and modelling work with urban greening, will be covered in the next section.

3.8 Research gaps in modelling urban micro-climates

Modelling tools are needed to resolve full temperature gradients (as well as wind speed and humidity in order to calculate HTC) across a modelled urban canyon. In addition, proper modelling of latent energy fluxes and vegetation is critical to WSUD studies, as a desired side effect of WSUD is localized cooling effects due to increased water and vegetation within the urban canyon.

While there are a number of models surveyed in the literature review which resolve at micro-climate scales, none of them are suitable to model WSUD due to either difficulties with these requirements or exclusion of these features by design. The majority of these models were originally designed to model air flow and particle dispersion. As surface energy balance fluxes help to drive those processes, those are also modelled, but this isn't the main focus of these models. The remaining micro-scale models, which start from radiation fluxes, lack vegetation and water modelling, so are missing much of what will be needed to assess WSUD features.

The TUF-3D model addresses many of these problems, however the lack of vegetation and water modelling leaves it incomplete. However, using the MAESPA model to model these missing features, coupling the two models, can create the tool needed for assessing WSUD features in support of HTC in urban areas and fill these gaps is this research area.

Once this tool is complete, a complete and systematic assessment of WSUD features at a micro-scale can be done. This is a very large gap which needs to be filled to use WSUD in the most effective way to protect human health in light of all the concerning trends progressing in urban areas.

4 Modifications to TUF-3D urban micro-climate model to support assessments of WSUD influences on HTC at a micro-scale in urban canyons

4.1 TUF-3D Modifications Design Details

Overview of changes

To model the impacts of increased water and vegetation on human thermal comfort in urban areas requires modifications to TUF-3D (Krayenhoff & Voogt 2007). TUF-3D in its unmodified form lacks functionality for the physical representation of vegetation along with their physiological processes. Also missing are latent energy fluxes and the water cycle associated with soil, vegetation, evaporation, and precipitation.

Two major changes have been made to the TUF-3D model to add this missing functionality. The first is representation of vegetation's physical form and radiative interactions within an urban canyon. This is done using placeholder vegetation structures which load data calculated by MAESPA (Duursma & Medlyn 2012) for vegetation absorption, transmission, and reflection of each individually modelled vegetation element. VTUF-3D uses cube shaped structures (as TUF-3D uses to represent buildings) to represent vegetation. These cubes store the surface properties and states and interact with the rest of the VTUF-3D domain. The vegetation's true shape is represented in MAESPA and accessed through the simulation by loading that calculated data. This allows quantifying shading effects and the cooling benefits that can bring.

The second major change is including the physiological workings of vegetation and soil in the model. Using a novel approach, MAESPA tiles replaces VTUF-3D ground surfaces with vegetated MAESPA surfaces and use MAESPA's photosynthesis and water cycle routines to modify VTUF-3D's energy balance calculations. Each embedded MAESPA surface calculates a full 3 dimensional tree (along with associated soil and movement of water within the stand) and feeds results back to VTUF-3D ground surface energy balances. Being able to model the soil/water, plant and atmosphere interactions allows the role of water to be quantified in urban areas. The entire cycle of soil moisture to vegetation transpiration and evaporation back to precipitation can be examined for its micro-climatic side effects.

In the following section, the three distinct models will be differentiated in the following way. TUF-3D will refer to the unmodified TUF-3D model. MAESPA is the unmodified MAESPA model. VTUF-3D refers to the modified TUF-3D model, including the extracted functionality from MAESPA, which will be the end product of this design document. The overall process flow of the VTUF-3D model is shown in Figure 7.

TUF-3D unmodified shading logic

In order to understand the changes made to create VTUF-3D, an overview of the previous TUF-3D logic is necessary. TUF-3D sets up a modelling domain by using user specified width/height ratios and calculating a domain of buildings and roads from those. (Other versions exist which allow more control over specific building heights and placements.) Both approaches lead to a basic starting point of building heights and locations. Two dimensional (x,y) locations of building locations are configured along with their heights (Figure 8) and stored in the bldht data object.

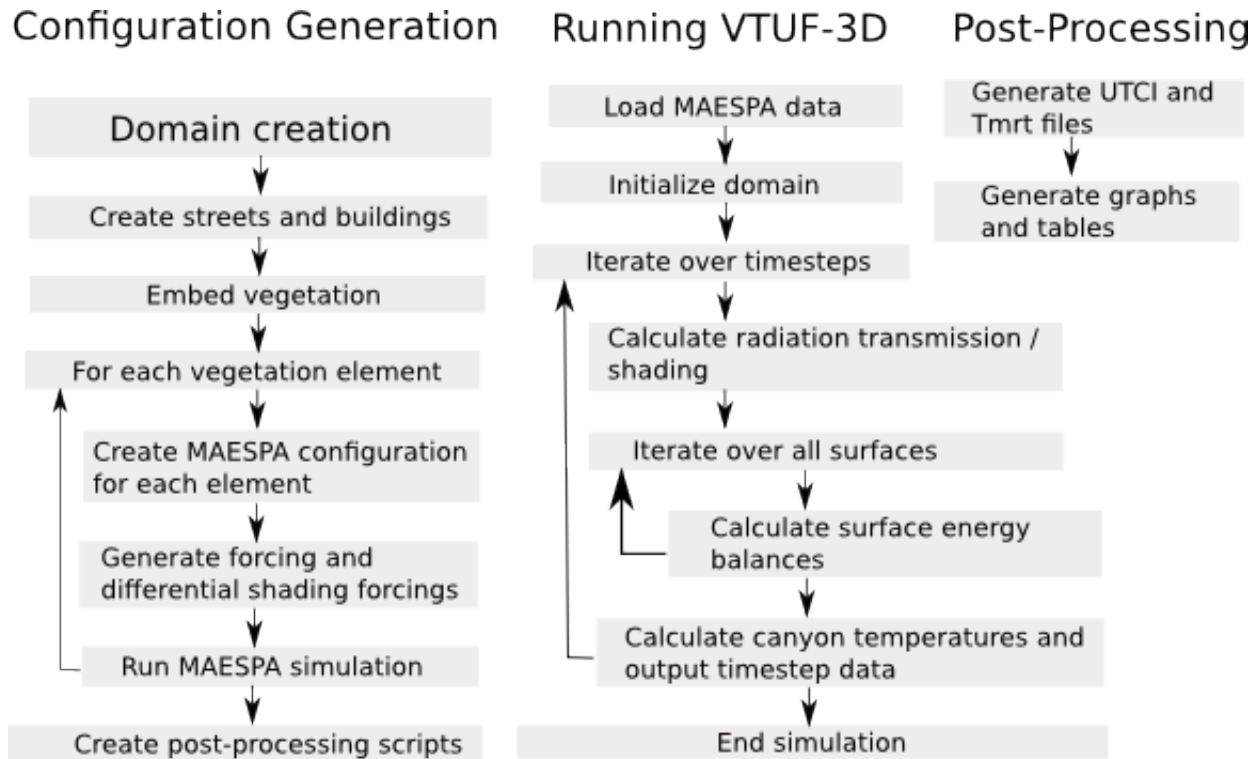


Figure 7: VTUF-3D model process flow

These values are used to calculate zH , mean building height, as in equation (4.1)

$$zH = (\text{patchlen} * \sum_{n=1}^{\text{numHeights}} \text{bldht}) / \text{numRoofs} \quad (4.1)$$

TUF-3D uses forcing data of temperature, humidity, incoming radiation levels, and wind speed and direction from a location at a specified z height (above the canopy). See Appendix (??) for more details. Wind is used in roughness calculations but isn't used to resolve movements around the buildings (as a CFD based model would). This simplification is a design decision trade-off to reduce the complexity of the model and the intensity of computations, while still producing accurate enough results.

The building height values ($bldht$) are then converted into a 3-dimensional (x,y,z) array ($surf_shade$). During the model initialization stage, ray tracing is done (Figure 9) between all the elements of the $surf_shade$ array to determine which surfaces are visible to from each surface. This step reduces the number of radiative interactions of surfaces which will need to be considered throughout the simulation run.

As the model runs a simulation, at each time step, TUF-3D runs a shading routine (Figure 10). In it, the model iterates through each surface in the domain (roads and building walls and roofs) and ray-traces towards the sun. Each of these surfaces are divided into quarters and each of these are ray-traced from the centre of each quarter. If the ray passes to the top of the domain without being obstructed (i.e. surface 4) then 0.25 is added to the shade coefficient for that surface. If the ray is obstructed before reaching the top of the domain (i.e. surface 3), then nothing is added. Each surface has potential values of 0, 0.25, 0.5, 0.75 and 1.0. During the later energy balance step, an appropriate amount of incoming radiation is allocated to this surface based on this coefficient.

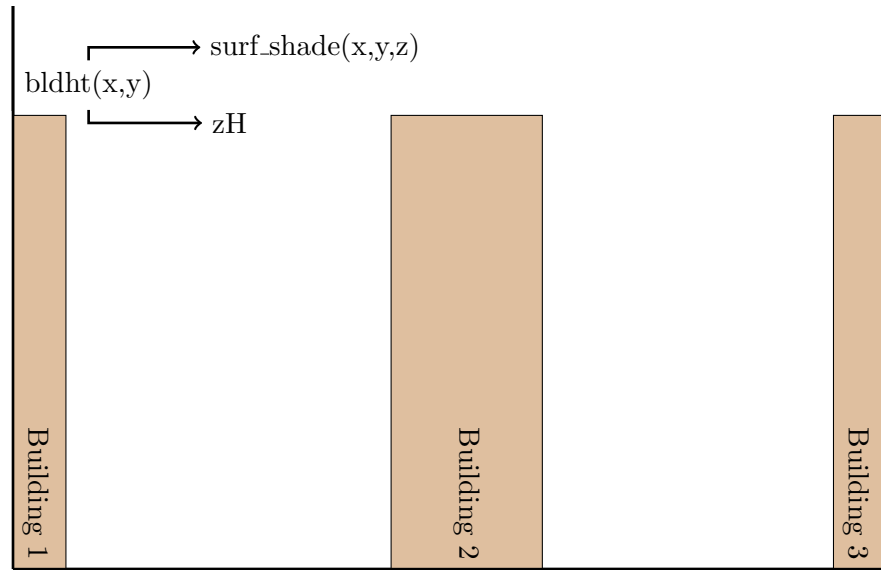


Figure 8: Building height arrays

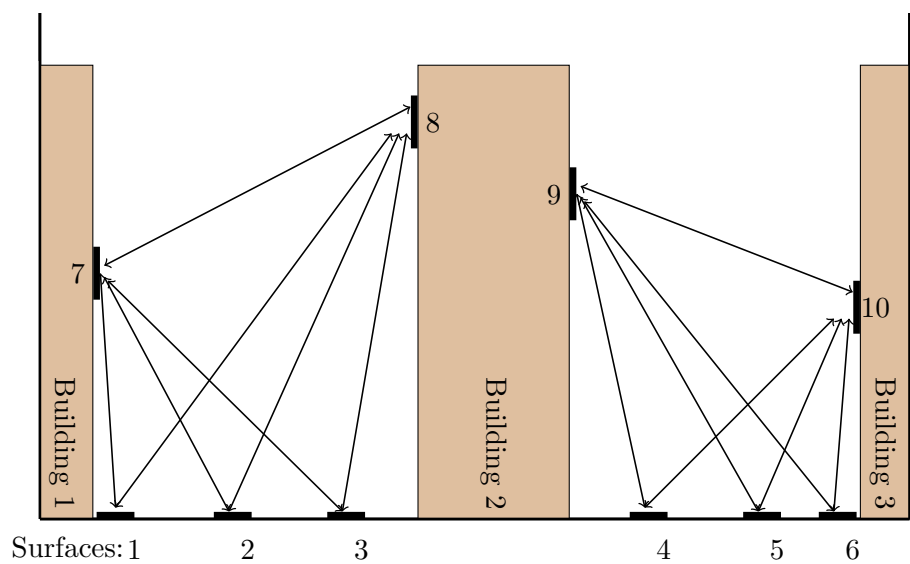


Figure 9: Initial view angles ray tracing

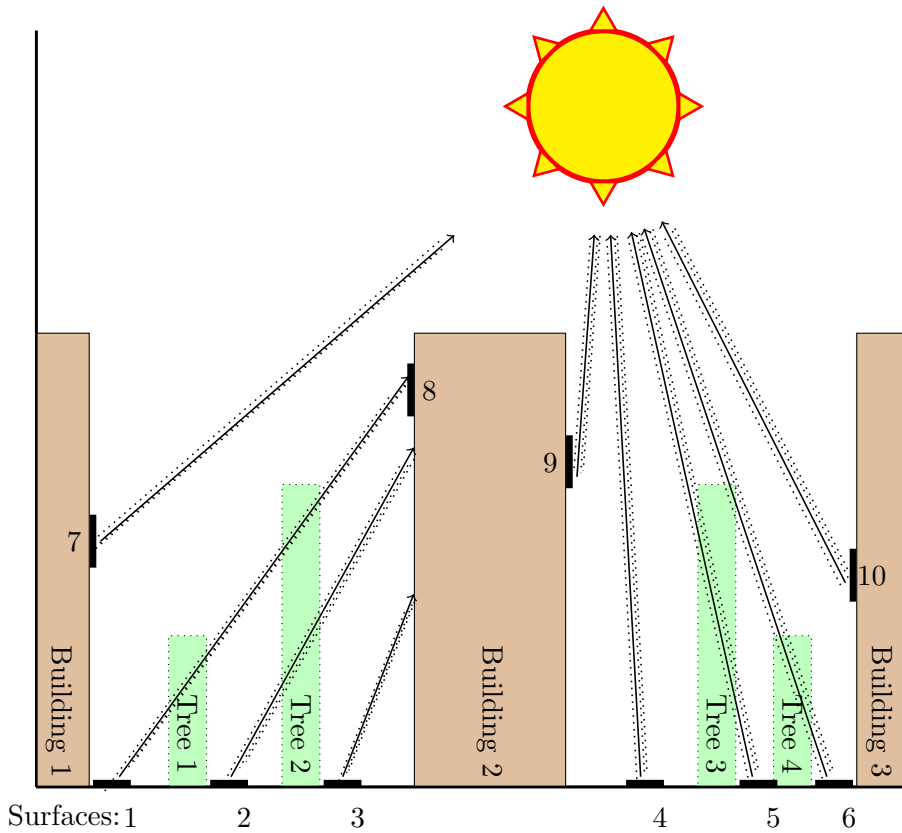


Figure 10: TUF-3D unmodified shading

Integrating vegetation shading and modified ray tracing logic in VTUF-3D

After model improvements to VTUF-3D, a similar parallel logic is used to represent the vegetation in the domain. A new user inputted data structure (the `veght` data structure) is added (Figure 11) to the model configuration. In this, the (x,y) locations of vegetation in the domain are specified along with their heights. As with the buildings, this is converted into a 3-dimensional (x,y,z) vegetation shade data structure (`vegshade`).

The domain initiation method has been modified to read in the configuration information. Previously, in TUF-3D, this method calculated and laid out a grid of buildings and roads based on a width/height ratio. The new modified version now reads in the domain layout directly from configuration files. These configuration files changes will be described in more detail in section (4.1.5).

These vegetation elements are ignored in the initializing ray-tracing (Figure 9). As this data is used to determine which surfaces will never be visible to each other, vegetation, depending on its density, may allow some level of transmission and must be considered on a case by case basis during the simulation run.

At each time step during the simulation, VTUF-3D now runs a modified shading routine (Figure 13). During the model iteration through each surface in the domain, ray-traces towards the sun are done as described previously. However, each step of the ray trace checks to see if vegetation has been encountered. If vegetation is encountered, a vegetation encountered flag is set. Then the ray trace continues and concludes when it either passes out of the domain or is blocked by a building.

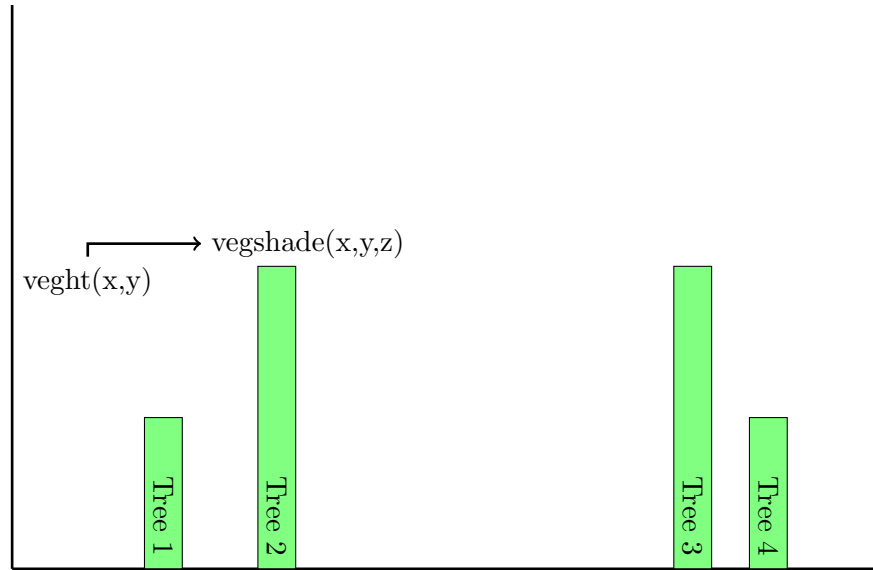


Figure 11: Vegetation height arrays

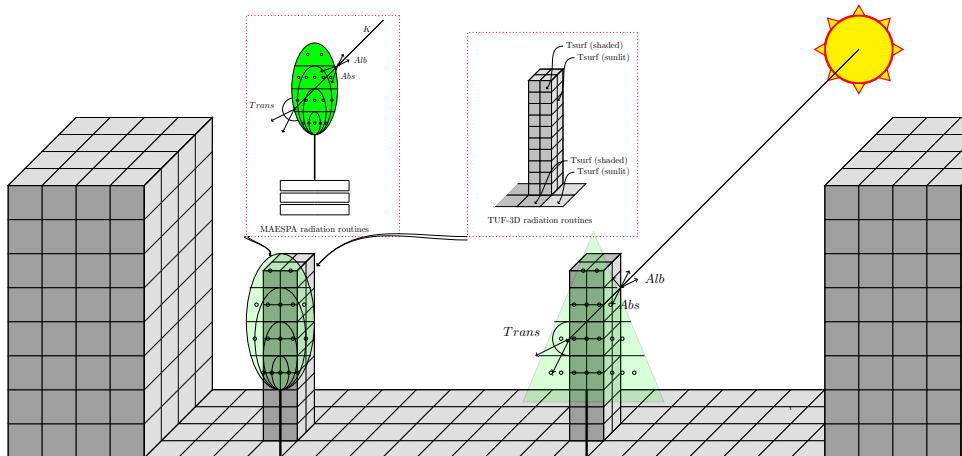


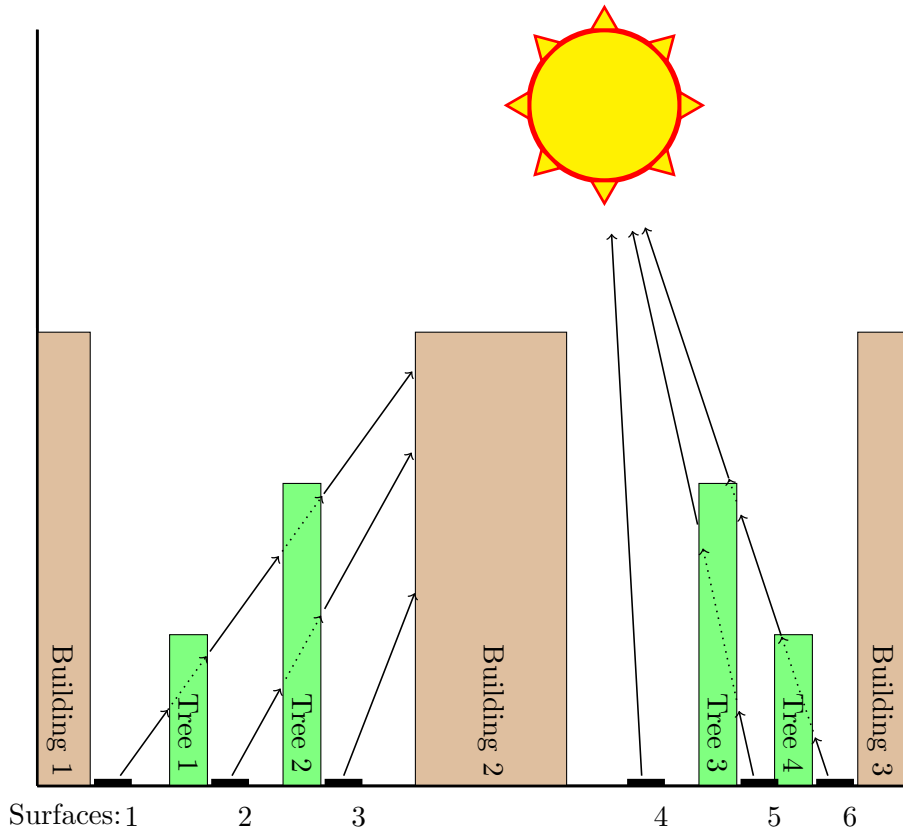
Figure 12: Integration of MAESPA tree model into VTUF-3D radiation fluxes routines

Table (1) summarizes the results for ray tracing the six surfaces of (Figure 13). As with the unmodified shading functionality, if a building is found shading the surface, the shading factor is zero, whether vegetation is encountered or not (surfaces 1, 2, 3, and 8) since no direct sunlight will reach that surface. If no building or vegetation is encountered, the surface receives the full sunlit factor of 1 (surfaces 4, 7, 9 and 10) (or some fraction of that if any of the ray traces from each quarter of the surface encounter an obstructing building). If vegetation is found but the ray leaves the domain otherwise unobstructed, the sunlit factor is currently unknown and requires more processing (surfaces 5 and 6).

To resolve the sunlit factor for surfaces with vegetation, reverse ray tracing is done for those beams (Figure 14). For surfaces 5 and 6, ray tracing is done from the top of the domain back along the radiation path. When the ray encounters vegetation (surface 5 and 6), VTUF-3D looks

Table 1: Ray tracing results

Surface	Sunlit factor	Vegetation in Ray
1	0	True
2	0	True
3	0	False
4	1	False
5	TBD	True
6	TBD	True
7	1	False
8	0	False
9	1	False
10	1	False

**Figure 13:** TUF-3D modified shading, timestep ray tracing

up the tree associated with the ground surface below and calculates the amount of radiation reflected, absorbed, and transmitted through the vegetation (further described in section 4.1.4).

The ray tracing continues, allocating the remaining radiation either to further intercepting vegetation or ultimately to the ground surface. Through this reverse ray tracing process, the problem of zero to many surface interceptions is solved by allocating radiation as it is transmitted from the sun and transmits through the zero to many objects it encounters along its path.

MAESPA vegetation transmission and energy balance functionality overview

MAESPA, as originally designed, allows modelling of a stand of trees or of a single grid square containing a single tree. VTUF-3D uses this functionality from MAESPA in two different ways. The first is MAESPA's calculations of radiation movement through the vegetation canopy. Each tree in the VTUF-3D modelling domain is individually modelled by MAESPA before the main modelling run and then this data is extracted by VTUF-3D and used throughout the simulation. In order to account for inner tree shading or shading by buildings, each tree in the domain is modelled three times, using varied amounts (20%, 60%, and 100%) of incoming shortwave.

The configuration of the individual trees will be described in a following section on modelling configuration (section 4.2.5). Through these shading modifications, VTUF-3D stores states of and represents vegetation through placeholder simple block structures in VTUF-3D (Figure 15), but calculates the underlying processes using their true shapes and types through the MAESPA representation.

VTUF-3D's configuration system has been expanded to allow mapping of individual trees to a (X,Y) location within its domain and to the placeholder vegetation cube and surface structure. These configuration changes (as well as the changes to VTUF-3D configuration) will be further detailed in section (4.1.5). During the simulation run (described in section 4.3), calculated transmission values are used to distribute radiation to the appropriate surfaces during the reverse ray tracing process to determine how much radiation is scattered by the vegetation, radiation absorbed by the vegetation, while the remaining amount of radiation is then distributed to subsequent vegetation, and ultimately to the ground surface at the end of the ray.

The second integration of MAESPA is used in the surface energy balances. Pre-calculated flux amounts for each vegetation element for each time step are loaded at the beginning of the simulation and used to repartition the energy fluxes for those surfaces with vegetation on them. The logic behind this will be described in section 4.3.

VTUF-3D and MAESPA configuration changes

In its unmodified form, TUF-3D is configured by two main user defined files, *parameters.dat* and *forcing.dat*. These files are described in more detail in Appendix (??). *Forcing.dat* supplies meteorological forcing data, including incoming shortwave and longwave, air temperature, and vapour pressure, for the duration of the simulation. *Parameters.dat* sets the main properties of the domain being simulated, such as location, orientation, width/height ratios, albedos and emissivities, and other modelling options. These files remain unmodified in their use in VTUF-3D.

In order to add new functionality and modelling options, new files have been added to the MAESPA configuration process. The normal configuration and usage of the default MAESPA configuration is described in Medlyn & Duursma (2014). To link TUF-3D and MAESPA within VTUF-3D, a new mapping file is introduced, *treemap.dat*. A sample configuration is shown in

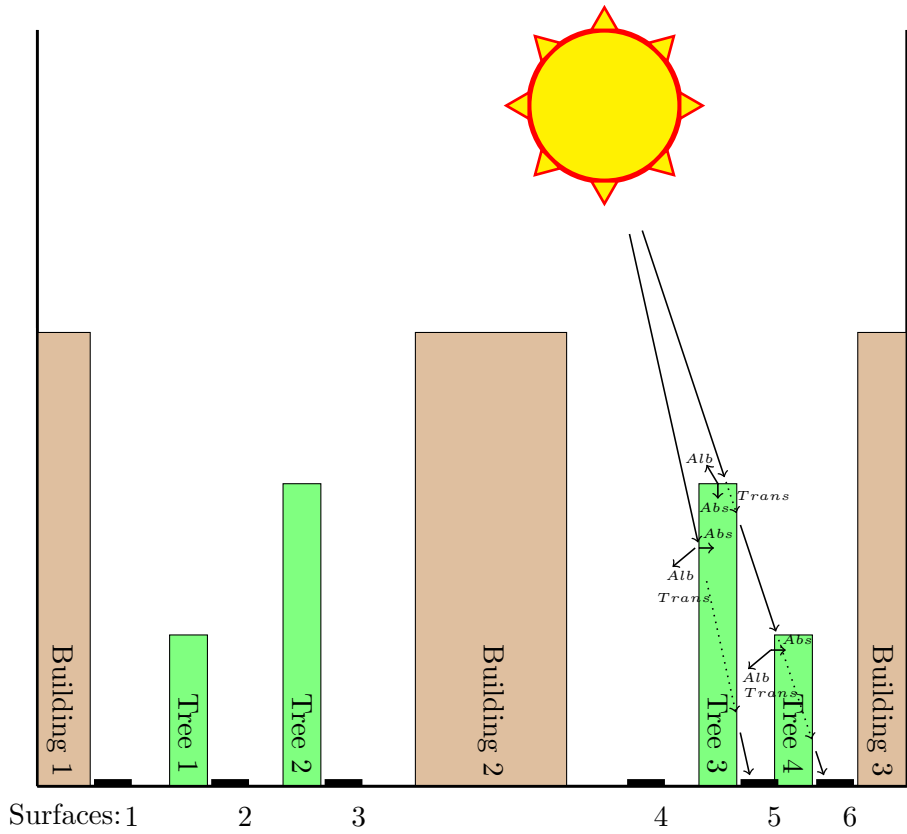


Figure 14: VTUF-3D modified shading, reverse ray tracing

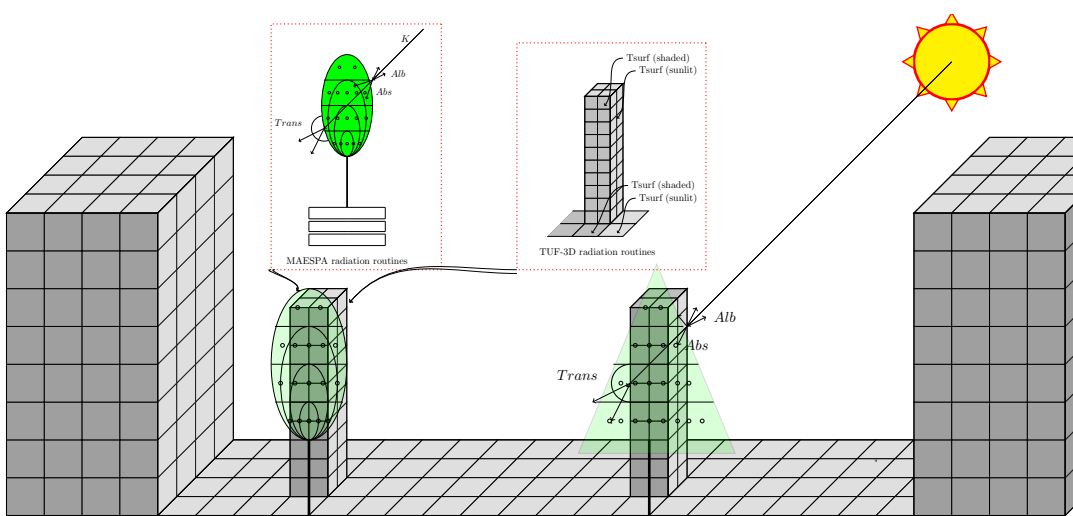


Figure 15: TUF-3D/MAESPA vegetation/radiation interactions

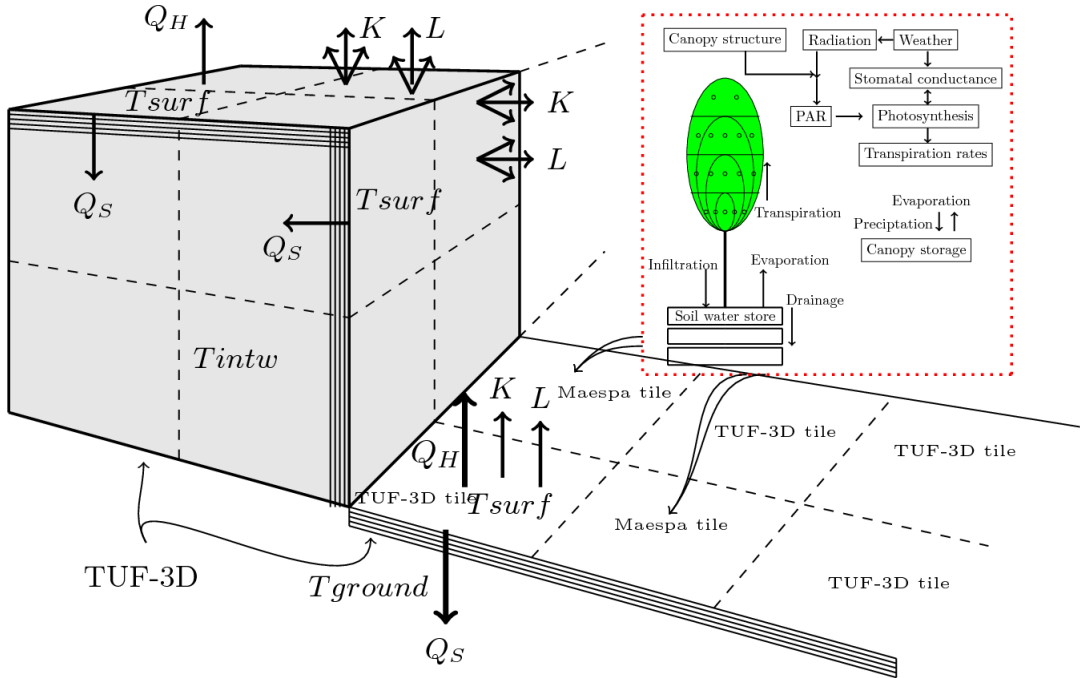


Figure 16: VTUF-3D energy balance modelling with vegetation MAESPA tiles

Appendix (??) and explained in detail in the configuration process (section 4.2.5). All other TUF-3D and MAESPA configuration files remain unchanged from the original models.

4.2 Configuration generation

Overview

In order to simplify the use of the VTUF-3D model, a number of utilities have been created to generate the configuration files needed to run a given simulation. The model will expect to find a number of configuration files and a specific directory structure to organize these files. The general pattern of these directories is:

```
<Run name>
  1
    1 <directory containing MAESPA tree 1, diffuse only>
    2 <directory containing MAESPA tree 1, 50% radiation>
    3 <directory containing MAESPA tree 1, 100% radiation>
  2
    1 <directory containing MAESPA tree 2, diffuse only>
    2 <directory containing MAESPA tree 2, 50% radiation>
    3 <directory containing MAESPA tree 2, 100% radiation>
  3 <tree directories continue sequentially>
    1
    2
    3
```

The overall model configuration, used by CreateMaespaRun, is given in the *messagesConfig.properties* file, setting values for run directory, Julian day start and end, year of run, grid

size in meters, and forcing data source (to be loaded from the appropriate Sqlite database), all referenced by the model run (i.e. "PBBBrush" in the listing below).

```
#PBBBrush
CreateMaespaRunAndProcess . runDirectory . PBBBrush=/home/kerryt/Documentation/Work/
    VTUF-Runs/PrestonBase/PrestonBrushbox
CreateMaespaRunAndProcess . start . PBBBrush=40
CreateMaespaRunAndProcess . end . PBBBrush=70
CreateMaespaRunAndProcess . gridSize . PBBBrush=5
CreateMaespaRunAndProcess . forcing . PBBBrush=Preston
CreateMaespaRunAndProcess . year . PBBBrush=2004
```

Create streets and buildings

As a first step, four comma separated value (CSV) files are read, containing x,y locations and values for building heights, vegetation heights, vegetation types, and a tree map. The heights are multiples of the grid size (i.e. with a 5m grid size, a 10m building's value is 2). Currently, supported vegetation types are:

```
OLIVE_CONFIG_TYPE = 1;
NO_TREE_CONFIG_TYPE = 2; //this is grass
BRUSHBOX_CONFIG_TYPE = 3;
NEW_GRASS_PARAMETERIZATION = 4;
```

All trees in a domain are given individual sequential numbers (i.e. 1, 2, 3, etc.), so they can be modelled separately. If a tree extends into another grid square, the grid square of the trunk is given a positive value while the other grid squares containing the canopy are given negative values (i.e. tree 3 might have neighboring grid square values of 3, -3, and -3). This allows non-vegetative surfaces to be overshadowed by a canopy.

Create post-processing scripts

A number of scripts are created to be used in the post-processing analysis. In this step, a number of Python and R scripts are created. They will be described in more detail in the post processing step (section 4.4).

Domain creation

Using the CSV files loaded in section 4.2.2, the *treemap.dat* file is created (and example given in Appendix ??). In this file, the number of grid spaces with trees is configured in *numberTreePlots*. For each of those tree plots, the *xLocation*, *yLocation*, *phyfileNumber*, *strfileNumber*, *treesfileNumber*, and *treesHeight* are specified. The (X,Y) location specifies its place in the domain.

MAESPA in its original form stores tree properties in the files *phy.dat* (physiology information), *str.dat* (canopy structure), and *trees.dat* (tree characteristics). Using the *treemap.dat* file, VTUF-3D maps each individual tree to its individual configuration and tree information will be loaded from files indexed by *phyX.dat*, *strX.dat*, and *treesX.dat* for each X value mapped in the *treemap.dat* configuration.

A similar structure in *treemap.dat* configures the buildings in the domain. Number of buildings are given in *numberBuildingPlots*. For each of those buildings, the *xBuildingLocation*, *yBuildingLocation*, and *buildingsHeight* are specified. The last domain properties values

specified in *treemap.dat* are the domain size, *width* and *height*, in number of grids in each direction.

The overall configuration for VTUF-3D, *parameter.dat*, is created. An example is shown in Appendix ???. Forcing data is loaded from a Sqlite database. The query for this database brings back the proper set of data for the time period as well as the given location. An example is shown in Appendix ??

MAESPA configurations creation

Each tree is modelled individually using MAESPA, so each of these also need to be configured. The same forcing data is used for each of these as the main modelling run. In order to account for shading of trees by buildings and other trees, each tree is modelled three times using modified forcing data.

The first tree variation uses unmodified forcing data, the incoming radiation set to 100%. The second tree variation uses 60% of the radiation from the forcing data. The final tree variation 20% direct radiation. This final value was derived from an average from a survey of mid-day shaded sites (Coutts 2015c). Each of these variations are put into the directory structure shown in section 4.2.1.

Currently, three tree parametrizations are available, *Olea europaea*, *Lophostemon Confertus*, and grass. Using the templates of parameters described below, configurations of *str.dat* (tree structure parameters), *phy.dat* (physiological parameters), and *tree.dat* (general tree parameters) are created. Some calculations are done to scale some parameters (crown radius, crown height, trunk height, stem diameter, and total leaf area) based on the grid size and user supplied tree height.

Stem diameter is calculated using the relationships described by Buba (2013) and Sumida et al. (2013). If the trunk height plus canopy height is greater than 7m, then stem diameter is calculated in equation (4.2) as:

$$stemDiam = ((trunkHeight + crownHeight) - 6.74) / 14.4 \quad (4.2)$$

Tree physical parameter templates (shown below) are based on a 5m tree. Using the modelled height, the parameters will be scaled according to the logic below. MAESPA uses total leaf area per tree as modelling input, so total leaf area per tree is calculated (in equation 4.4) using the scaled tree canopy dimensions (equation 4.3) and leaf area index of the specified species. These specific values for each species will be detailed in the following section (4.2.6).

$$canopyArea = (crownRadiusX * crownRadiusY) * 3.1415; \quad (4.3)$$

$$totalLeafArea = leafAreaIndex * canopyArea \quad (4.4)$$

MAESPA tree parameterizations

As all tree parametrizations in VTUF-3D are pluggable, individual trees are added to a domain using a specific set of configuration files with many of the physical properties scaled from a base template. All parametrizations share some common attributes summarized in Table 2.

Table 2: MAESPA tree parameterizations common attributes

Parameter	Value
Stomatal conductance	Ball-Berry-Opti model (Medlyn et al. 2011)
Number of layers in the crown assumed when calculating radiation interception	6
Number of points per layer	12
Number of zenith angles for which diffuse transmittances are calculated	5
Number of azimuth angles for which the calculation is done	11

4.2.6.1 MAESPA olive tree (*Olea europaea*) parameterization The first complete parameterization for VTUF-3D is the olive tree (*Olea europaea*). The physical and meteorological parameters for a 5x5 meter grid square are given in Table 3. The configuration scripts will re-scale these parameters for a given modelling domain grid size. The specific physiological parameters for this species are given in Table 4 and are used to generate the appropriate *trees.dat*, *str.dat* and *phy.dat* for each olive tree in the domain.

Table 3: MAESPA olive tree (*Olea europaea*) parameterization, tree dimensions for 5x5m grid (rescale for taller/shorter), values adapted from Coutts (2014)

Parameter	Value
crown radius (m)	2.5
crown height (m)	3.75
trunk height (m)	1.25
leaf area index	2.48
crown shape	round
zht (m)	4.0
zpd (m)	1.6
z0ht (m)	3.0

4.2.6.2 MAESPA brushbox tree (*Lophostemon Confertus*) parameterization The second complete parameterization for VTUF-3D is the brushbox tree (*Lophostemon Confertus*). The physical and meteorological parameters for a 5x5 meter grid square are given in Table 5. The configuration scripts will re-scale these parameters for a given modelling domain grid size. The specific physiological parameters for this species are given in Table 6 and are used to generate the appropriate *trees.dat*, *str.dat* and *phy.dat* for each brushbox tree in the domain.

Table 4: MAESPA olive tree (*Olea europaea*) parameterization

Parameter	Value(s)	Source
Leaf reflectance (%PAR, %NIR and %IR)	0.082, 0.49, 0.05	Baldini et al. (1997)
Minimum stomatal conductance g_0 (mol/m ² s)	0.0213	Coutts (2014)
Slope parameter g_1	3.018	Coutts (2014)
# of sides of the leaf with Stomata	2	
Width of leaf (m)	0.0102	
CO ₂ compensation point (μmol/m ² s)	46	Sierra (2012); 56=Coutts (2014)
Max rate electron transport (μmol/m ² s)	135.5	135.5=Sierra (2012); 134=Coutts (2014)
Max rate rubisco activity (μmol/m ² s)	82.7	82.7=Sierra (2012); 94=Coutts (2014)
Curvature of the light response curve	0.9	Sierra (2012)
Activation energy of Jmax (kJ/mol)	35350	Díaz-Espejo et al. (2006)
Deactivation energy of Jmax (J/mol)	200000	Medlyn et al. (2005)
XX Entropy term (kJ/mol)	644.4338	
Quantum yield of electron transport (mol electrons/mol)	0.2	
Dark respiration (μmol/m ² s)	1.12	Sierra (2012); 1.79=Coutts (2014)
Specific leaf area	5.1	3.65=Villalobos et al. (1995); 5.1=Marise et al. (2000)

Table 5: MAESPA brushbox tree (*Lophostemon Confertus*) parameterization, tree dimensions for 5x5m grid (rescale for taller/shorter), values adapted from Coutts (2015b)

Parameter	Value
crown radius (m)	2.5
crown height (m)	3.75
trunk height (m)	1.25
leaf area index	2.0
crown shape	round
zht (m)	4.0
zpd (m)	1.6
z0ht (m)	3.0

4.2.6.3 MAESPA grass parameterization The third complete parameterization for VTUF-3D is for grass. This parameterization is a adaptation of the normal MAESPA tree parameterizations. In it, the vegetation is modelled as a box shaped canopy with a crown height of 0.2 meters. This and the rest of the physical and meteorological parameters for a 5x5 meter grid square are given in Table 7. The configuration scripts will re-scale these parameters for a given modelling domain grid size. The specific physiological parameters for this species are given in Table 8 and are used to generate the appropriate *trees.dat*, *str.dat* and *phy.dat* for each grass grid square in the domain.

Table 6: MAESPA brushbox tree (*Lophostemon Confertus*) parameterization

Parameter	Value(s)	Source
Leaf reflectance (%PAR, %NIR and %IR)	0.04, 0.35, 0.05	Fung-yan (1999)
Minimum stomatal conductance g_0 (mol/m ² s)	0.01	Coutts (2015b)
Slope parameter g_1	3.33	Coutts (2015b)
# of sides of the leaf with Stomata	1	Beardsell & Considine (1987)
Width of leaf (m)	0.05	
CO ₂ compensation point (μmol/m ² s)	53.06	Coutts (2015b)
Max rate electron transport (μmol/m ² s)	105.76	Coutts (2015b)
Max rate rubisco activity (μmol/m ² s)	81.6	Coutts (2015b)
Curvature of the light response curve	0.61	Coutts (2015b)
Activation energy of Jmax (kJ/mol)	35350	Bernacchi et al. (2001)
Deactivation energy of Jmax (J/mol)	200000	Medlyn et al. (2005)
XX Entropy term (kJ/mol)	644.4338	
Quantum yield of electron transport (mol electrons/mol)	0.06	Coutts (2015b)
Dark respiration (μmol/m ² s)	1.29	Coutts (2015b)
Specific leaf area	25.3	Wright & Westoby (2000)

Table 7: MAESPA grass layer as a box tree on the ground covering the plot area, values adapted from Coutts (2015a)

Parameter	Value	Source
crown radius (m)	2.5	
crown height (m)	0.2	Simmons et al. (2011)
trunk height (m)	0.01	
stem diameter (m)	0.2	
leaf area index	7.13	ave from Bijoor et al. (2014)
crown shape	box	
zht (m)	4.0	
zpd (m)	0.066	
z0ht (m)	0.02	

The final piece of configuration to generate is the MAESPA *points.dat* files. The use of these is described in section 4.3.4.

The final step in configuration generation is to run each of the MAESPA instances over the period being modelled. This data will then be available for use during the VTUF-3D run.

4.3 Running VTUF-3D

Overview of changes in TUF-3D

There are two major integration points within the newly changed VTUF-3D model. These are in the radiation distribution logic and in the surface energy balance routines. The first item will read vegetation transmission data from MAESPA and use it in the distribution of shortwave radiation and calculation of shading effects. The second item will use MAESPA predictions of latent energy fluxes and water evaporation and vegetation transpiration and use

Table 8: MAESPA grass layer as a box tree on the ground covering the plot area

Parameter	Value(s)	Source
Soil reflectance (%PAR, %NIR and %IR)	0.10 0.05 0.05	Observed, Levinson et al. (2007), Oke (1987)
Leaf transmittance (%PAR, %NIR and %IR)	0.01 0.28 0.01	Olive: Baldini et al. (1997) (Adaxial side of leaf)
Leaf reflectance (%PAR, %NIR and %IR)	0.05 0.42 0.08	Olive: Baldini et al. (1997) (Adaxial side of leaf)
Minimum stomatal conductance g0 (mol/m ² s)	0.0	De Kauwe et al. (2015)
Slope parameter g1	5.25	C3 grasses, from De Kauwe et al. (2015)
# of sides of the leaf with Stomata	2	
Width of leaf (m)	0.006	Rademacher & Nelson (2001)
CO ₂ compensation point (μmol/m ² s)	57	Brown & Morgan (1980) @ 25 degrees
Max rate electron transport (μmol/m ² s)	80.95	Tall Fescue from Yu et al. (2012))
Max rate rubisco activity (μmol/m ² s)	36.14	Tall Fescue from Yu et al. (2012))
Curvature of the light response curve	0.9	
Activation energy of Jmax (KJ/mol)	35350	Bernacchi et al. (2001)
Deactivation energy of Jmax (J/mol)	200000	Medlyn et al. (2005)
XX Entropy term (KJ/mol)	644.4338	
Quantum yield of electron transport (mol electrons/mol)	0.19	PAR curves; PSICO2=Absorb*8*0.5
Dark respiration (μmol/m ² s)	0.6	Estimated for Tall Fescue from Yu et al. (2012)
Specific leaf area	23.16	Average from Table 1 in Bijoor et al. (2014) for 3 turfgrasses.

these values to re-partition energy fluxes on those surfaces which contain vegetation. Also, surface temperatures of those surfaces will use values from MAESPA.

MAESPA energy flux conversions

As MAESPA outputs hourly transpiration in units of *mm*, they must be converted to w/m² of latent energy, there is a conversion step required using the 2-dimensional area of the tree and the time duration of each timestep (equation 4.5).

$$et_{w/m_2} = et * A_{mm} * 18.0152g/mol * \Delta H_{vap} * 1W/1000KJ/sec * Time \quad (4.5)$$

where *et* is mm of evapotranspiration, *A_{mm}* is the 2-dimensional tree area in mm, *Time* in seconds, ΔH_{vap} is the heat of vaporization of water (equal to 40.7KJ/mol), and 18.0152 is taken from 18.0152g/mol of water.

Loading MAESPA data

As the VTUF-3D model initializes, it loads all of the generated MAESPA data for all the trees and all the different shading configurations. Three main MAESPA output files are accessed for each tree (and their 20%, 60%, and 100% incoming radiation variations).

The first set of these is loaded when `readMaespaTestData()` is called. For each `testflx.dat` output file (output for calculations of PAR transmission to user-defined xyz points) the `TD` variable (relative diffuse transmission (0-1)) is read for each hour of the simulation. During the VTUF-3D simulation, these values will be used to allocate the transmission of shortwave radiation through the tree canopies and determine the amount of radiation reaching the surfaces beyond them.

The second set of data, used for energy flux and energy balance calculations, is loaded from the `watbal.dat` (water balance calculations for each timestep) and `hrflux.dat` (hourly flux files, contains all flux estimates for each target tree for each timestep) files. The variables used from these files are shown in Table 9.

Table 9: MAESPA variables loaded

Variable	Description	Units
canopystore	storage of intercepted rain	mm
evapstore	evaporation of wet canopy	mm
soilevap	soil evaporation	mm
et	modelled canopy transpiration	mm
Tcan	Average foliage temperature	degrees C

After loading, the amount of Q_e is calculated using equation 4.6.

$$Q_e = (et + soilevap + canopystore + evapstore)/a_{tree} \quad (4.6)$$

where a_{tree} is the 2-dimensional area of the tree in mm and et , $soilevap$, $canopystore$, $evapstore$ are calculated using the conversion in equation 4.5

Radiation transmission in Maespa

Calculations of radiation transmission use the test points functionality from MAESPA. This allows modelling of PAR transmissions to user-defined xyz points within the tree canopy. The xyz point used to calculate transmission through the tree is half of the grid size (i.e. 2.5 for a 5m grid) and 0.1m to be at the bottom of the tree. This is configured in the `points.dat` configuration file by setting `XYZCOORDS` to '2.5 2.5 0.1' and setting `NOPOINTS` and `INPUTTYPE` to '1'.

The method `getDataForTimeAndDayAndPoint()` in the VTUF-3D `reverseRayTrace()` method reads the hourly output of the test points, the `testflx.dat` data file using the TD, diffuse transmittance to grid point (fraction), value.

VTUF-3D use of Maespa shading values

For each surface, VTUF-3D ray traces four rays (each surface is split into quarters) to the sun. As described in section 4.1.3, if vegetation is found in a ray trace from the surface towards the sun, then a flag is set to also perform a reverse ray trace from the sun back to the surface. The return value from this function is the transmission percentage (0 to 100%) for that ray. Overall then, the sunlit factor for each surface will then be the addition of those four rays, ranging from 0.0 to 4.0, corresponding giving a range of 0 to 100% illuminated. The value then is later divided by 4 when it is used to allocate energy transmissions.

The logic to allocate radiation to vegetation surfaces and surfaces shaded by vegetation uses a reverse ray trace from the top of the domain (coming from the sun) to the ground surface. As vegetation is encountered, `getDataForTimeAndDayAndPoint()` is called to read the transmission value for that tree (calculated using the `points.dat` functionality of MAESPA) and reduce the ray strength by that percentage. Tracing continues through any additional vegetation, eventually reaching the ground and allocating the remaining amount of direct shortwave to the ground surface.

VTUF-3D use of Maespa differential shading values

In order to account for vegetation shaded by buildings and other vegetation, VTUF-3D uses a differential shading scheme to choose the appropriate MAESPA data throughout a simulation. Creation of MAESPA configurations for each tree creates three different model runs with differing forcing data. The incoming shortwave is varied in three different ways. The first uses 100% values. The second reduces incoming shortwave to 60%. The third uses 20% incoming shortwave. These percentages are based on observations of incoming shortwave at shaded locations (Coutts 2015c)

Two data structures, `treeXYMapSunlightPercentageTotal` and `treeXYMapSunlightPercentagePoints` are used to keep track of the amount of direct radiation hitting each tree. This is calculated in `reverseRay()`, as described in section 4.3.5. When a ray trace finds vegetation, the total for the tree at coordinates x,y is increased by the `finalTransmissionPercentage`. `FinalTransmissionPercentage` is the cumulative percentage of the incoming shortwave radiation beam, accounting for possible shading of buildings or other trees. If this beam had previously encountered other vegetation, its current value will be decreased by the new transmission percentage. Also, the number of Points is increased by 1.

Once these values are set for each timestep for each tree for each surface which potentially could be sunlit, the ratio of `treeXYMapSunlightPercentageTotal` to `treeXYMapSunlightPercentagePoints` determines which forcing configuration (20%, 60%, or 100% shortwave radiation forcing values) to use during the energy balance partitioning of each ground surface (section 4.3.8). If the ratio is greater than 0.75, the 100% shortwave radiation configuration is used. If the ratio is between 0.75 and 0.25, the 60% configuration is used. Otherwise, the 20% configuration is used.

Adding physiological vegetation processes

At the conclusion of each timestep, the unmodified TUF-3D model calculates the energy balance of each surface. Incoming radiation energy and existing stored energy is partitioned into new values of storage and radiated heat. In order to account for the addition of vegetation, these energy balances have been modified to account for latent energy fluxes and the physiological processes of vegetation. In VTUF-3D, a variable for latent energy is added and energy allocated to it from the pool of available energy. The vegetation is treated as a flat two dimensional ground surface tile.

This is done by tiling multiple instances of MAESPA (each individual tree with its unique configuration) into surfaces which have vegetation (Figure 17). These instances have calculated, in three dimensions using the canopy structure, radiation transmission, energy fluxes, and soil and soil water storage for each individual tree.

If a surface does not contain vegetation, VTUF-3D runs its normal energy balance calculations. If a surface does contain vegetation, VTUF-3D loads the pre-calculated fluxes (in section 4.3).

The tiling is structured by the *treemap.dat* configuration file (section 4.3.3). This file maps an X,Y grid location to its unique tree configurations, properties, and characteristics.

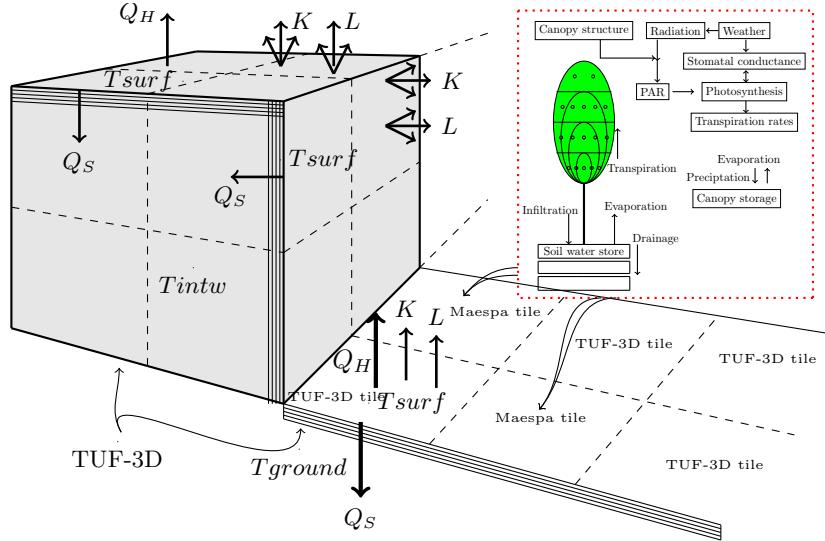


Figure 17: TUF-3D energy balance modelling with MAESPA tiles

Energy balance partitioning during simulation timesteps

As the simulation proceeds through each time step, an energy balance is performed on each surface. For each surface with vegetation, the surface temperature ($T_{sf c}$) is set to the value calculated by MAESPA for that tree. The following describe the differences from the normal calculations the unmodified TUF-3D uses to calculate the energy balances needed by VTUF-3D to partition the energy fluxes of a vegetated surface.

For net radiation (Q_*), the $Q_{*prelim}$ value for that surface would have previously be calculated (equation 4.7) before the partitioning calculations using the albedo and emissivity of the vegetation, where the α_{veg} of vegetation is set to 0.20 and and ϵ_{veg} of vegetation set to 0.97 (Oke 1987, p. 12), instead of the TUF-3D asphalt surface values .

$$Q_{*prelim} = K \downarrow - (\alpha_{veg} K \downarrow) + \epsilon_{veg} L \downarrow \quad (4.7)$$

The calculation of upwelling longwave, which has been deferred until the partitioning, and its subtraction from the pool of net energy will complete the calculation of Q_* (equation 4.8).

$$Q_{*veg} = Q_{*prelim} - \epsilon_{veg} \sigma T_{sf c_{veg}}^4 \quad (4.8)$$

where $Q_{*prelim}$ is the net radiation calculated in equation 4.7, ϵ_{veg} is set to 0.97, σ is the Stefan-Boltzmann constant, and $T_{sf c_{veg}}$ is the vegetation surface temperature. The two differences between vegetated and non-vegetated calculations are the albedos, emissivities, the source of the surface temperatures.

For sensible heat fluxes (Q_h), vegetation is accounted for differently by using the $T_{sf c}$ of the vegetation instead of the TUF-3D $T_{sf c}$ value (equation 4.9). will yield a different result using the MAESPA vegetation $T_{sf c}$ than if the TUF-3D surface temperature had been used.

$$Q_{h_{veg}} = h_i * (T_{sf c_{veg}} - T_{conv}) \quad (4.9)$$

where h_i is the previously calculated heat transfer coefficient, $Tsf c_{veg}$ is the vegetation surface temperature and T_{conv} is the converging canyon temperature.

For latent energy fluxes (Qe), which is a new variable added to VTUF-3D (equation 4.10).

$$Qe_{veg} = Qe_{MAESPA} \quad (4.10)$$

where Qe_{MAESPA} is the value for the grid square calculated in the MAESPA tree calculations, loaded from the MAESPA data, and using the conversion in equation 4.6.

Finally, ground storage fluxes (Qg) will be calculated as a residual of $Rnet - Qh - Qe$ (equation 4.11) instead of the normal TUF-3D method (equation 4.12) to calculate the street ground storage fluxes..

$$Qg_{veg} = Q *_{veg} - Qh_{veg} - Qe_{veg} \quad (4.11)$$

$$Qg_{street} = k_1 * (Tsf c - T_1) * 2/T_m \quad (4.12)$$

where k_1 is the thermal conductivity of the surface, T_1 is the temperature of the shallowest layer, and T_m is the temperature of the deepest layer

4.4 VTUF-3D Post-processing

In order to complete analysis of a simulation, and to provide additional output not built into the VTUF-3D model, a number of additional scripts are available. These scripts are generated during the configuration generation with characteristics specific to each scenario. These include:

- TUF_ave_graphs.R, used to generates figures for 30 day hourly averages of the $Q*$, Qh , Qe , and Qg fluxes. If applicable, (the run uses Preston forcing data), these fluxes will be compared to observation fluxes.
- TUF_Graphs.R is used to generate numerous figures of every item in the output.
- GenerateUTCIFiles.py is used to read the VTUF-3D output (and forcing data input) and generate UTCI and Tmrt data for each surface in each time step.
- MatlabPatchesPlot3.py is used to create 3D figures of Tsfc predictions. If applicable, (the run uses City of Melbourne Gipps and George St. or Lincoln Square data), points will be annotated on these figures with observation data.
- MatlabPatchesPlot4.py is the same as MatlabPatchesPlot3.py but plots UTCI predictions.
- MatlabPatchesPlot6.py is used to generate 30 day hourly aggregates of predicted VTUF-3D points vs. observations.
- MatlabPatchesPlot8.py is used to create ground level z-slices for each time step of UTCI, Tmrt, and Tsfc predictions.
- UTCI.py is the utility script used by the other scripts to calculate Tmrt and UTCI values.
- TUF_EnergyClosure_graph.R is used to look at the 30 day $Q* - Qh - Qe - Qg = 0$ values to ensure that the model is conserving energy and achieving energy closure.

Tmrt and UTCI

VTUF-3D provides output of downward and upward shortwave and Tsfc for each surface at each time step. Using these and values of air temperature, wind speed, vapor pressure from the forcing data, the values for Tmrt and UTCI are calculated for each surface.

The calculation of relative humidity is completed using a form of the Clausius-Clapeyron equation (equation 4.13):

$$rh = 100 \cdot ea / (Po \cdot e^{-H/R \cdot T}) \quad (4.13)$$

where ea is the vapor pressure (read from the forcing data), Po the vapor pressure of water at infinite temperature (7.5152×10^8), H is the enthalpy of evaporation (42809 J/mol), R is the ideal gas constant (8.314 J/Kmol), T is the temperature in Kelvin

Calculations of mean radiant temperature $Tmrt$ use a slightly modified version of the Thorsson et al. (2007) scheme. The first step is the calculation of the mean radiant flux density (S_{str}) in equation 4.14:

$$S_{str} = \alpha_k(k \downarrow \cdot 0.5 + k \uparrow \cdot 0.5) + \epsilon_p(l \downarrow \cdot 0.5 + l \uparrow \cdot 0.5) \quad (4.14)$$

where ϵ_p , the emissivity of the human body (0.97), α_k , the absorption coefficient for short-wave radiation (0.7), and the summation of the products of the six angular factors and shortwave and longwave up and down fluxes ($k \uparrow, l \uparrow, k \downarrow, l \downarrow$) have been simplified to a single up and down angular factor of 0.5.

Then, in the second step, the $Tmrt$ is calculated in equation 4.15:

$$Tmrt = \sqrt[4]{S_{str}/(\epsilon_p \sigma)} - 273.15 \quad (4.15)$$

where σ = the Stefan-Boltzmann constant ($5.67 \times 10^{-8} \text{ W m}^{-2} \text{ K}^{-4}$)

Finally, the UTCI for each surface is calculated in equation 4.16

$$UTCI = f(Ta, ws, rh, Tmrt) \quad (4.16)$$

generating a UTCI value for each surface, using input of Ta , air temperature (read from forcing data), ws , wind speed (read from forcing data), rh , relative humidity, and $Tmrt$, mean radiant temperature, calculated using the Bröde et al. (2009) UTCI formula.

Design conclusions

TODO Using the loading data, running, post processing, all the changes, blah blah, VTUF-3D does accounts for latent energy and vegetation and works

5 Validation and assessment of improved performance of the VTUF-3D model to model urban areas

5.1 VTUF-3D Validation Details

Overview of validation process

In order to ensure VTUF-3D can make accurate predictions, an extensive validation process was undertaken. A variety of observation data sets allowed validations of a number of different aspects of the model. A validation matrix (Table 10) details the specific validations for each data set. These include validations against observations of air temperature (Ta) and canopy temperatures (Tcan), UTCI human thermal index observations (which include Tmrt observations), evapotranspiration (ET) and tree physiological observations, and flux (energy balance) observations.

Items in table cells colored green have completed validation. Those cells colored yellow are still in progress. Cells colored red have not been started and are still awaiting the observations to be finalized.

Table 10: VTUF-3D validation matrix

Scenario	Ta	Tcan	UTCI	ET	Energy balance
Preston (Coutts et al. 2007)					
Gipps/George St, Melbourne (Coutts et al. 2015)	Yellow	Yellow	Green		
Lincoln Sq, Melbourne (Motazedian 2015)	Yellow		Green		
Hughesdale				Red	
Smith St, Melbourne (Gebert et al. 2012)		Red		Red	

Model testing and validation using Preston dataset

Validations using the Preston data set were undertaken. Preston is a homogeneous, medium density suburb in the northern part of Melbourne, Australia. The data set contains complete flux observations recorded 2003-2004 (Coutts et al. 2007) from a 30 meter flux tower, allowing validation of surface energy balances against modelled predictions.

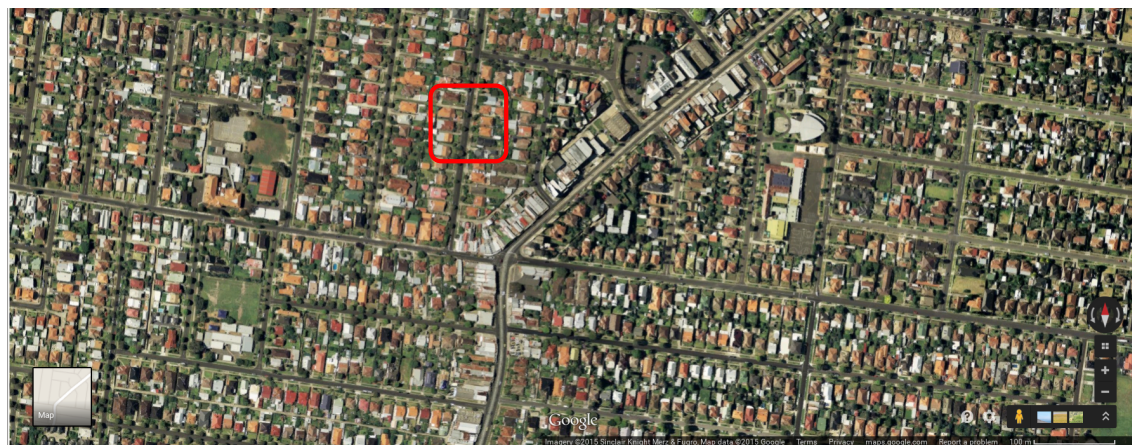


Figure 18: Preston suburb and modelled area (Google 2015)

The modelled area (500x500m, Figure 19) was chosen to be representative of the overall area observed by flux tower. The mix of vegetation types modelled (Figure 21), consisting of grass

(18.5%), olive (*Olea europaea*) and brushbox (*Lophostemon Confertus*) trees (7.25%), match closely to published values for data set. Modelled building densities (Figure 20), consisting of 46.75% buildings and 27.5% impervious surfaces, also match closely to published data set values. Domain resolution is 5m grids.

ADD IN ANDY'S Values for Preston

Buildings Road Concrete Trees Grass Water Total IMP Total VEG 251266 161687 109594 79686
 183496 0 785729 PRESTON 500m radius EXPERT 44.0 13.0 3.0 29.0 11.0 0.0 60.0 40.0
 MANUAL 45.0 13.0 6.0 16.0 19.0 1.0 64.0 36.0 AVERAGE (Coutts et al 2007) 44.5 13.0 4.5
 22.5 15.0 0.5 62.0 38.0 NURY 32.0 20.6 13.9 10.1 23.4 0 66.5 33.5 34.5 Difference from Nury

KERRY NICE MODEL AREA NICE (5m resolution model) 46.75 27.5 7.25 18.5 74.3 25.8 NICE
 (from nury 1 m res) 3848 1408 1874 791 2416 10337 NICE (from nury 1 m res) NICE (from
 nury 1 m res) 21.7 21.7 0.0



Figure 19: Digitization of Preston suburban street. (1=building heights, green=vegetation heights)

30 days of simulation were run between the dates 10 February 2004 and 10 March 2004, forced by the observations for those days. Individual fluxes (R_{net} , Q_h , Q_g , K_{dn} , and Q_e) were aggregated into hourly averages over the 30 days and compared to the observations (Figure 24).

A number of partitioning schemes were considered during the model development. The following schemes are described in Table 11 and overall error performance shown in Figure 22 and Figure 23.

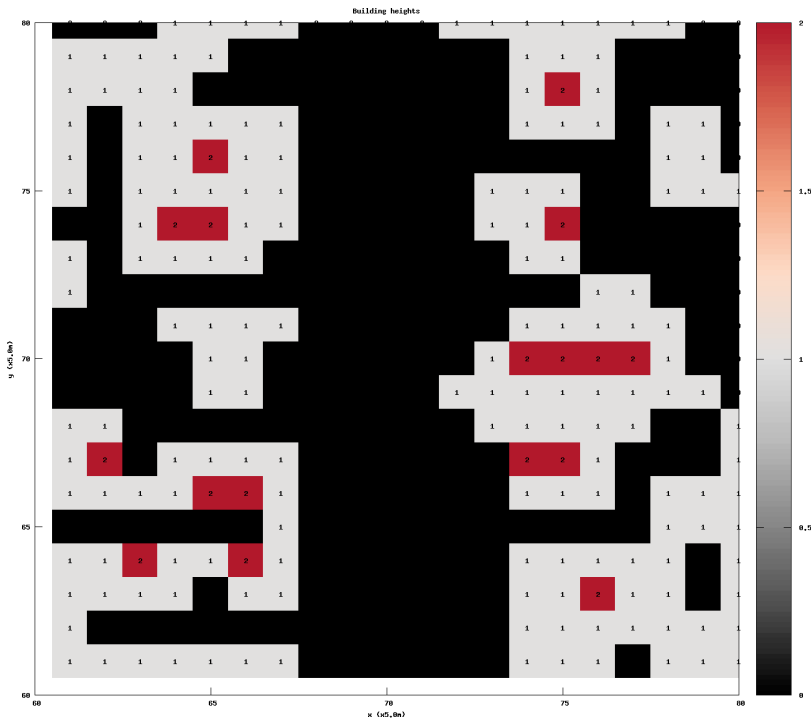


Figure 20: Building heights (0, 5, 10m)

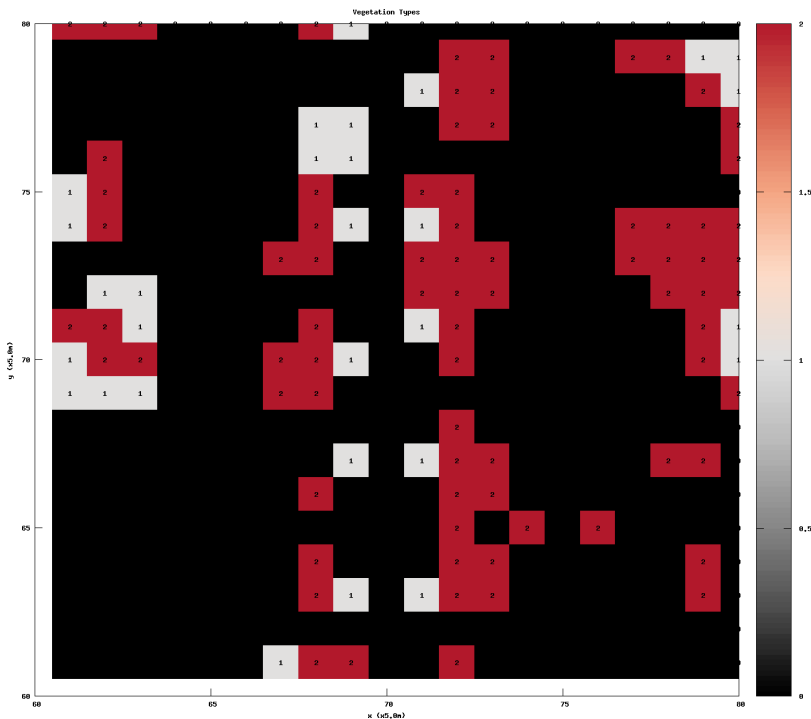


Figure 21: Vegetation heights (0, 5, 10m)

Table 11: Preston simulations compared

Name	Description
PrestonBaseNoVeg1	Baseline no-vegetation simulation showing unimproved VTUF-3D
IntercomparisonMax	Grimmond et al. (2010) intercomparison performance maximum (using Grimmond & Oke (1999) VL92 dataset)
IntercomparisonMin	Grimmond et al. (2010) intercomparison performance minimum (using Grimmond & Oke (1999) VL92 dataset)
IntercomparisonMean	Grimmond et al. (2010) intercomparison performance mean (using Grimmond & Oke (1999) VL92 dataset)
PrestonBase6	Section 4.3.8 scheme and Q_e equation 4.6 (divide by tree area) using Olive trees
PrestonBase5	Section 4.3.8 scheme and Q_e equation 4.6 (divide by grid area) using Olive trees
PrestonBrushbox	Section 4.3.8 scheme and Q_e equation 4.6 (divide by tree area) using Brushbox tree
PrestonBrushboxDiff	Section 4.3.8 scheme and Q_e equation 4.6 (divide by tree area) using Brushbox tree differential shading
PrestonBrushboxDiff2	Section 4.3.8 scheme and Q_e equation 4.6 (divide by tree area) using Brushbox tree with differential shading switch off
PrestonValidation13	Section 4.3.8 scheme (but using Maespa Rnet) and Q_e equation 4.6 (divide by grid area) using Olive trees

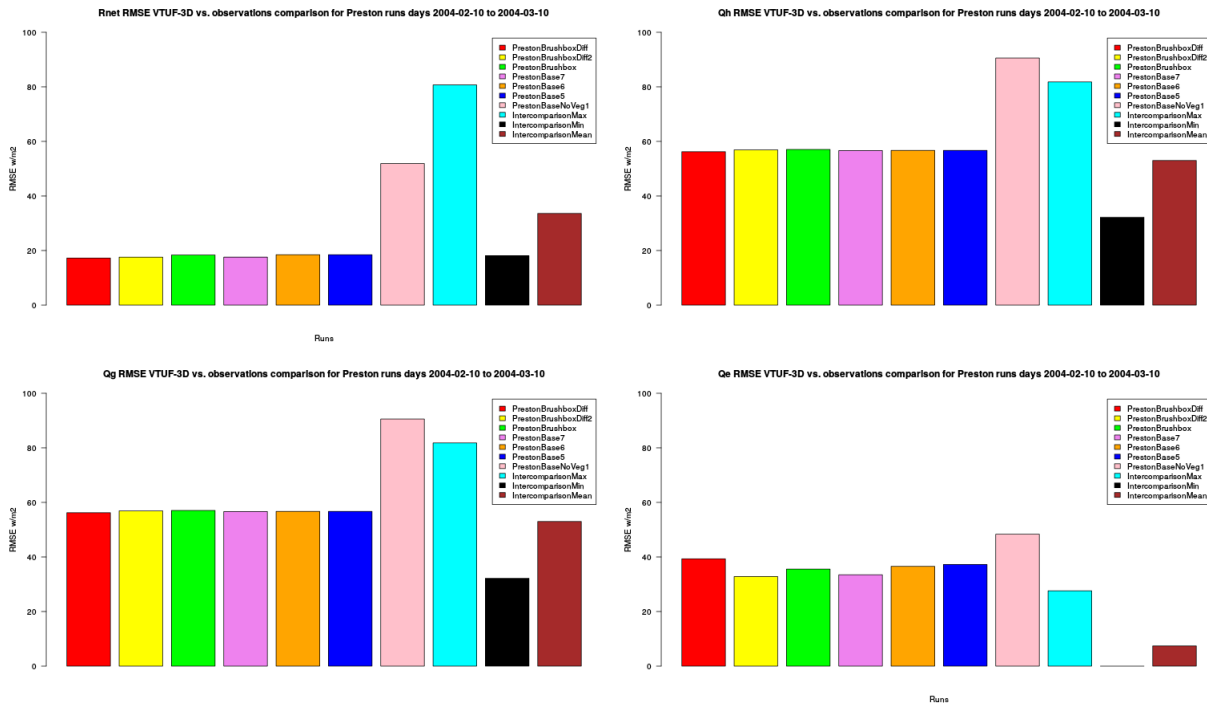


Figure 22: R_{net} RMSE VTUF-3D vs. observations comparison for Preston runs

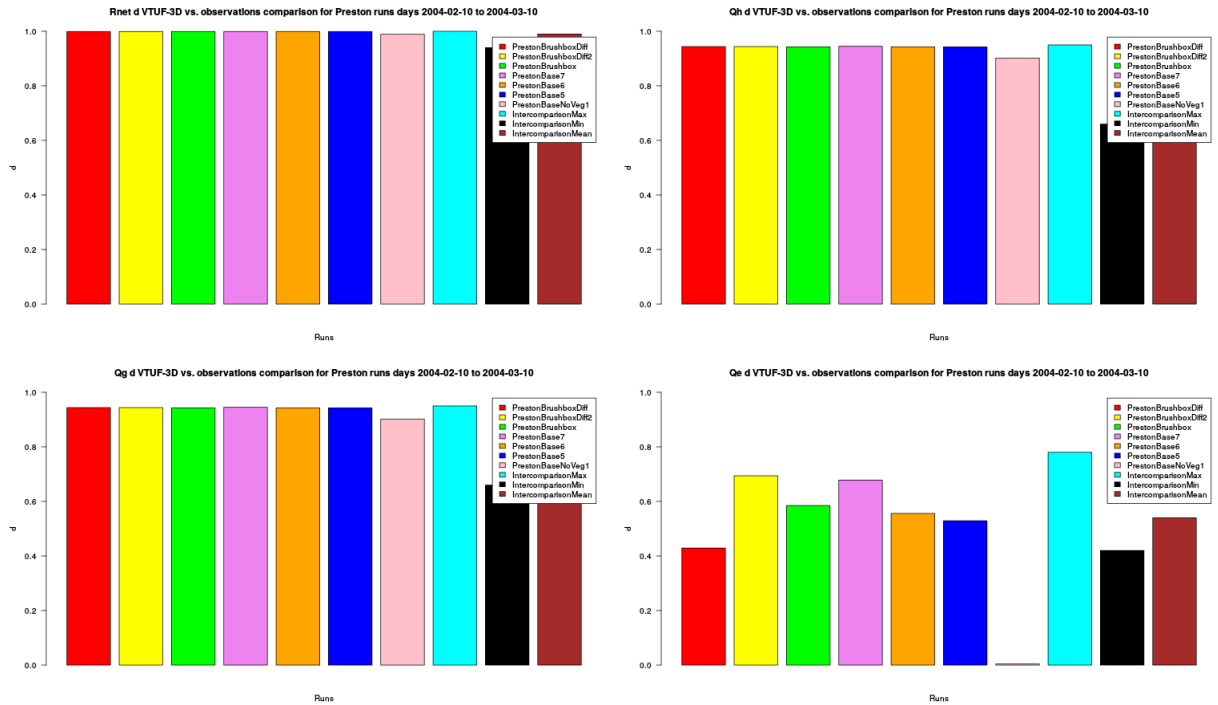


Figure 23: *Rnet d VTUF-3D vs. observations comparison for Preston runs*

Runs PrestonBase6 and PrestonBrushbox both use the same scheme described in Section 4.3.8 scheme and Q_e equation 4.6. PrestonBase6 uses olive trees while PrestonBrushbox uses Brushbox trees as the modelled tree species. Both simulations show good energy closure (PrestonBase6 shown in Figure 25).

Both simulations show reasonably good agreement between modelled and observed fluxes. 30 day hourly averages for PrestonBase6 (Figure 24) show close agreement with a slight over prediction of Q_h during the afternoons, a slight under prediction of Q_g during late afternoons, and a under prediction of Q_e during the day.

Error analysis for PrestonBase6 (Figure 26) shows d values of 0.943, 0.556, 0.999, and 0.939 for Q_h , Q_e , Q_* , and Q_g respectively, and RMSE (w/m^2) values of 56.7, 36.5, 18.5, and 60.6. Daytime and nighttime values (Figures 27 and 28) do not show a detectable improvement or worsening for those times.

These values show an improvement over the unimproved VTUF-3D model (PrestonBaseNoVeg1, shown in Figures 30 and 29). The unimproved model yields results of d of 0.902, 0, 0.989, and 0.871 and RMSE (w/m^2) of 90.6, 48.4, 51.9, 77.7 for Q_h , Q_e , Q_* , and Q_g respectively.

Results of d and RMSE are also compared to results from the Grimmond et al. (2010) intercomparison project in Figures 22 and 23 and perform within the range of other models. However, these results cannot be compared directly as most models in this comparison project were local scaled (not micro-scaled) and these results used a different data set (the Grimmond & Oke (1999) VL92 dataset).

In considering the tree differential shading scheme, these have shown a slight worsening in flux predictions. This scheme yields results of d of 0.945, 0.17, 0.999, and 0.945 and RMSE (w/m^2) values 57.1, 45.1, 17.5, 57.8 for Q_h , Q_e , Q_* , and Q_g respectively. Also, overall performance of these schemes is shown in Figure 22 and Figure 23.

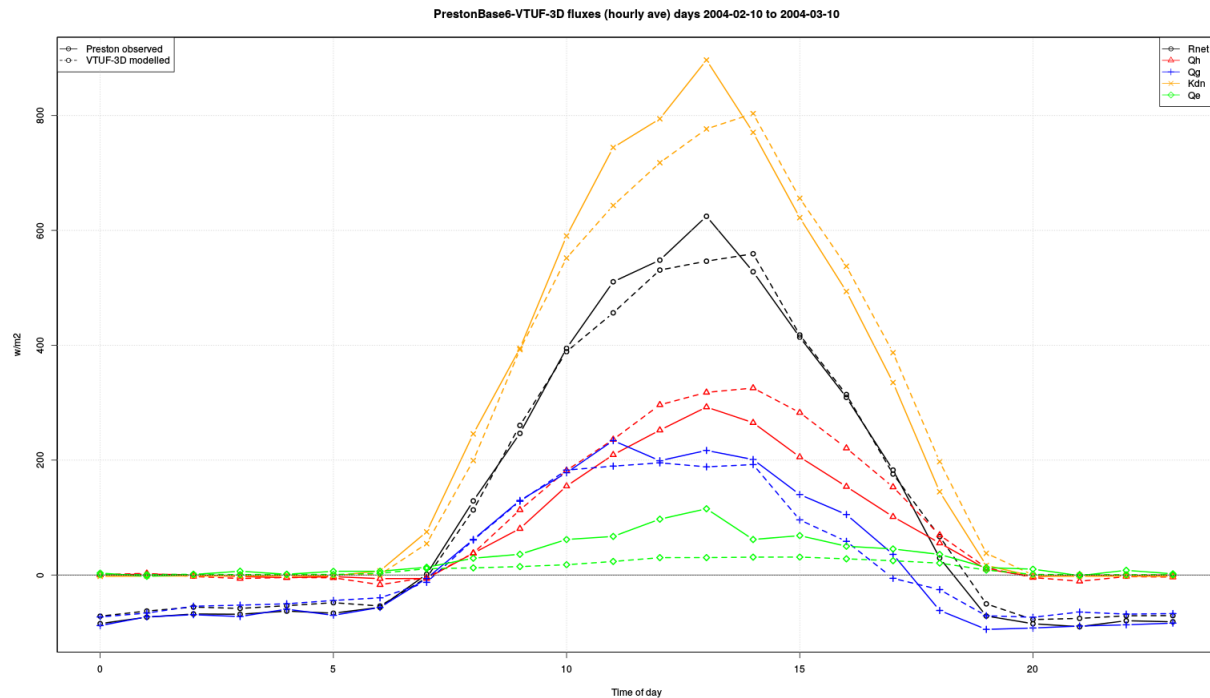


Figure 24: PrestonBase6 run 30 day hourly average VTUF-3D flux comparisons to Preston flux observations

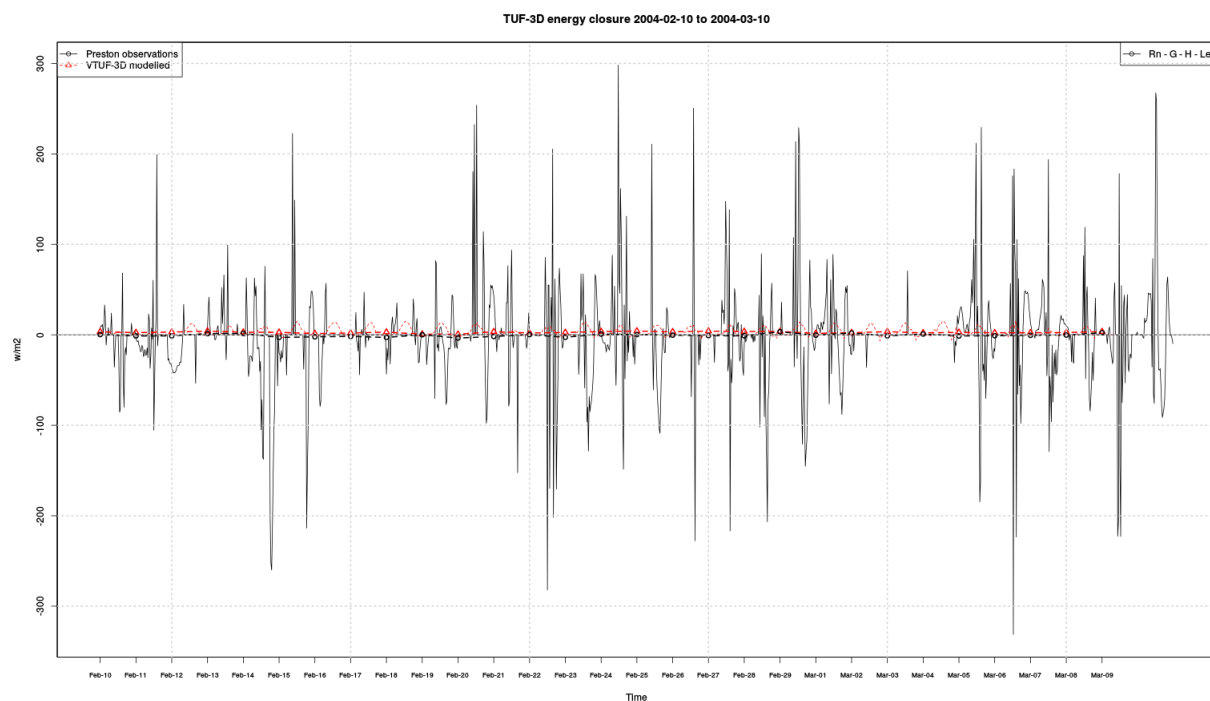


Figure 25: PrestonBase6 energy closure (VTUF-3D and observations), $Q * -Qg - Qh - Qe = 0$

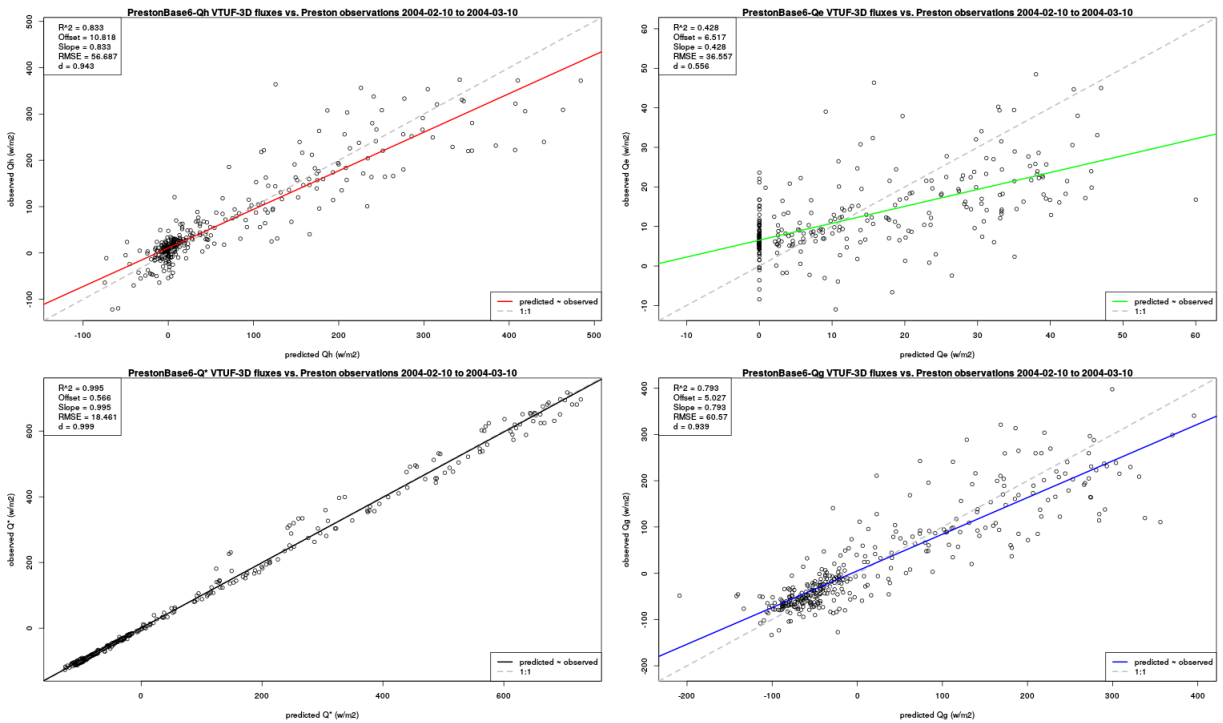


Figure 26: PrestonBase6 predicted vs. observations

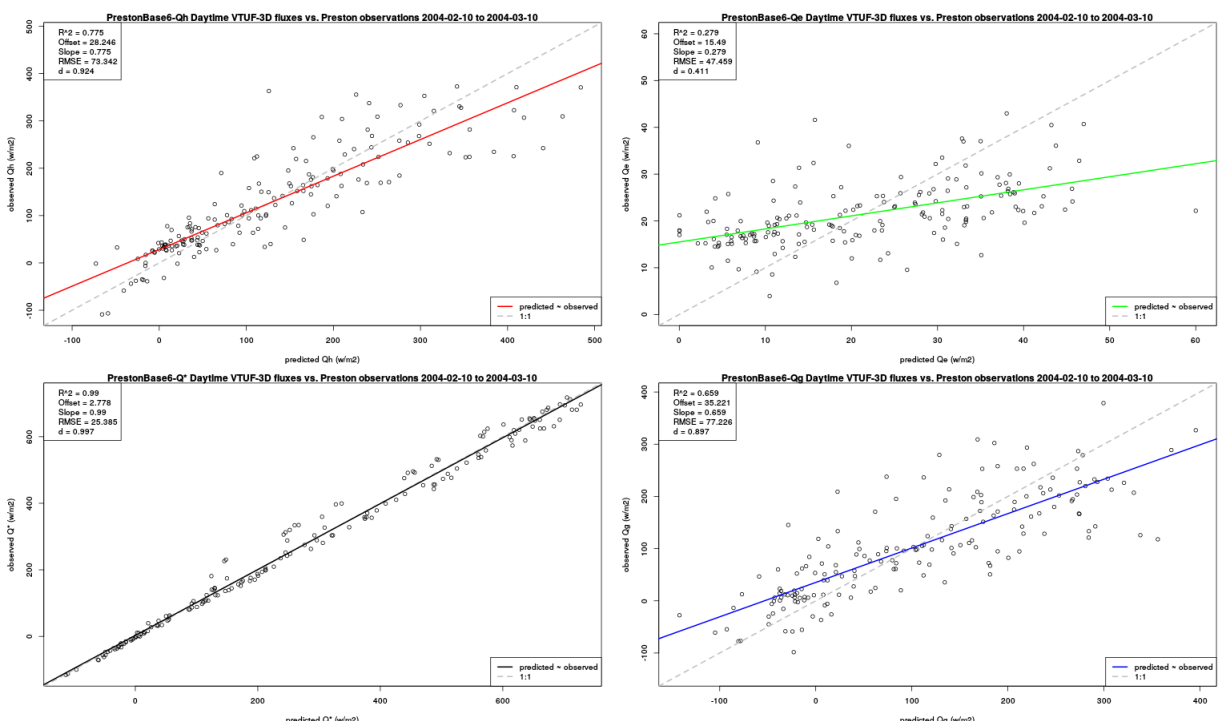


Figure 27: PrestonBase6 daytime predicted vs. observations

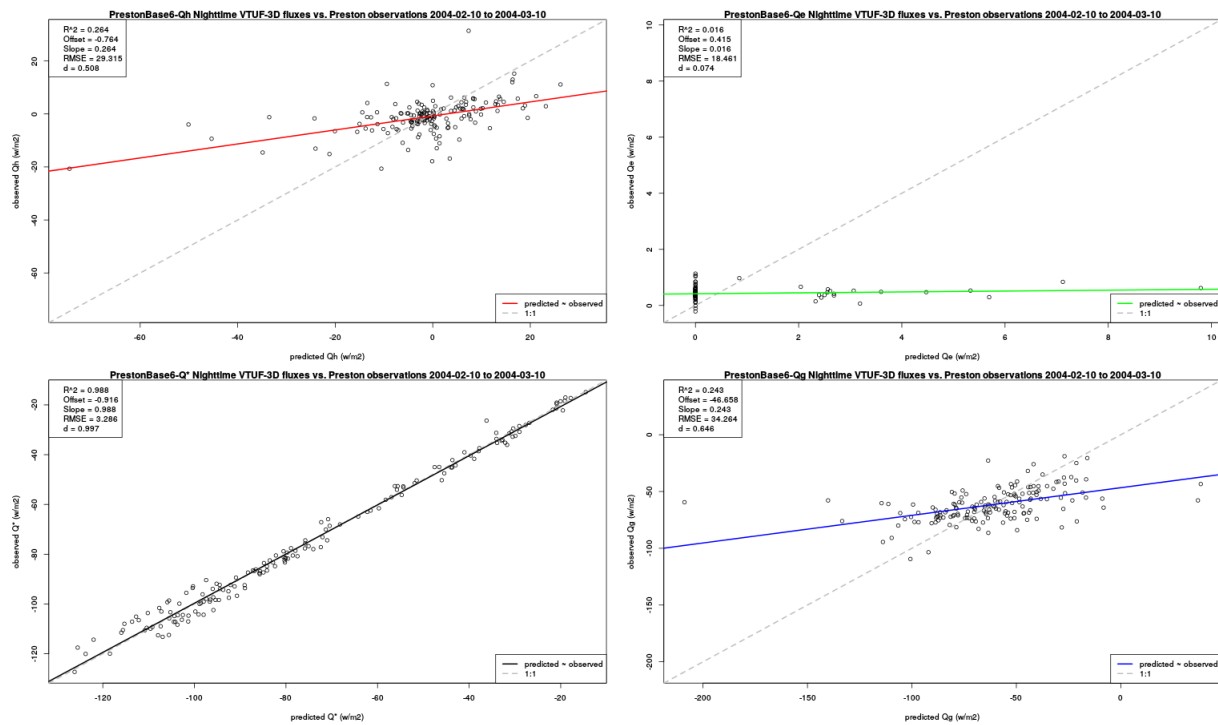


Figure 28: PrestonBase6 nighttime predicted vs. observations

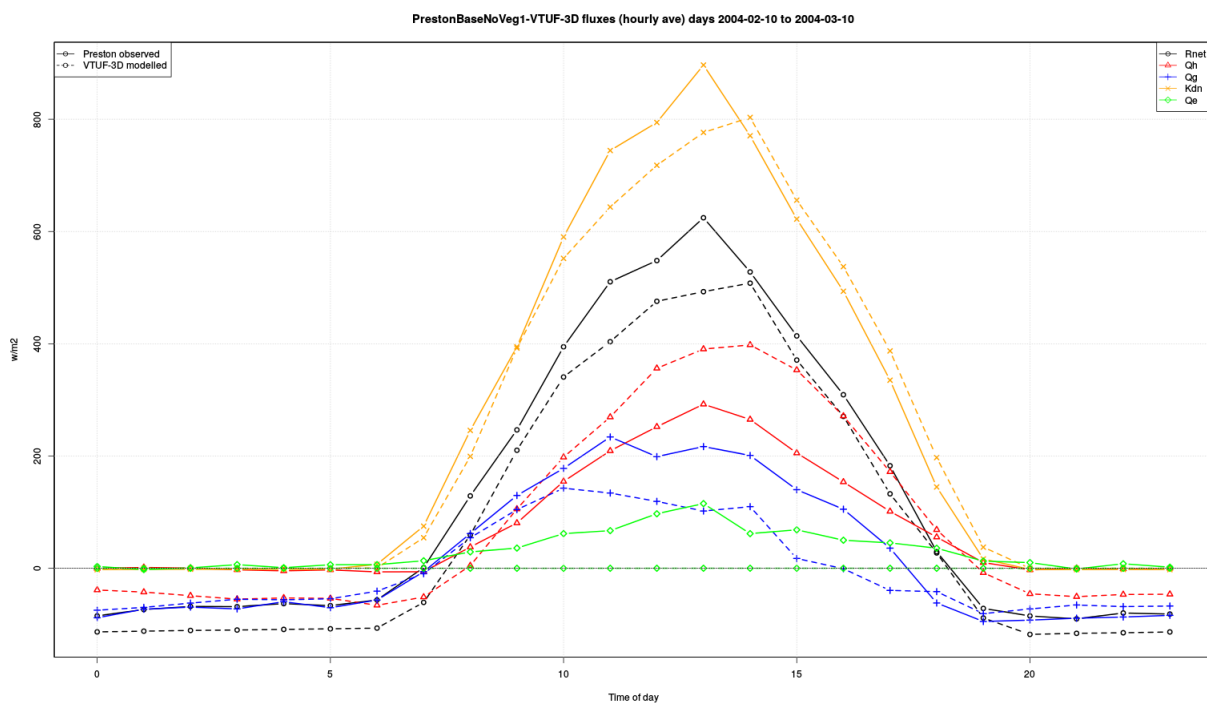


Figure 29: PrestonBaseNoVeg1 run 30 day hourly average VTUF-3D flux comparisons to Preston flux observations

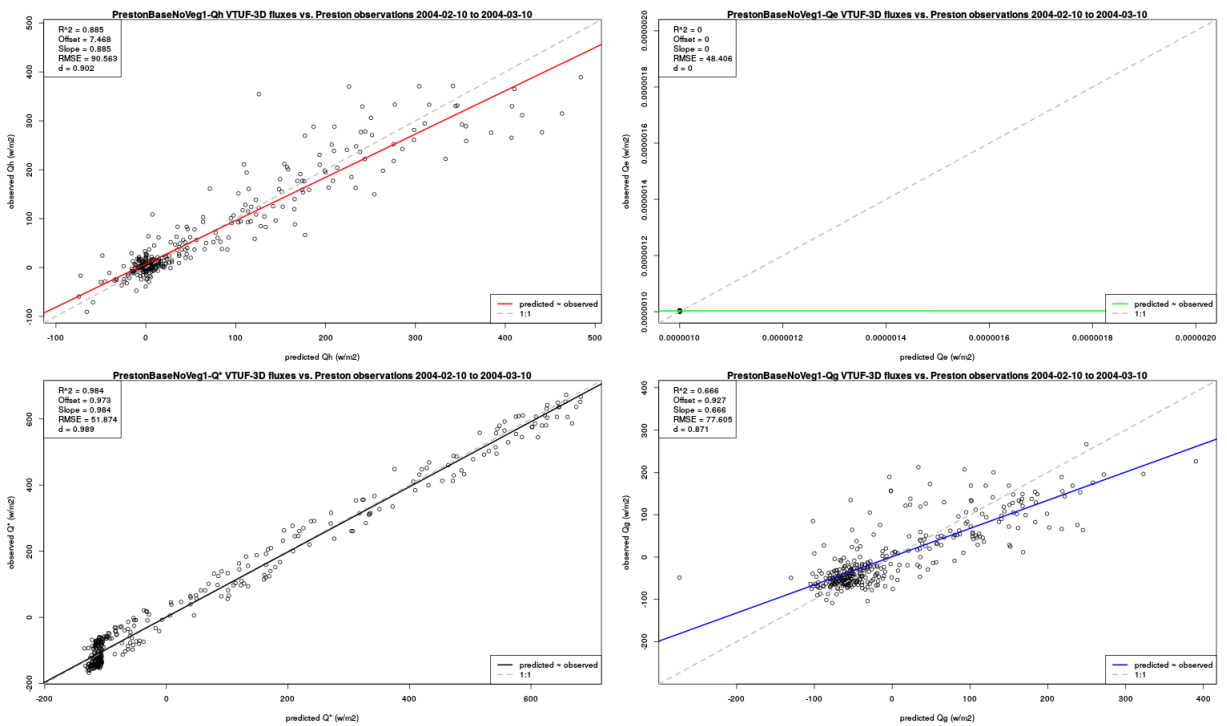


Figure 30: PrestonBaseNoVeg1 predicted vs. observations

Model testing and validation using City of Melbourne, George and Gipps St. dataset

A second set of validations was undertaken using observations from George St. and Gipps St. in the City of Melbourne (Coutts et al. 2015). These observations were taken at a number of observation stations, recording air temperature, wind speed, humidity, and incoming short wave, located along the two streets. Observation data set also contains values for Tmrt and UTCI for each observation station.



Figure 31: George St/Gipps St - Modelled domains with 4 and 3 observation stations located on street

Station locations, noted on Figure 31 as yellow pins (and station name, EM12, EM9, etc.), also shows the modelled domains. Both streets (George St. and Gipps St.) are shallow urban canyons (average building heights 7 and 8m, H:W 0.32 and 0.27) with varying canopy cover (45% and 12%). These domains were configured accordingly (Figure 32). The model was run for both streets for the period 1 February 2014 to 1 March 2014. Domain resolution is 5m grids.

Model testing and validation using George St. dataset

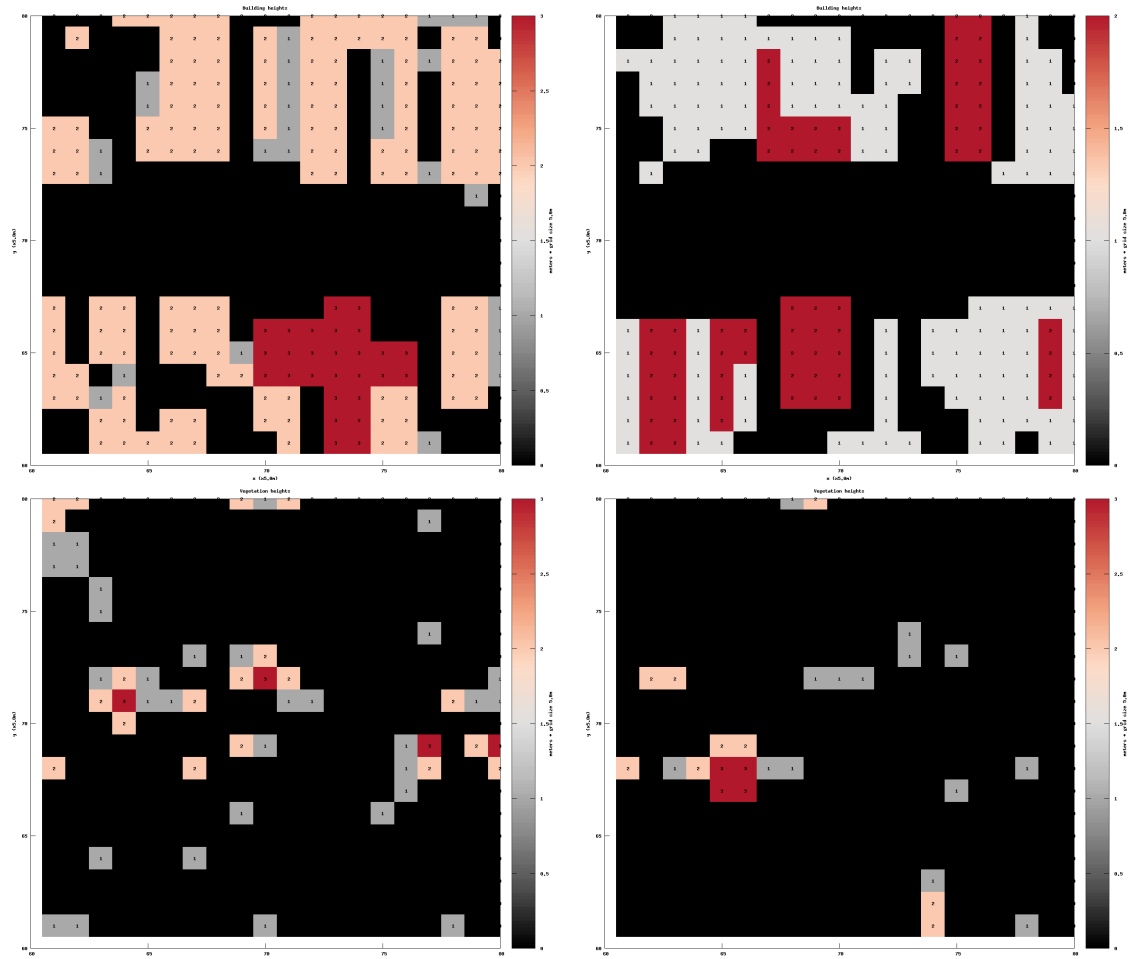


Figure 32: Building heights (top) / Vegetation cover (bottom) - George St (left), Gipps St. (right)

Energy closure for George St. (Figure 33) shows some energy gain during the modelled period. Further work will address this issue.

In a point by point comparison, using 30 day hourly averages (Figure 38), the model over predicts Tmrt during the day and under predicts it at night. This leads to UTCI, which is calculated from the Tmrt, also reflecting those patterns. More work on improving the Tmrt calculations is another item on the future improvement list (Appendix ??). Tables 12, 13, and 14 summarize the RMSE and d index of agreement for Tmrt, Tsfc, and UTCI respectively (from Figures 35, 36, and 37). Tsfc values show a strong level of agreement, with d values ranging from 0.902 to 0.066, while Tmrt and UTCI show slightly less strong agreement with d values ranging from 0.804 to 0.896.

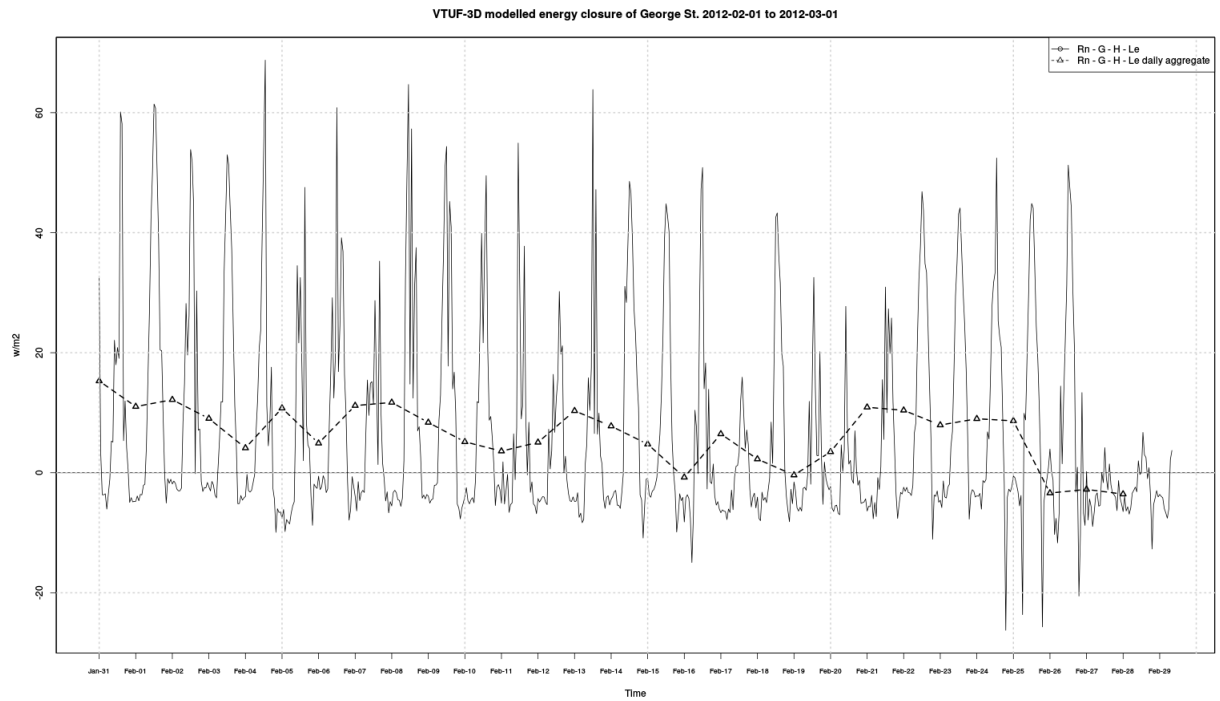


Figure 33: Energy closure of George St

Table 12: George St Tmrt predicted vs. observations

Observation point	RMSE ($^{\circ}\text{C}$)	d
EM12	12.6	0.846
EM9	13.9	0.804
EM3	11.6	0.896
EM2	15.0	0.832

Table 13: George St Tsfc predicted vs. observations

Observation point	RMSE ($^{\circ}\text{C}$)	d
EM12	2.875	0.966
EM9	3.353	0.952
EM3	4.631	0.907
EM2	7.226	0.902

Table 14: George St UTCI predicted vs. observations

Observation point	RMSE ($^{\circ}\text{C}$)	d
EM12	6.035	0.832
EM9	6.613	0.8
EM3	6.055	0.848
EM2	7.039	0.807

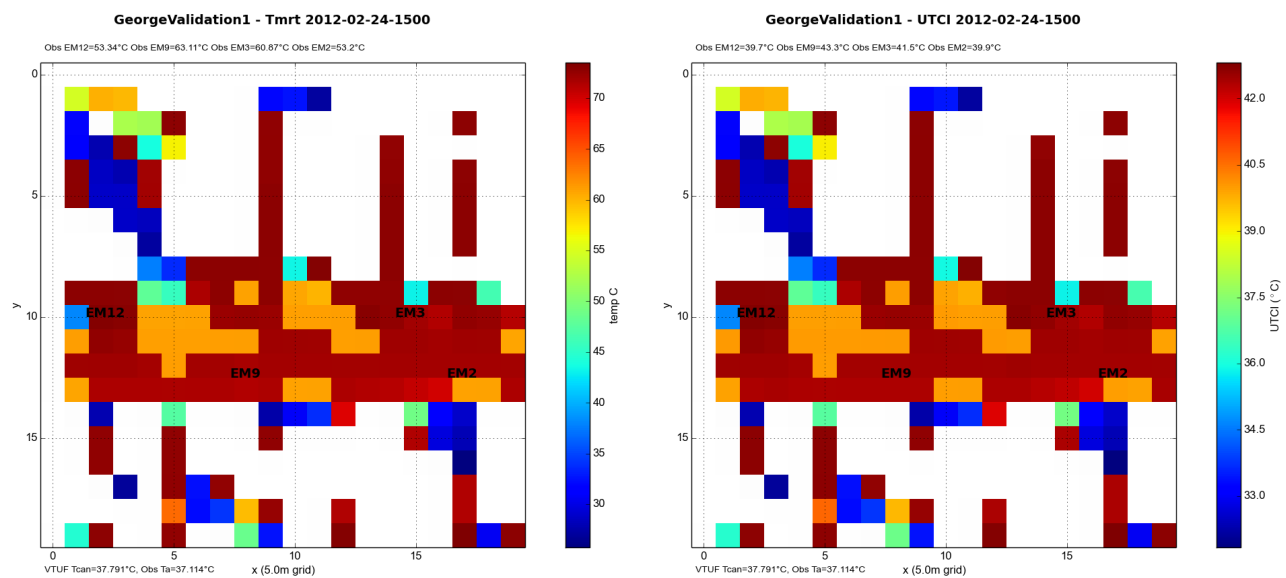


Figure 34: Results of George St. Tmrt and UTCI for 24 February 2014 1500.

Model testing and validation using City of Melbourne, Gipps St. dataset

In the Gipps St. validation, the energy balances (Figure 39) are much closer to full closure. Other analysis, predicted vs. three observed locations (Tables 15, 16, and 17, as well as Figures 41, 40, and 42) comparisons of Tmrt, Tsfc, and UTCI achieve results very similar to the George St. validations.

Table 15: Gipps St. Tmrt predicted vs. observations

Observation point	RMSE ($^{\circ}\text{C}$)	d
EM5	5.892	0.915
EM11	4.463	0.931
EM8	6.086	0.906

(Improved) micro-climate modelling assessment of the influence of WSUD on HTC

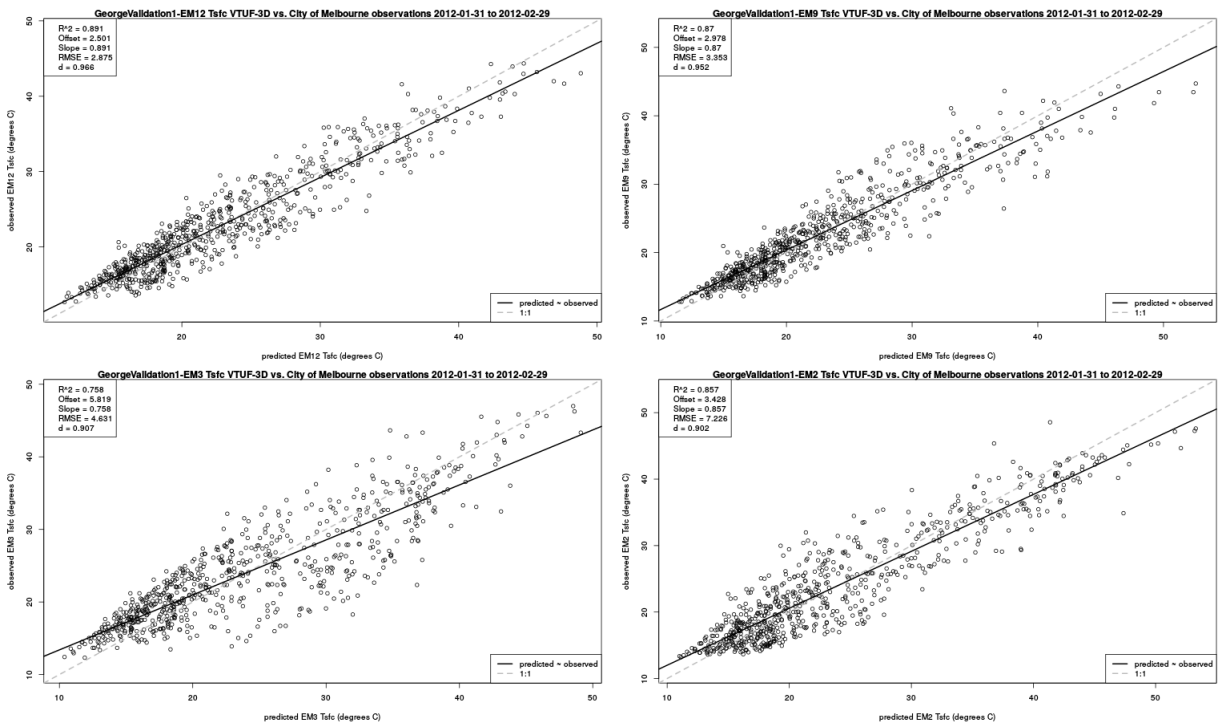


Figure 35: George St. point comparison of Tsfc of 4 observation stations to modelled points

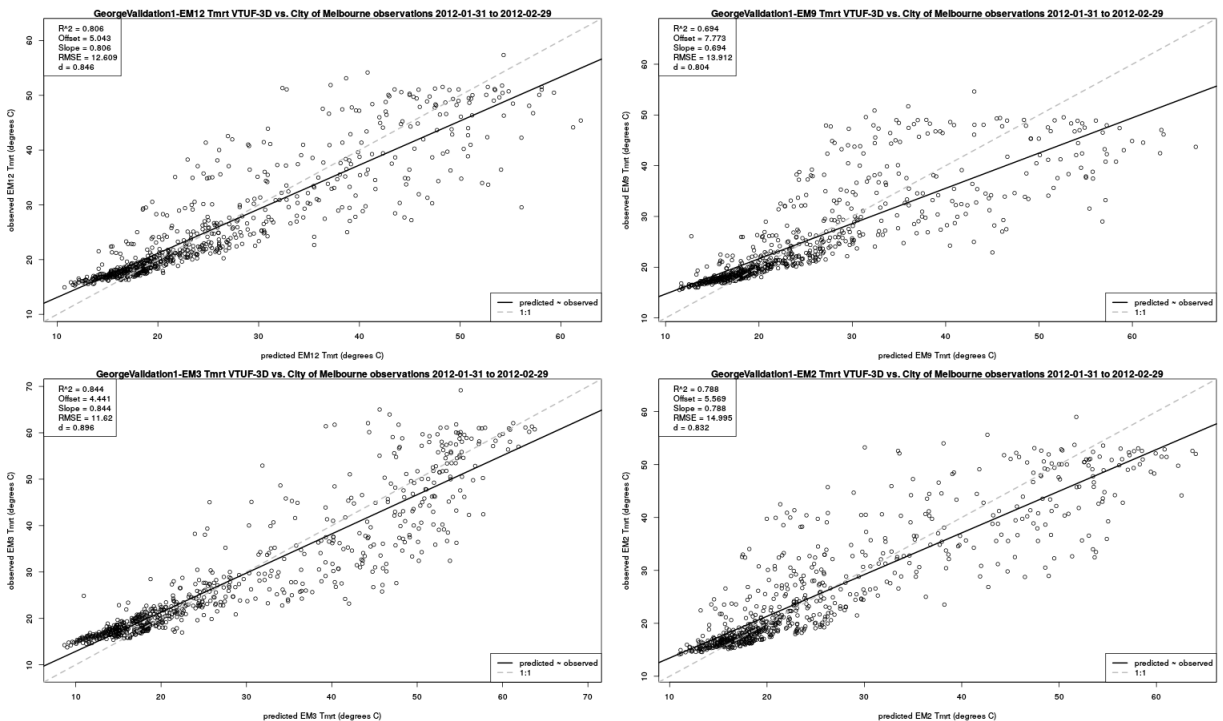


Figure 36: George St. point comparison of Tmrt of 4 observation stations to modelled points

Table 16: Gipps St. Tsfc predicted vs. observations

Observation point	RMSE (°C)	d
EM5	12.398	0.896
EM11	12.959	0.865
EM8	12.781	0.889

(Improved) micro-climate modelling assessment of the influence of WSUD on HTC

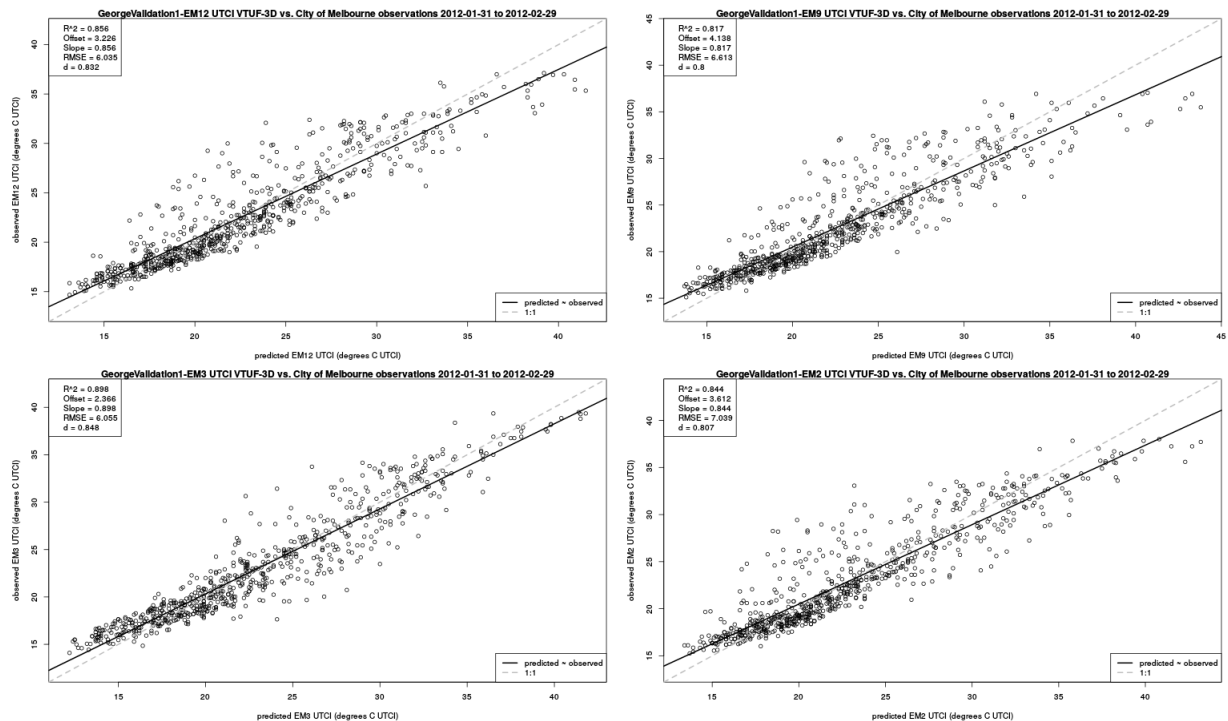


Figure 37: George St. point comparison of UTCI of 4 observation stations to modelled points

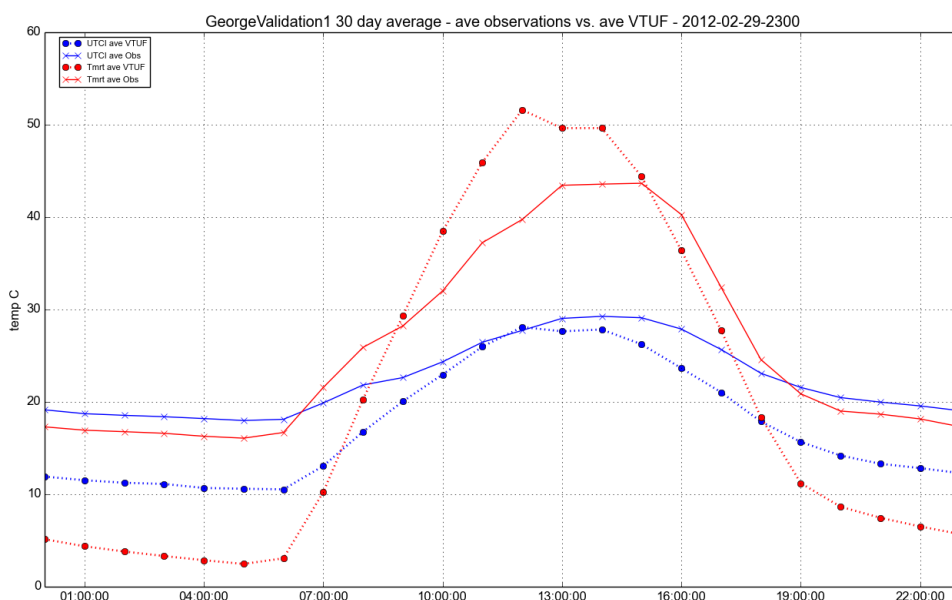


Figure 38: George St. 30 day averages, 4 observation stations compared to modelled points

Table 17: Gipps St. UTCI predicted vs. observations

Observation point	RMSE (°C)	d
EM5	5.773	0.874
EM11	6.289	0.834
EM8	6.085	0.854

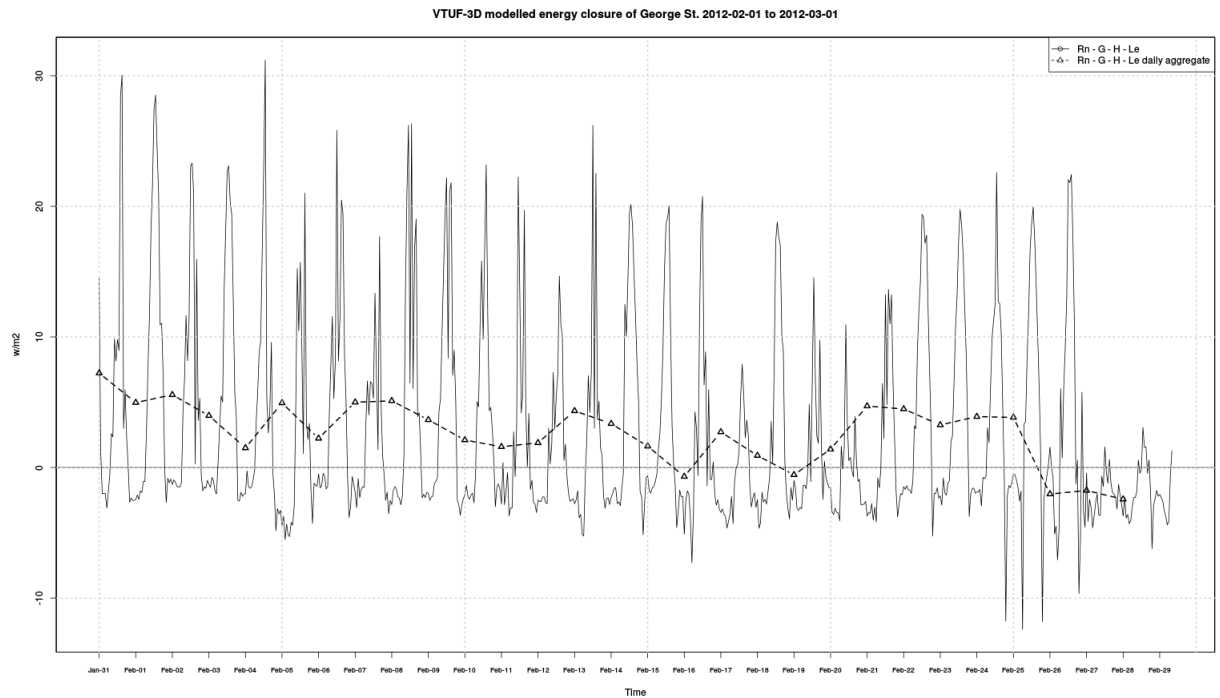


Figure 39: Energy closure of VTUF-3D and observations for Gipps St.

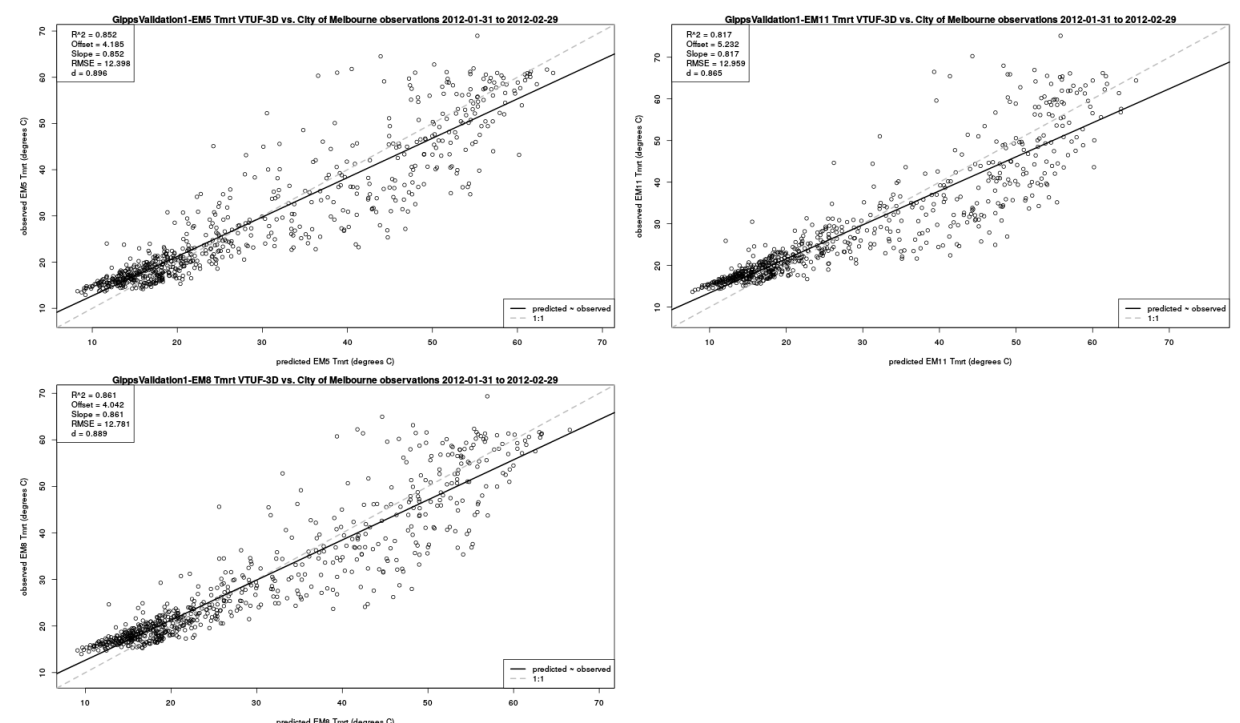


Figure 40: Gipps St. point comparison of Tmrt of 3 observation stations to modelled points

(Improved) micro-climate modelling assessment of the influence of WSUD on HTC

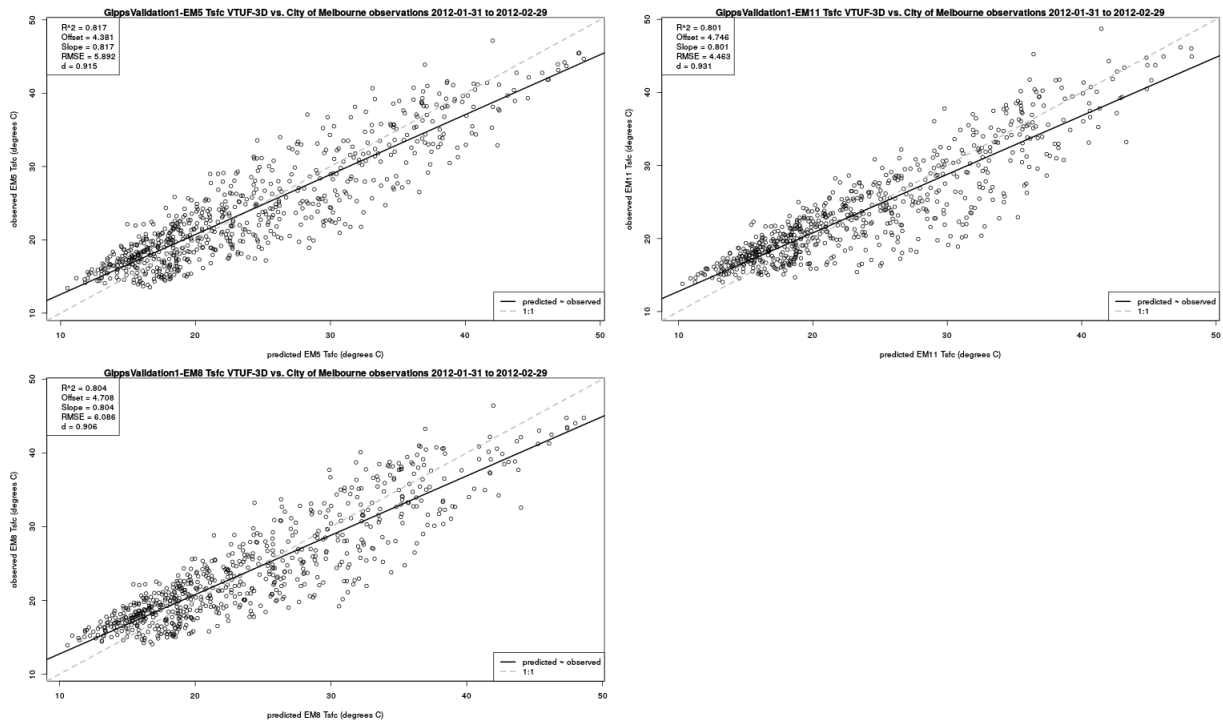


Figure 41: Gipps St. point comparison of T_{sfc} of 3 observation stations to modelled points

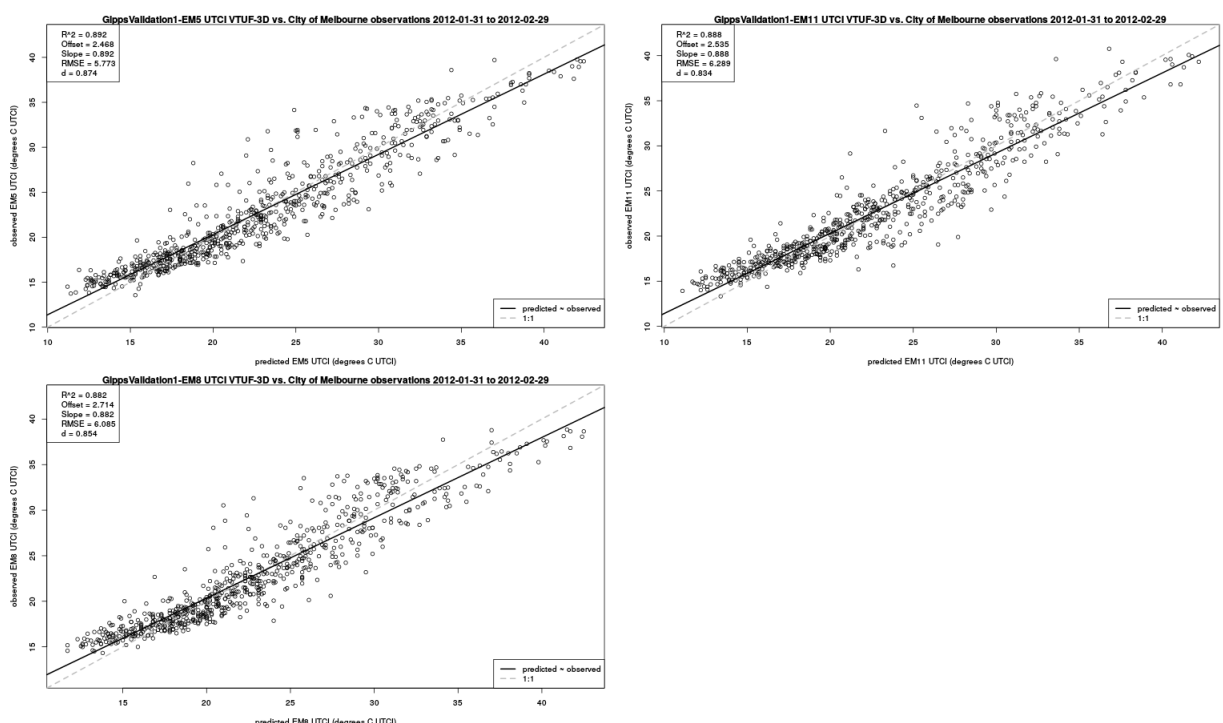


Figure 42: Gipps St. point comparison of $UTCI$ of 3 observation stations to modelled points

Model testing and validation using Lincoln Sq dataset

A third set of validations was run against the Lincoln Square data set (Motazedian 2015). This is a Melbourne urban square (Figure 43) with a mix of open grass and mature trees (Figure 45) within a dense urban canyon (Figure 44). Domain resolution was 10m grids.

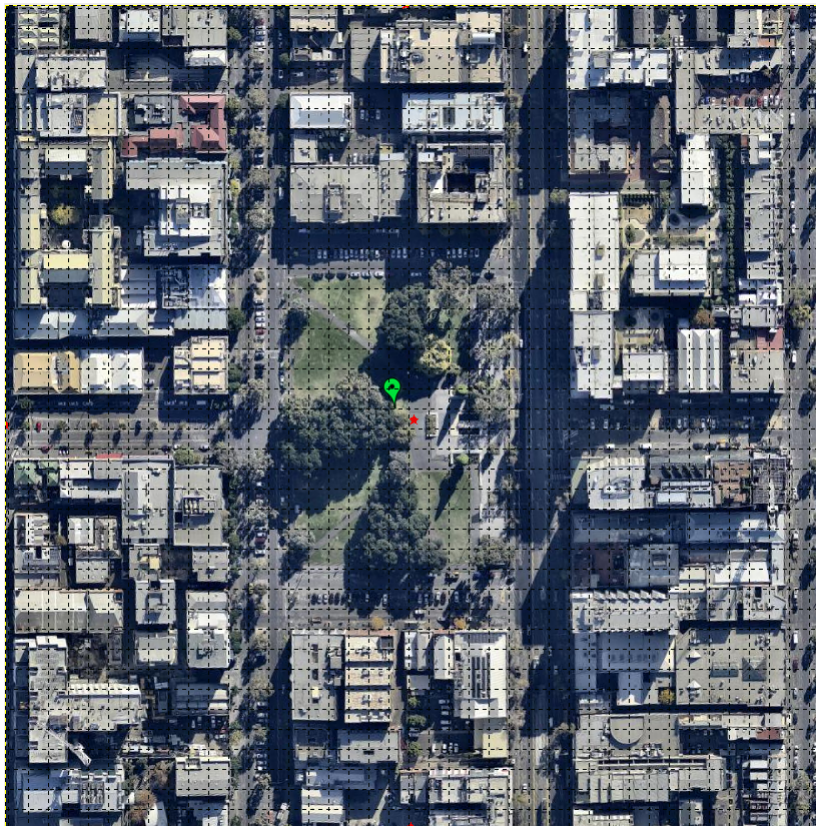


Figure 43: *Lincoln Square domain*

The modelled results were compared to transits of Tsfc (Figure 46) and UTCI (Figure 47) and showed broad agreement with the spatial patterns in the observations.

5.2 Future tasks

Model testing and validation using Hughesdale dataset

Future validations are to be done against the Hughesdale data set. These observations are currently being recorded and finalized. Hughesdale (Figure 48) is a medium density homogeneous suburb in the south east of Melbourne, Australia. These observations will include evapotranspiration and other tree physiology observations in addition to climate (air temperature, humidity, shortwave radiation, and wind speed) observations.

Model testing and validation using Smith St dataset

A final set of validations are to be done against the Smith Street data set (Gebert et al. 2012). This is an inner suburb of Melbourne, Australia. This street is a higher density/retail area, with a high percentage of impervious surfaces and very sparse tree cover. Observations were done of physiological processes of isolated trees in addition to the regular climate parameters. These validations will compare modelled values of evapotranspiration and photosynthesis to observed values.



Figure 44: Lincoln Square building heights

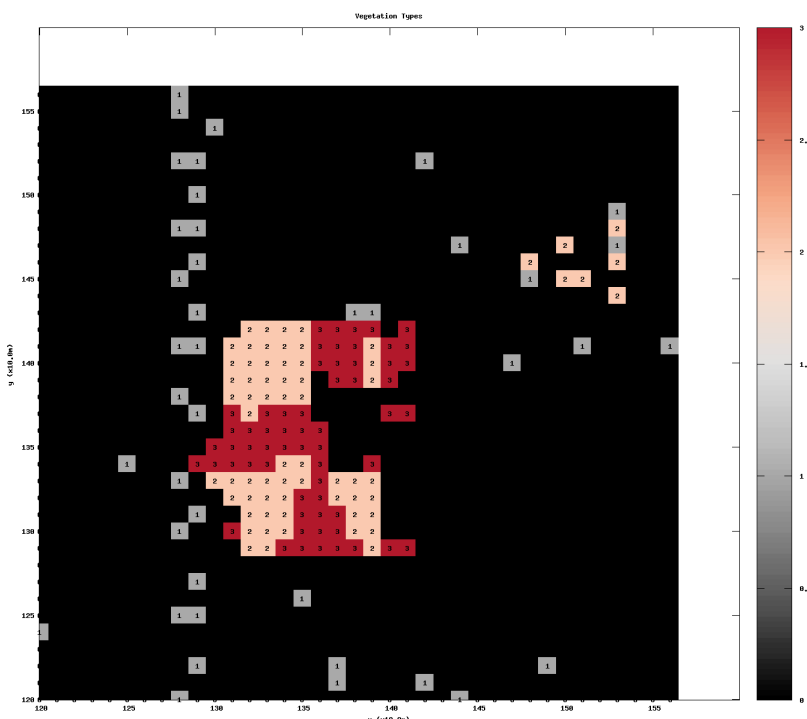


Figure 45: Lincoln Square vegetation heights

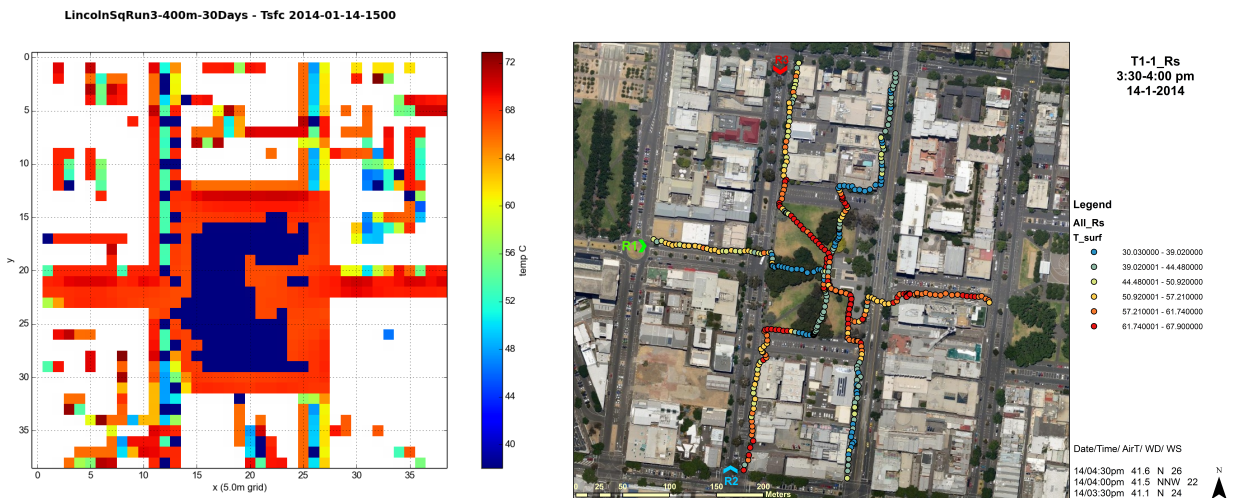


Figure 46: Comparisons of modelled T_{sf} to observed transits of Lincoln Sq. on 14 January 2014 3pm

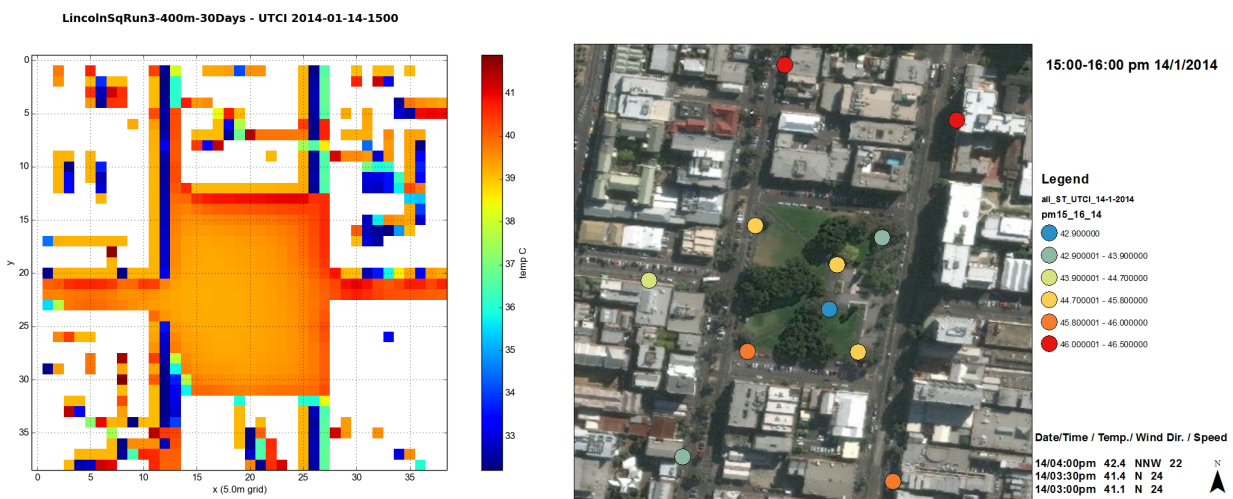


Figure 47: Comparisons of modelled UTCI to observed transits of Lincoln Sq. on 14 January 2014 3pm

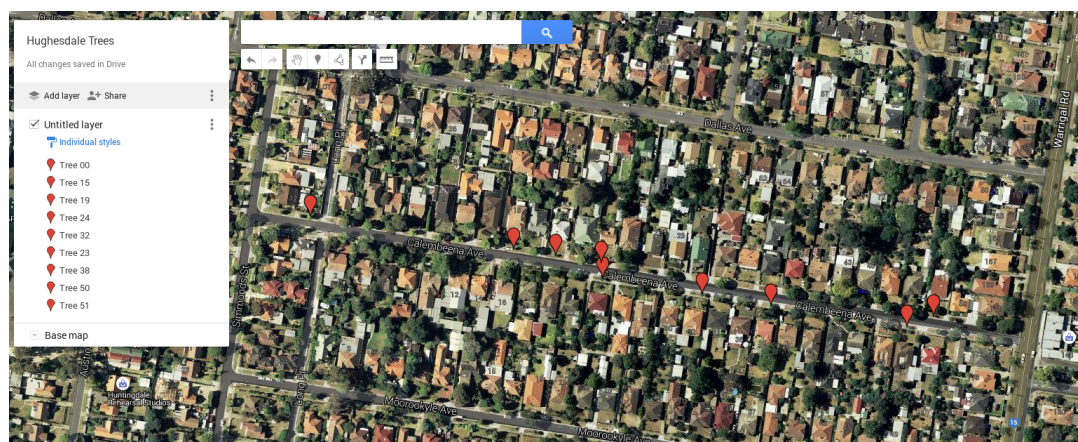


Figure 48: Hughesdale suburb and observation station locations



Figure 49: Smith St. contains detailed physiological observations of isolated trees

6 A systematic assessment of WSUD scenarios and urban morphologies using newly improved VTUF-3D model in support of HTC at a micro-climate level in urban areas

6.1 VTUF-3D Scenarios Details

Overview of scenarios

A first group of scenarios were set up, building on the domains from the validations. For each domain, a baseline existing tree cover was used. Then, additional domains were set up with zero trees, half trees, and double trees (as well as quadruple for some domains). The model was run for each variation generating two days of simulation data. Analysis compared UTCI and canopy temperature values to find the differences between the different scenarios.

A second group of scenarios will be set up to conduct a sensitivity study based on an idealized canyon, varying a number of variables to determine their relative importance in influencing HTC in urban areas.

Preston Scenarios

The Preston scenarios were built using the Preston validation domain (Figure 18). Three variations from the existing trees cover were designed of zero, half, and double trees (configurations shown in Figure 50). The model was run for 13-14 February 2004 using forcing data used in the validation steps.

Post-processing analysis generated Tmrt and UTCI calculations for each surface in the domain. Figures were generated, showing UTCI values for only surfaces at 0m (Figure 51, showing 14 February 2004 2pm for each scenario). All 0m UTCI values for 13-14 February 2004 were averaged for each timestep and charted in Figure 52 as well as differences between the baseline existing scenario and the other three scenarios.

Finally, canopy temperatures over the modelling period are shown (Figure 53), including the Tair forcing air temperature value, as well as differences between the baseline existing scenario and the other three scenarios. Note that canopy temperatures are averaged across the entire domain, while UTCI temperatures are only averaged across 0m surfaces.

The highlights of these scenarios are:

- UTCI (street level, 0m, average) variations of 0.9°C between the no tree scenario and double trees
- Double trees scenario gives 0.3°C UTCI reduction over existing Preston tree canopy
- Preston canopy temperature differences of 0.25°C between the scenarios.

City of Melbourne Gipps St. scenarios

The City of Melbourne Gipps St. scenarios where built using the Gipps St. validation domain (Figure 31). Four variations from the existing tree cover were designed of zero, half, double, and quadruple trees (configurations shown in Figure 54). The model was run for 23-24 February 2014 using forcing data used in the validation steps.

Post-processing analysis generated Tmrt and UTCI calculations for each surface in the domain. Figures were generated, showing UTCI values for only surfaces at 0m (Figure 55, showing

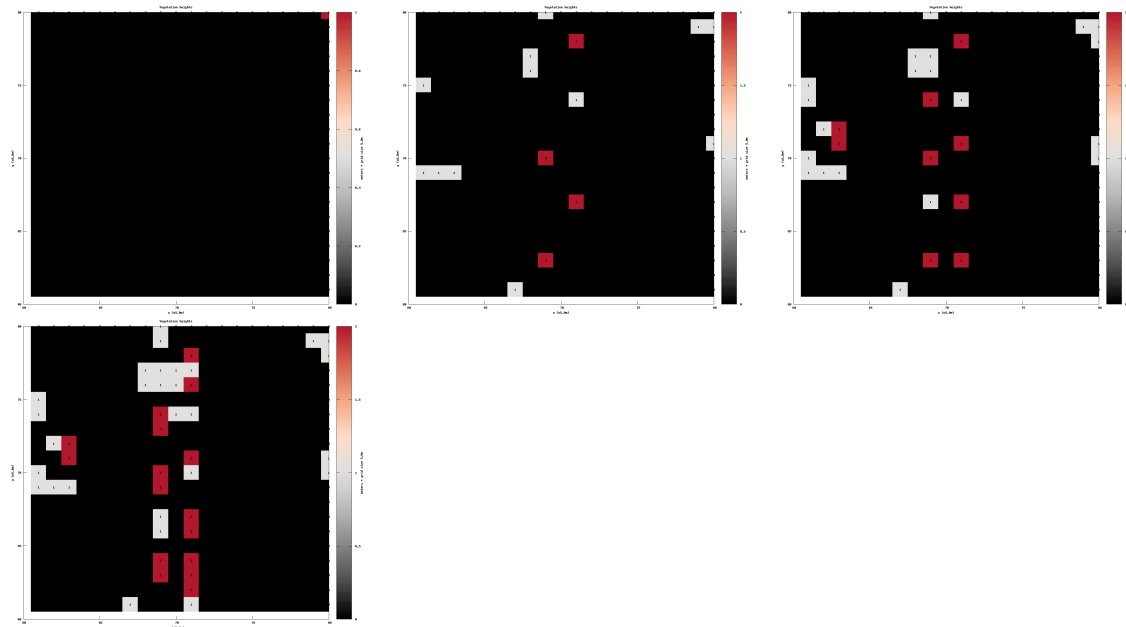


Figure 50: Preston, 4 scenarios of zero trees, half trees, existing Preston tree canopy cover, and double trees

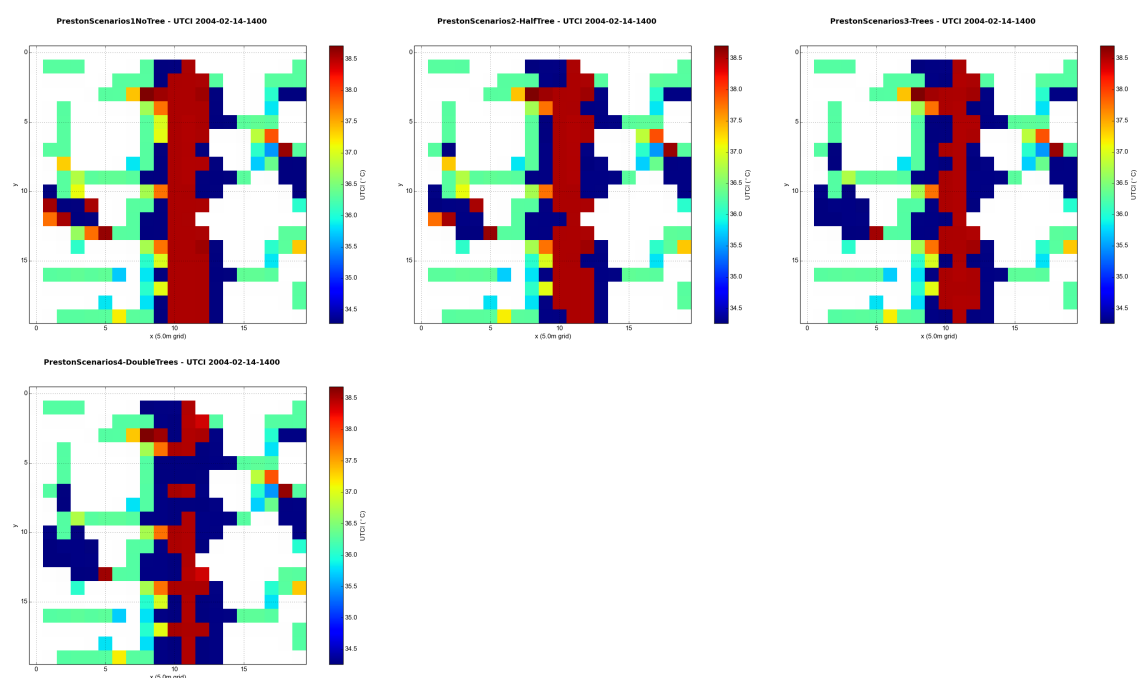


Figure 51: Preston Scenarios-UTCI at 0m for 4 scenarios of zero trees, half trees, existing Preston tree canopy cover, and double trees

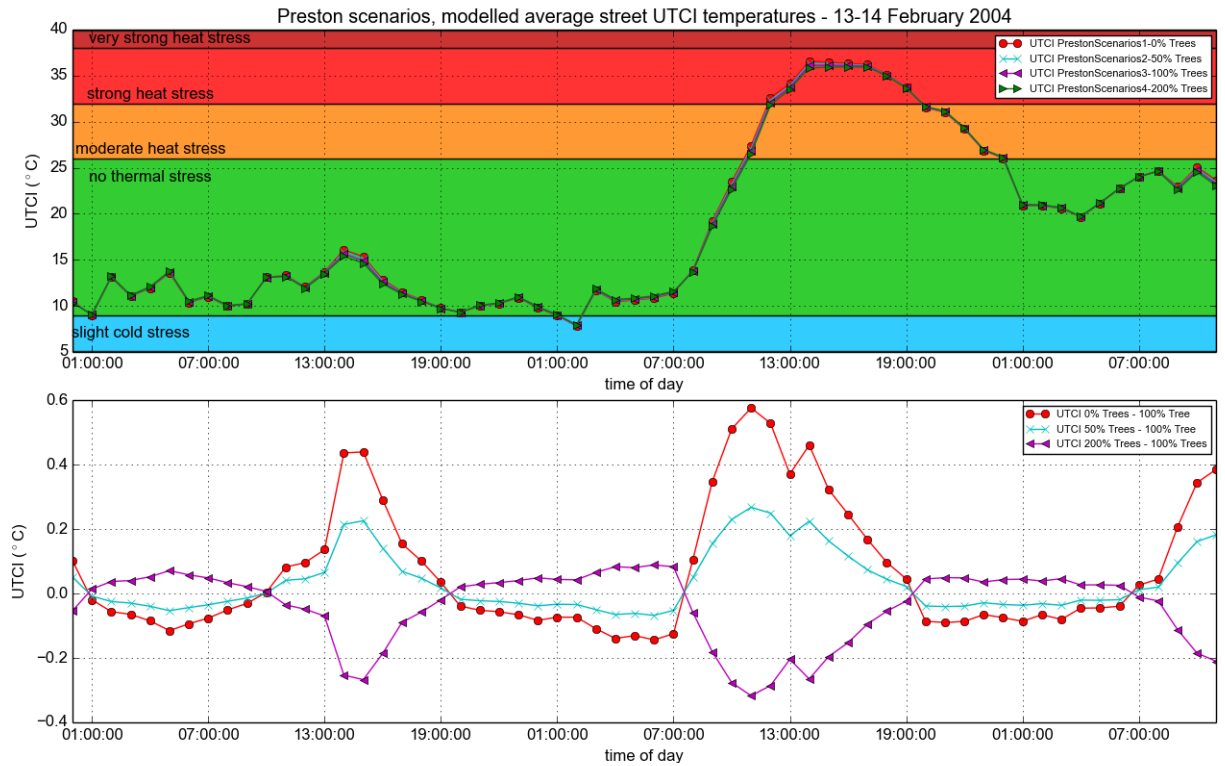


Figure 52: Modelled UTCI of 4 Preston scenarios over 13-14 February 2004 / UTCI differences between baseline existing Preston trees and other scenarios

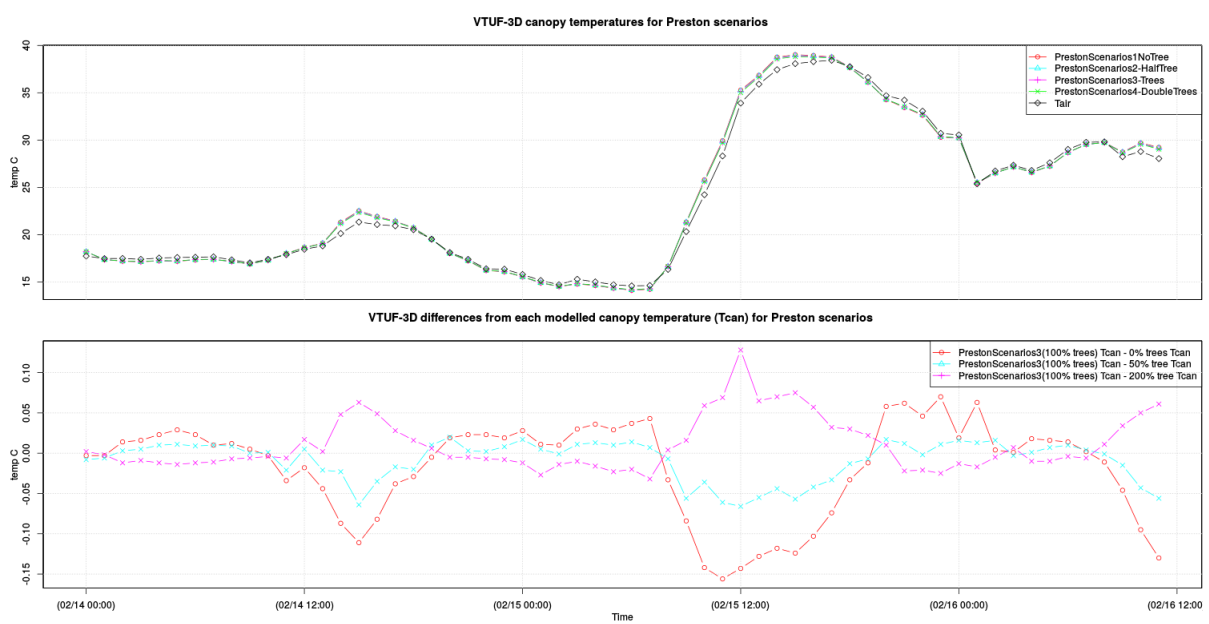


Figure 53: Modelled Tcan of 4 Preston scenarios over 13-14 February 2004 / Tcan differences between baseline existing Preston trees and other scenarios

24 February 2014 3pm for each scenario). All 0m UTCI values for 23-24 February 2014 were averaged for each timestep and charted in Figure 56, as well as differences between the baseline existing scenario and the other four scenarios.

Finally, canopy temperatures over the modelling period are shown (Figure 57), including the Tair forcing air temperature value, as well as differences between the baseline existing scenario and the other three scenarios. Note that canopy temperatures are averaged across the entire domain, while UTCI temperatures are only averaged across 0m surfaces.

The highlights of these scenarios are:

- UTCI (averaged at 0m height) maximum variations of 1.0°C between Gipps St. zero tree scenario and double trees
- UTCI (averaged at 0m height) maximum variations of 2.3°C between Gipps St. zero tree scenario and quadruple trees
- Gipps St. canopy temperature differences range from 0.2°C to 0.4°C between the scenarios.

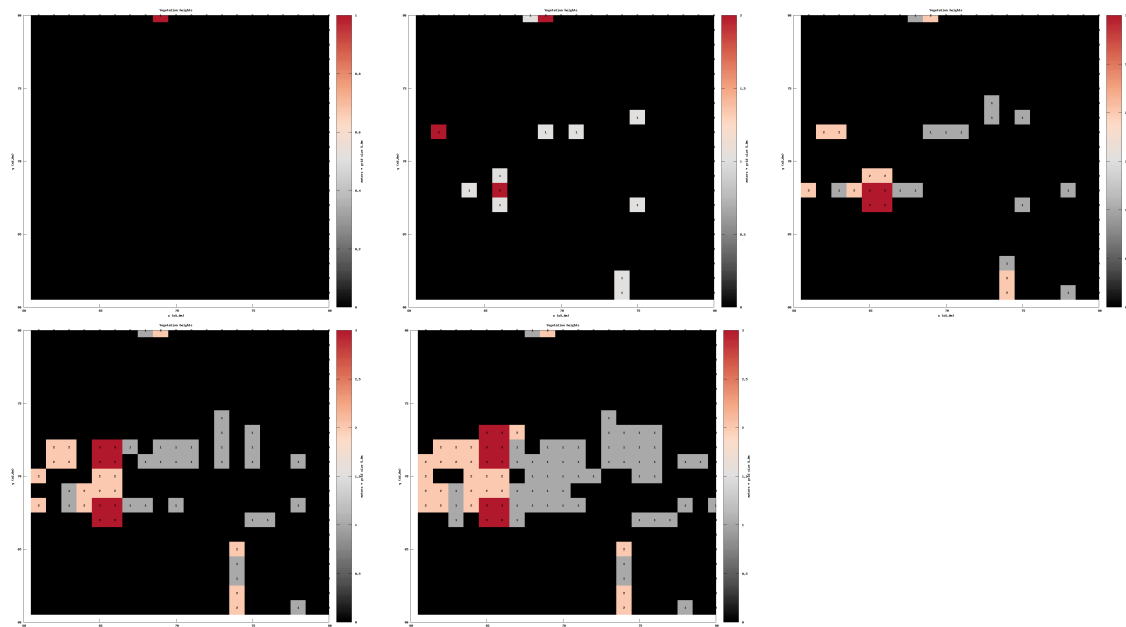


Figure 54: Gipps St. 5 scenarios of zero trees, half trees, existing Gipps St. tree canopy cover, double trees, and quadruple trees.

Sensitivity scenarios

A final set of scenarios will be built to examine the different variables in urban vegetation. These will be built using an idealized urban canyon. In these scenarios, the following variables will be varied to determine their individual impact on HTC:

- tree height,
- leaf area index,
- number of trees,

(Improved) micro-climate modelling assessment of the influence of WSUD on HTC

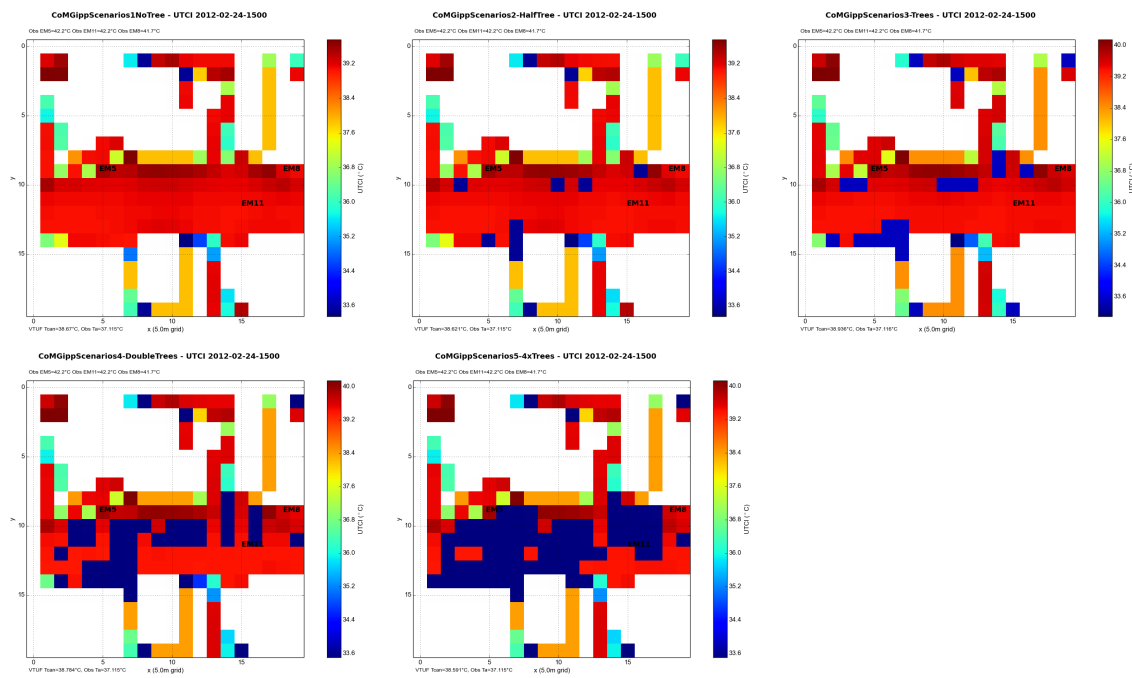


Figure 55: Gipps St. UTCI (averaged at 0m height) of scenarios of zero trees, half trees, existing Gipps St. tree canopy cover, double trees, and quadruple trees.

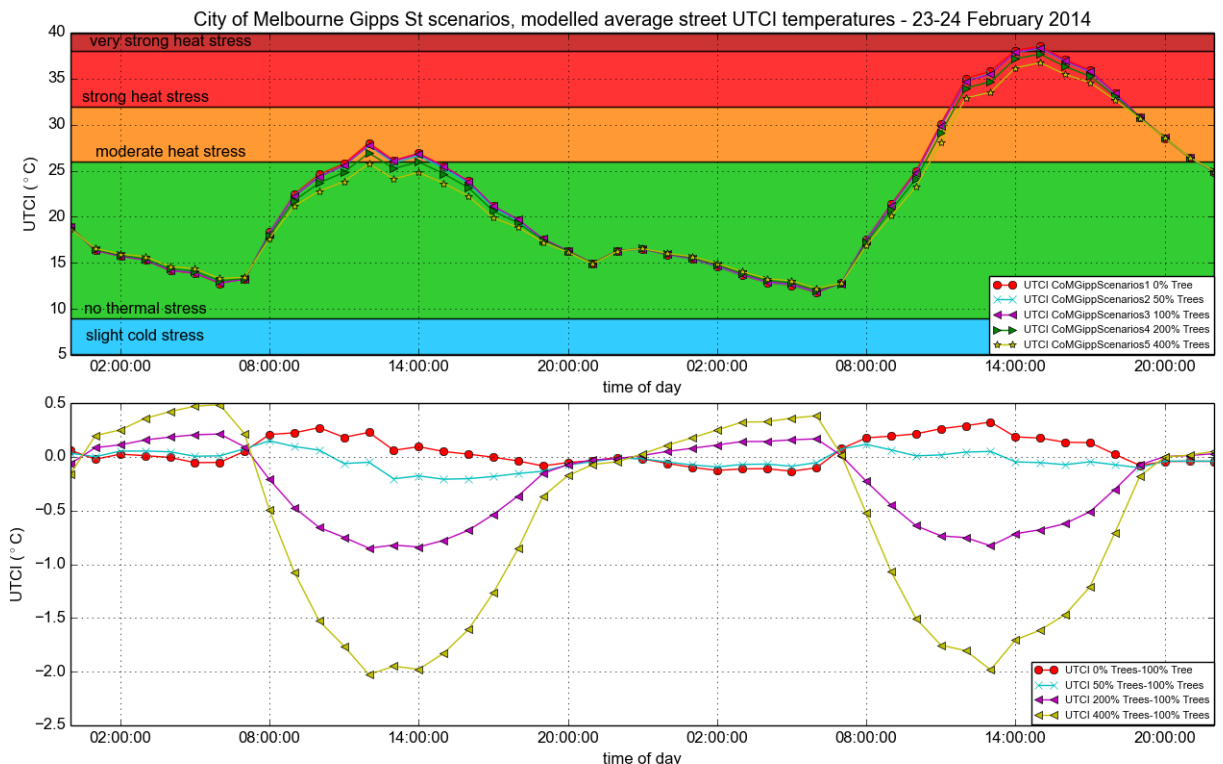


Figure 56: Gipps St. UTCI (averaged at 0m height) for 5 scenarios over 23-24 February 2014 / UTCI differences between baseline scenario and other Gipps St. scenarios

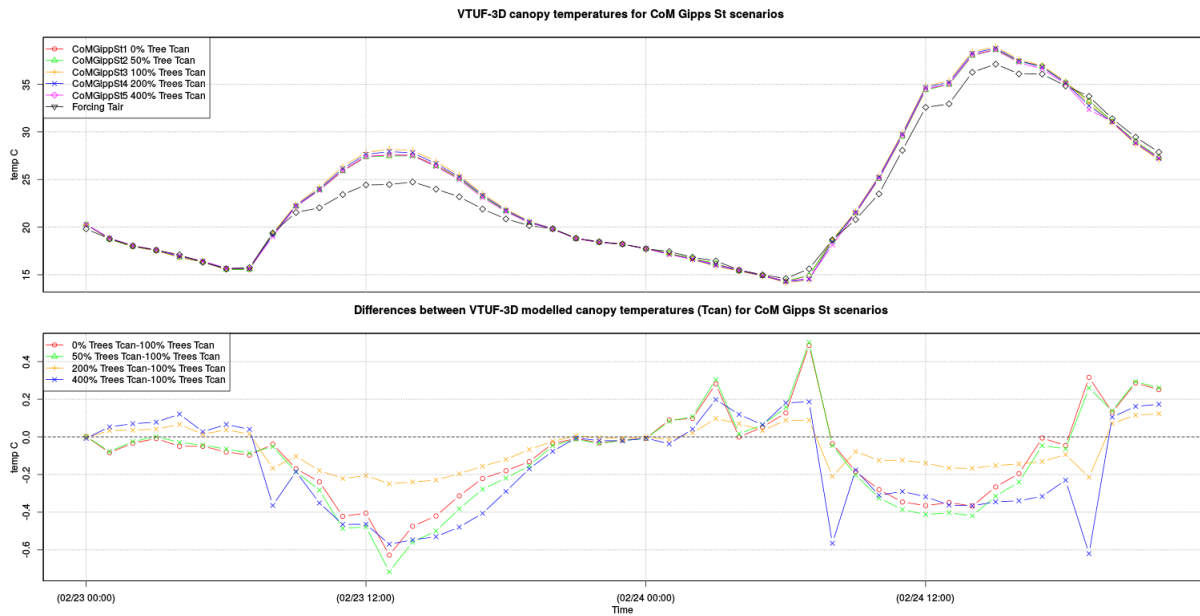


Figure 57: Modelled Tcan of 5 Gipps St. scenarios (and forcing Tair) over 23-24 February 2014 /
Tcan differences between baseline existing Gipps St. trees scenario and other scenarios

- tree placement (side of street, grouping or solitary,
- soil moisture.

7 Future plans

8 Conclusion

References

- Alitoudert, F and Mayer, H. (2006), Numerical study on the effects of aspect ratio and orientation of an urban street canyon on outdoor thermal comfort in hot and dry climate. *Building and Environment*, 41:pp. 94–108.
- Baldini, E., Facini, O., Nerozzi, F. & Arboree, C. (1997), Leaf characteristics and optical properties of different woody species. *Trees*, 12:pp. 73–81.
- Beardsell, D.V. & Considine, J.A. (1987), Lineages, Lineage Stability and Pattern Formation in Leaves of Variegated Chimeras of *Lophostemon confertus* (R. Br.) Wilson & Waterhouse and *Tristaniopsis laurina* (Smith) Wilson & Waterhouse (Myrtaceae). *Aust. J. Bot.*, 35(6):pp. 701–714.
- Bernacchi, C.J., Singsaas, E.L., Pimentel, C., Portis, A.R. & Long, S.P. (2001), Improved temperature response functions for models of Rubisco-limited photosynthesis. *Plant, Cell and Environment*, 24(2):pp. 253–259.
- Bijoor, N.S., Pataki, D.E., Haver, D. & Famiglietti, J.S. (2014), A comparative study of the water budgets of lawns under three management scenarios. *Urban Ecosystems*, 17(4):pp. 1095–1117.
- Bowler, D.E., Buyung-Ali, L., Knight, T.M. & Pullin, A.S. (2010), Urban greening to cool towns and cities: A systematic review of the empirical evidence. *Landscape and Urban Planning*, 97(3):pp. 147–155.
- Bröde, P., Fiala, D., Blazejczyk, K., Epstein, Y., Holmér, I., Jendritzky, G., Kampmann, B., Richards, M., Rintamäki, H., Shitzer, A. & Havenith, G. (2009), Calculating UTCI Equivalent Temperatures. In: *Environmental Ergonomics XIII, Proceedings of the 13th International Conference on Environmental Ergonomics*, Boston, MA, 2 - 7 August 2009, University of Wollongong, Wollongong, pp. 49–53.
- Brown, R.H. & Morgan, J.a. (1980), Photosynthesis of Grass Species Differing in Carbon Dioxide Fixation Pathways 1. *Plant Physiology*, 66(4):pp. 541–544.
- Bruse, M. (1999), *The influences of local environmental design on microclimate- development of a prognostic numerical Model ENVI-met for the simulation of Wind, temperature and humidity distribution in urban structures*. Ph.D. thesis, University of Bochum, Germany (in German).
- Buba, T. (2013), Relationships between stem diameter at breast height (DBH), tree height, crown length, and crown ratio of *Vitellaria paradoxa* C. F. Gaertn in the Nigerian Guinea Savanna. *African journal of Biotechnology*, 12(22):pp. 3441–3446.
- CD-adapco (2011), CD-adapco website. <http://www.cd-adapco.com/>, (accessed 2 November 2011).
- Chen, D., Wang, X., Thatcher, M., Barnett, G., Kachenko, A. & Prince, R. (2014), Urban vegetation for reducing heat related mortality. *Environmental Pollution*, 192:pp. 275–284.
- Coutts, A.M. (2014), pers. comm., 24 January. Email, "Maespa single tree - Olive".
- Coutts, A.M. (2015a), pers. comm., 1 December. Email, "Re: Simulating shaded trees in MAESPA?".
- Coutts, A.M. (2015b), pers. comm., 15 June. Email, "L Confertus (Brushbox) files".

- Coutts, A.M. (2015c), pers. comm., 27 November. Email, "Re: Simulating shaded trees in MAESPA?".
- Coutts, A.M., Beringer, J. & Tapper, N. (2010), Changing Urban Climate and CO₂ Emissions: Implications for the Development of Policies for Sustainable Cities. *Urban Policy and Research*, 28(1):pp. 27–47.
- Coutts, A.M., Beringer, J. & Tapper, N.J. (2007), Impact of Increasing Urban Density on Local Climate: Spatial and Temporal Variations in the Surface Energy Balance in Melbourne, Australia. *Journal of Applied Meteorology and Climatology*, 46(4):pp. 477–493.
- Coutts, A.M., Tapper, N.J., Beringer, J., Loughnan, M. & Demuzere, M. (2012), Watering our cities: The capacity for Water Sensitive Urban Design to support urban cooling and improve human thermal comfort in the Australian context. *Progress in Physical Geography*, 37(1):pp. 2–28.
- Coutts, A.M., White, E.C., Tapper, N.J., Beringer, J. & Livesley, S.J. (2015), Temperature and human thermal comfort effects of street trees across three contrasting street canyon environments. *Theoretical and Applied Climatology*:pp. 1–14.
- De Kauwe, M.G., Kala, J., Lin, Y.S., Pitman, A.J., Medlyn, B.E., Duursma, R.A., Abramowitz, G., Wang, Y.P. & Miralles, D.G. (2015), A test of an optimal stomatal conductance scheme within the CABLE land surface model. *Geoscientific Model Development*, 8(2):pp. 431–452.
- Declet-Barreto, J., Brazel, A.J., Martin, C.a., Chow, W.T.L. & Harlan, S.L. (2012), Creating the park cool island in an inner-city neighborhood: heat mitigation strategy for Phoenix, AZ. *Urban Ecosystems*.
- Díaz-Espejo, A., Walcroft, A.S., Fernández, J.E., Hafredi, B., Palomo, M.J. & Girón, I.F. (2006), Modeling photosynthesis in olive leaves under drought conditions. *Tree Physiology*, 26(11):pp. 1445–1456.
- Dupont, S., Otte, T. & Ching, J. (2004), Simulation of meteorological fields within and above urban and rural canopies with a mesoscale model. *Boundary-Layer Meteorology*, 113:pp. 111–158.
- Duursma, R.A. & Medlyn, B.E. (2012), MAESPA: a model to study interactions between water limitation, environmental drivers and vegetation function at tree and stand levels, with an example application to [CO₂] x drought interactions. *Geoscientific Model Development*, 5(4):pp. 919–940.
- Fung-yan, M. (1999), *Hyperspectral Data Analysis of Typical Surface Covers in Hong Kong*. Ph.D. thesis, The Chinese University of Hong Kong.
- Gebert, L., Coutts, A. & Beringer, J. (2012), Response of trees to the urban environment. Technical report, Monash University.
- Google (2015), Preston, Victoria 3072. <http://maps.google.com.au/maps>.
- Grimmond, C.S.B., Blackett, M., Best, M.J., Barlow, J., Baik, J.J., Belcher, S.E., Bohnenstengel, S.I., Calmet, I., Chen, F., Dandou, a., Fortuniak, K., Gouvea, M.L., Hamdi, R., Hendry, M., Kawai, T., Kawamoto, Y., Kondo, H., Krayenhoff, E.S., Lee, S.H., Loridan, T., Martilli, a., Masson, V., Miao, S., Oleson, K., Pigeon, G., Porson, a., Ryu, Y.H., Salamanca, F., Shashua-Bar, L., Steeneveld, G.J., Tombrou, M., Voogt, J., Young, D. & Zhang, N. (2010), The International Urban Energy Balance Models Comparison Project: First Results from Phase 1. *Journal of Applied Meteorology and Climatology*, 49(6):pp. 1268–1292.

- Grimmond, C. & Oke, T. (1999), Aerodynamic properties of urban areas derived from analysis of surface form. *Journal of Applied Meteorology*, 38:pp. 1262–1292.
- Gromke, C., Blocken, B., Janssen, W., Merema, B., van Hooff, T. & Timmermans, H. (2015), CFD analysis of transpirational cooling by vegetation: Case study for specific meteorological conditions during a heat wave in Arnhem, Netherlands. *Building and Environment*, 83:pp. 11–26.
- Harman, I.N. & Belcher, S.E. (2006), The surface energy balance and boundary layer over urban street canyons. *Quarterly Journal of the Royal Meteorological Society*, 132(621):pp. 2749–2768.
- Järvi, L., Grimmond, C. & Christen, A. (2011), The Surface Urban Energy and Water Balance Scheme (SUEWS): Evaluation in Los Angeles and Vancouver. *Journal of Hydrology*, 411(3-4):pp. 219–237.
- Kanda, M., Kawai, T., Kanega, M., Moriwaki, R., Narita, K. & Hagishima, a. (2005), A Simple Energy Balance Model for Regular Building Arrays. *Boundary-Layer Meteorology*, 116(3):pp. 423–443.
- Konarska, J., Lindberg, F., Larsson, A., Thorsson, S. & Holmer, B. (2014), Transmissivity of solar radiation through crowns of single urban trees-application for outdoor thermal comfort modelling. *Theoretical and Applied Climatology*, 117(3-4):pp. 363–376.
- Kondo, H., Genchi, Y., Kikegawa, Y., Ohashi, Y., Yoshikado, H. & Komiyama, H. (2005), Development of a Multi-Layer Urban Canopy Model for the Analysis of Energy Consumption in a Big City: Structure of the Urban Canopy Model and its Basic Performance. *Boundary-Layer Meteorology*, 116(3):pp. 395–421.
- Krayenhoff, E.S., Christen, A., Martilli, A. & Oke, T.R. (2014), A Multi-layer Radiation Model for Urban Neighbourhoods with Trees. *Boundary-Layer Meteorology*, 151(1):pp. 139–178.
- Krayenhoff, E.S., Santiago, J.L., Martilli, A., Christen, A. & Oke, T.R. (2015), Parametrization of Drag and Turbulence for Urban Neighbourhoods with Trees. *Boundary-Layer Meteorology*, 156(2):pp. 157–189.
- Krayenhoff, E.S. & Voogt, J.A. (2007), A microscale three-dimensional urban energy balance model for studying surface temperatures. *Boundary-Layer Meteorology*, 123(3):pp. 433–461.
- Krüger, E., Minella, F. & Rasia, F. (2011), Impact of urban geometry on outdoor thermal comfort and air quality from field measurements in Curitiba, Brazil. *Building and Environment*, 46(3):pp. 621–634.
- Kunz, R., Khatib, I. & Moussiopoulos, N. (2000), Coupling of mesoscale and microscale models - an approach to simulate scale interaction. *Environmental Modelling & Software*, 15(6-7):pp. 597–602.
- Kusaka, H., Kondo, H., Kikegawa, Y. & Kimura, F. (2001), A simple single-layer urban canopy model for atmospheric models: Comparison with multi-layer and slab models. *Boundary-Layer Meteorology*, 101(ii):pp. 329–358.
- Lee, S.H. (2011), Further Development of the Vegetated Urban Canopy Model Including a Grass-Covered Surface Parametrization and Photosynthesis Effects. *Boundary-Layer Meteorology*, 140(2):pp. 315–342.

- Lee, S.H. & Park, S.U. (2008), A Vegetated Urban Canopy Model for Meteorological and Environmental Modelling. *Boundary-Layer Meteorology*, 126(1):pp. 73–102.
- Lehmann, I., Mathey, J., Rößler, S., Bräuer, A. & Goldberg, V. (2014), Urban vegetation structure types as a methodological approach for identifying ecosystem services - Application to the analysis of micro-climatic effects. *Ecological Indicators*, 42:pp. 58–72.
- Lemonsu, A., Masson, V., Shashua-Bar, L., Erell, E. & Pearlmuter, D. (2012), Inclusion of vegetation in the Town Energy Balance model for modelling urban green areas. *Geoscientific Model Development*, 5(6):pp. 1377–1393.
- Levinson, R., Berdahl, P., Akbari, H., Miller, W., Joedicke, I., Reilly, J., Suzuki, Y. & Vondran, M. (2007), Methods of creating solar-reflective nonwhite surfaces and their application to residential roofing materials. *Solar Energy Materials and Solar Cells*, 91(4):pp. 304–314.
- Mariscal, M.J., Orgaz, F. & Villalobos, F.J. (2000), Modelling and measurement of radiation interception by olive canopies. *Agricultural and Forest Meteorology*, 100(2-3):pp. 183–197.
- Martilli, A., Clappier, A. & Rotach, M. (2002), An urban surface exchange parameterisation for mesoscale models. *Boundary-Layer Meteorology*, 104:pp. 261–304.
- Masson, V. (2000), A physically-based scheme for the urban energy budget in atmospheric models. *Boundary-Layer Meteorology*, 94(3):pp. 357–397.
- Matzarakis, A., Rutz, F. & Mayer, H. (2007), Modelling radiation fluxes in simple and complex environments—application of the RayMan model. *International Journal of Biometeorology*, 51(4):pp. 323–34.
- Matzarakis, A., Rutz, F. & Mayer, H. (2010), Modelling radiation fluxes in simple and complex environments: basics of the RayMan model. *International Journal of Biometeorology*, 54(2):pp. 131–9.
- Medlyn, B.E. & Duursma, R.A. (2014), MAESTRA Manual. <http://bio.mq.edu.au/research/projects/maestra/manual.htm>, (accessed 3 July 2014).
- Medlyn, B.E., Duursma, R.A., Eamus, D., Ellsworth, D.S., Prentice, I.C., Barton, C.V.M., Crous, K.Y., De Angelis, P., Freeman, M. & Wingate, L. (2011), Reconciling the optimal and empirical approaches to modelling stomatal conductance. *Global Change Biology*, 17(6):pp. 2134–2144.
- Medlyn, B.E., Robinson, A.P., Clement, R. & McMurtrie, R.E. (2005), On the validation of models of forest CO₂ exchange using eddy covariance data: some perils and pitfalls. *Tree Physiology*, 25(7):pp. 839–857.
- Motazedian, A. (2015), pers. comm., 1 June. Email: "Lincoln Sq".
- Noilhan, J. & Planton, S. (1989), A simple parameterization of land surface processes for meteorological models. *Monthly Weather Review*, 117:pp. 536–549.
- Oke, T. (1982), The energetic basis of the urban heat island. *Quarterly Journal of the Royal Meteorological Society*, 108:pp. 1–24.
- Oke, T. (1987), *Boundary Layer Climates*. Routledge, London and New York, 2nd edition.
- Oleson, K.W., Bonan, G.B., Feddema, J., Vertenstein, M. & Grimmond, C.S.B. (2008), An Urban Parameterization for a Global Climate Model. Part I: Formulation and Evaluation for Two Cities. *Journal of Applied Meteorology and Climatology*, 47(4):pp. 1038–1060.

- OpenFOAM (2011), OpenFOAM website. <http://www.openfoam.com/>, (accessed 2 November 2011).
- Otte, T. & Lacser, A. (2004), Implementation of an urban canopy parameterization in a mesoscale meteorological model. *Journal of Applied Meteorology*, (2002):pp. 1648–1665.
- Rademacher, I.F. & Nelson, C. (2001), Nitrogen Effects on Leaf Anatomy within the Intercalary Meristems of Tall Fescue Leaf Blades. *Annals of Botany*, 88(5):pp. 893–903.
- Schlünzen, K.H., Gräwe, D., Bohnenstengel, S.I., Schlüter, I. & Koppmann, R. (2011), Joint modelling of obstacle induced and mesoscale changes - Current limits and challenges. *Journal of Wind Engineering and Industrial Aerodynamics*, 99(4):pp. 217–225.
- Shahidan, M.F., Jones, P.J., Gwilliam, J. & Salleh, E. (2012), An evaluation of outdoor and building environment cooling achieved through combination modification of trees with ground materials. *Building and Environment*, 58:pp. 245–257.
- Sierra, A.M. (2012), *Measuring and modeling canopy photosynthesis of olive orchards*. Msc thesis plant production systems, Instituto de Agricultura Sostenible (IAS - CSIC).
- Simmons, M., Bertelsen, M., Windhager, S. & Zafian, H. (2011), The performance of native and non-native turfgrass monocultures and native turfgrass polycultures: An ecological approach to sustainable lawns. *Ecological Engineering*, 37(8):pp. 1095–1103.
- SOLWEIG (2011), SOLWEIG website. <http://www.gvc.gu.se/Forskning/klimat/stadsklimat/gucg/software/solweig/>, (accessed 2 November 2011).
- Sumida, A., Miyaura, T. & Torii, H. (2013), Relationships of tree height and diameter at breast height revisited: analyses of stem growth using 20-year data of an even-aged Chamaecyparis obtusa stand. *Tree Physiology*, 33(1):pp. 106–118.
- Tan, C.L., Wong, N.H., Jusuf, S.K. & Chiam, Z.Q. (2015), Impact of plant evapotranspiration rate and shrub albedo on temperature reduction in the tropical outdoor environment. *Building and Environment*, 94(P1):pp. 206–217.
- Thorsson, S., Lindberg, F., Elasson, I. & Holmer, B. (2007), Different Methods for Estimating the Mean Radiant Temperature in an Outdoor Urban Setting. *International Journal of Climatology*, 27:pp. 1983–1993.
- Tominaga, Y., Sato, Y. & Sadohara, S. (2015), CFD simulations of the effect of evaporative cooling from water bodies in a micro-scale urban environment: Validation and application studies. *Sustainable Cities and Society*, 19:pp. 259–270.
- Villalobos, F., Orgaz, F. & Mateos, L. (1995), Non-destructive measurement of leaf area in olive (*Olea europaea* L.) trees using a gap inversion method. *Agricultural and Forest Meteorology*, 73(1-2):pp. 29–42.
- Vu, T.C., Ashie, Y., Asaeda, T., Ca, V.T., Ashie, Y. & Asaeda, T. (2002), A k-e turbulence closure model for the atmospheric boundary layer including urban canopy. *Boundary-Layer Meteorology*, 102(3):pp. 459–490.
- Wang, Y.P. & Jarvis, P.G. (1990), Description and validation of an array model - MAESTRO. *Agricultural and Forest Meteorology*, 51:pp. 257–280.
- Wang, Y., Bakker, F., de Groot, R., Wortche, H. & Leemans, R. (2015), Effects of urban trees on local outdoor microclimate: synthesizing field measurements by numerical modelling. *Urban Ecosystems*, 18(4):pp. 1305–1331.

- White, E., Coutts, A., Tapper, N. & Beringer, J. (2012), Urban microclimate & street trees: Understanding the effects of street trees on human thermal comfort. Technical report, CRC for Water Sensitive Cities, Monash University.
- Wong, T.H.F & Brown, R.R. (2009), The water sensitive city: principles for practice. *Water Science and Technology*, 60(3):pp. 673–82.
- Wright, I.J. & Westoby, M. (2000), Cross-species relationships between seedling relative growth rate, nitrogen productivity and root vs leaf function in 28 Australian woody species. *Functional Ecology*, 14(1):pp. 97–107.
- Yu, J., Chen, L., Xu, M. & Huang, B. (2012), Effects of Elevated CO₂ on Physiological Responses of Tall Fescue to Elevated Temperature, Drought Stress, and the Combined Stresses. *Crop Science*, 52(4):p. 1848.